Change in variability in the Columbia River estuary: a habitat perspective

By

Mojgan Rostaminia

A dissertation presented to the faculty of the

Division of Environmental and Biomolecular System

School of Medicine

Oregon Health & Science University

In partial fulfillment of the requirements for the degree of

Doctor of Philosophy in

Environmental Science and Engineering

March 2017

School of Medicine

Oregon Health & Science University

CERTIFICATE OF APPROVAL

This is to certify that the PhD dissertation of

Mojgan Rostaminia

has been approved

Dr. António M. Baptista
(Advisor)

Dr. Tawnya Peterson
(Chair)

Dr. G. Curtis Roegner

Dr. Richard Johnson

Dedication

I dedicate this thesis to my daughter, Elsa. You and future generations deserve to live on a healthy planet; I am doing what I can to make it so.

Table of Contents

Table of Contents ..... *i*
List of Tables ..... *iii*
List of Figures ..... *v*
Acknowledgements ..... *ix*
Abstract ..... *xi*

CHAPTER 1 1
INTRODUCTION 1
1.1. The Columbia River estuarine habitat *1*
1.2. Research objectives and structure of the dissertation *5*

CHAPTER 2 7
CHARACTERIZING JUVENILE CHINOOK SALMON HABITAT AND ITS VARIABILITY IN A RIVERINE ESTUARY 7
Abstract *8*
2.1. Introduction *9*
2.2. Method *13*
2.2.1. Circulation simulations 13
2.2.2. Review of the calculation of Physical Habitat Opportunity 14
2.2.2.1. Depth criterion 15
2.2.2.2. Velocity criterion 15
2.2.2.3. Temperature criterion 16
2.2.2.4. Salinity criterion 16
2.2.3. New calculation of salmon habitat 16
2.3. Results *20*
2.3.1. Contrasting definitions of salmon habitat 20
2.3.2. Nursery habitat vs. migratory habitat 21
2.3.3. Sensitivity of salmon habitat to life stage 22
2.3.4. Natural variability of nursery habitat for emergent fry 25
2.3.4.1. Intra–annual variability 25
2.3.4.2. Inter–annual variability 25
2.3.5. Nursery habitat anomalies 26
2.3.6. Spring–neap effects on salmon habitat 28
2.4. Discussion *31*
2.4.1. Methodology for salmon habitat calculation 31
2.4.2. Nursery and migratory habitat 32
2.4.3. Sensitivity of salmon habitat to life stage 33
2.4.4. Nursery and migratory habitat variability and anomalies 34
2.4.5. Sensitivity of salmon habitat to spring–neap tide 35
2.5. Conclusion *36*
Tables *38*
Figures *41*

CHAPTER 3 53
POTENTIAL IMPACTS OF A LARGE CASCADIA SUBDUCTION ZONE EARTHQUAKE IN THE COLUMBIA RIVER ESTUARY: A HABITAT PERSPECTIVE 53
Abstract *54*
3.1. Introduction *55*

3.2. Method ... *57*
3.2.1. Estuarine habitat: relevant indicators ... 57
3.2.1.1. Salinity Intrusion Length ... 57
3.2.1.2. Plume Volume ... 57
3.2.1.3. Shallow Water Habitat ... 58
3.2.1.4. Salmon Habitat ... 59
3.2.2. Cascadia earthquake scenario ... 60
3.2.3. Numerical model configuration ... 62
3.3. Results ... *63*
3.4. Discussion ... *66*
3.5. Conclusion ... *70*
Table ... *71*
Figure ... *72*

CHAPTER 4 ... 83
IMPACT OF SEA LEVEL CHANGES ON SALMON HABITAT IN THE COLUMBIA RIVER ESTUARY ... 83
Abstract ... *84*
4.1. Introduction ... *85*
4.2. Method ... *87*
4.2.1. Indicators ... 87
4.2.2. Numerical model ... 89
4.2.3. Sea level change scenarios ... 90
4.2.3.1. Global sea level change ... 90
4.2.3.2. Relative sea level changes ... 92
4.2.3.3. Relative SLC scenarios ... 92
4.3. Results ... *95*
4.4. Discussion ... *101*
4.4.1. Uncertainty and limitations of the study ... 104
4.5. Conclusion ... *105*
Tables ... *107*
Figures ... *116*

CHAPTER 5 ... 128
CONCLUSIONS AND FUTURE WORK ... 128
5.1. Contributions ... *128*
5.1.1. Refined set of criteria to characterize juvenile Chinook salmon habitat as a function of predictable physical factors ... 129
5.1.2. Characterized temporal and spatial variability of salmon habitat over a 15 year period (2000-2014) 130
5.1.3. Determined the effect of a large CSZ subduction on the estuary and its ability to provide estuarine salmon habitat ... 131
Determined the influence of SLC on the estuary and its ability to provide estuarine salmon habitat ... 132
5.2. Contributions to management ... *134*
5.3. Uncertainty ... *135*
5.4. Future work ... *138*

REFERENCE ... 140

List of Tables

Table 2. 1. Seasonal mean and range of daily Coefficient of Variation in nursery habitat for emergent fry at 8 reaches, river discharge and temperature at Bonneville Dam, continental shelf temperature, and tidal range at Tongue Point (2000-2014). 38
Table 2. 2. Seasonal mean and standard deviation (SD) of log-transformed nursery habitat for emergent fry at 8 reaches, river discharge at Bonneville Dam, temperature at Bonneville Dam, ocean temperature, and tidal range at Tongue point for years 2000-2014. 39
Table 2. 3. 2000-2014 Mean nursery habitat for emergent fry for 8 hydrogeomorphic reaches of the Columbia River estuary, separated by season and tidal cycle (spring and transition). Units are percentage of the nursery habitat at neap tidal cycle at each reach.....40

Table 3. 1. Percentage change in six salmon-relevant indicators for the XXL1-CSZ scenario relative to the contemporary condition.....71
Table 4. 1. Relative sea level change projection for year 2100. Gauge: 9439040, Astoria, OR. NOAA's regional rate: -0.00040 m/yr. All values are expressed in meters relative to the local mean sea level. 107
Table 4. 2. Yearly minimum, mean, and maximum of daily (tidally averaged) values for the indicators: salinity intrusion length (SIL), salt volume (SV), plume volume (PV), shallow water habitat (SWH), and salmon habitat (SH) for the contemporary condition and six scenarios of sea level change. 108
Table 4. 3. Yearly minimum, mean, and maximum of difference values for the indicators: salinity intrusion length (SIL), salt volume (SV), plume volume (PV), shallow water habitat (SWH), and salmon habitat (SH) for six scenarios of sea level change minus the contemporary condition. 109
Table 4. 4. Yearly minimum, mean, and maximum of percent changes for indicators: salinity intrusion length (SIL), salt volume (SV), plume volume (PV), shallow water habitat (SWH), and salmon habitat (SH) for six scenarios of sea level change relative to the contemporary condition. 110
Table 4. 5. Yearly minimum, mean, and maximum of daily (tidally averaged) values for shallow water habitat (SWH) at eight reaches in the contemporary condition and for six scenarios of sea level change. 111
Table 4. 6. Yearly minimum, mean, and maximum of percent changes for shallow water habitat (SWH) at eight reaches for six scenarios of sea level change relative to the contemporary condition. 112
Table 4. 7. Shallow water habitat (SWH) changes for six scenarios of sea level change relative to the contemporary system. Shallow water habitat is calculated in each element on June 14th, when most reaches show the highest value of shallow water habitat. 113

Table 4. 8. Yearly minimum, mean, and maximum of daily (tidally averaged) values for salmon habitat (SH) at eight reaches in the contemporary condition and for six scenarios of sea level change. 114
Table 4. 9. Yearly minimum, mean, and maximum of percent changes for salmon habitat (SH) at eight reaches for six scenarios of sea level change relative to the contemporary condition. 115

List of Figures

Figure 2. 1. Juvenile Chinook salmon performance depends on criteria that include population structure and life history, habitat opportunity (access), and habitat capacity (quality and quantity) criteria, all of which are influenced by regional physical factors (adapted from Bottom et al. 2005). 41
Figure 2. 2. Horizontal view of unstructured grid for Columbia River estuary and shelf, extending from Bonneville dam to the Pacific Ocean with 8 hydrogeomorphic reaches of the Columbia River Estuary Ecosystem Classification (Simenstad et al., 2011b). (a) The full extent of the model domain, from California to British Columbia; (b) zoom-in of the Columbia River estuary; (c) coastal lowlands entrance mixing and coastal uplands salinity gradient; (d) volcanic current reversal, Western Cascades tributary confluences, and tidal flood plain basin constriction; (e) middle tidal flood plain basin; (f) upper tidal flood plain basin and Western Gorge. 42
Figure 2. 3. Schematic representation of the method used to determine juvenile Chinook salmon habitat. The method distinguishes between (a) nursery and (b) migratory habitat, and operates through a combination of thresholds and penalty functions. For nursery habitat, the method distinguishes between four life stages through the velocity threshold 43
Figure 2. 4. Illustration of the effect of the changes introduced in the habitat criteria, for 2011 time series of daily averaged values of either PHO (Bottom et al., 2005) or salmon habitat (as in this work). (a) Contrast between area- (blue) and volume-based (orange) calculations of PHO. (b) Effect of using different threshold velocities on the calculation of volume-based PHO. (c) Contrast between volume-based PHO and nursery habitat tailored for emerging fry ($v<0.4$m/s). (d) Comparison of nursery habitat for emerging fry, migratory habitat, and total habitat. 44
Figure 2. 5. 2000-2014 Mean habitat for each of the 8 reaches of the estuary, separated by season and habitat type (migratory versus nursing habitat for emerging fry). Units are percentage of the total volume of the reach. Here and in other figures, seasons are defined as follows: Seasons: W = winter (Jan, Feb, Mar); Sp = spring (Apr, May, Jun); Su = summer (Jul, Aug, Sep); F = fall (Oct, Nov, Dec).....45
Figure 2. 6. 2000-2014 Mean habitat for each of the 8 reaches of the estuary, separated by season and life stage (resident fry, fingerling A, and fingerling B). Colored by percentage change of the nursery habitat for emergent fry of the reach. X-axis: 1: ((Resident fry-emergent fry)/emergent fry)*100; 2: ((Fingerling A-emergent fry)/emergent fry*100; 3: (Fingerling B-emergent fry)/emergent fry)*100. 46
Figure 2. 7. Climatology of: (a) nursery habitat for emergent fry at each reach; (b) river; (c) water temperature at Bonneville Dam; (d) ocean temperature; (e) nursery habitat for resident fry at each reach; (f) nursery habitat for fingerling A at each reach; and (g) nursery habitat for fingerling B at each reach. The statistics are computed for 2000-2014. Individual years referred in text are displayed as colored lines. 47

Figure 2. 8. Z-scores of nursery habitat for emergent fry at all reaches of the estuary, for the four seasons and contextualized by: Z-scores of river discharge at Bonneville Dam (RD (BON)), temperature at Bonneville Dam (T (BON)), tidal range (TR) and ocean temperature (T); and values of the seasonal averages of the Cumulative Upwelling Index (CUI) divided by 100, the Pacific Decadal Oscillation (PDO), and the El Niño–Southern Oscillation (ENSO).....51
Figure 2. 9. 2000-2014 Mean nursery habitat for emergent fry for 8 reaches of the estuary, separated by season and tidal cycle (spring and transition). Colored by percentage of the nursery habitat at neap tidal cycle at each reach. X-axis: 1: ((nursery habitat at transition tidal cycle- nursery habitat at neap tidal cycle)/ nursery habitat at neap tidal cycle) *100; 2: ((nursery habitat at spring tidal cycle- nursery habitat at neap tidal cycle)/ nursery habitat at neap tidal cycle) *100.....52

Figure 3. 1. (a) Horizontal view of the model domain, along the west coast of the U.S. from California to British Columbia and the Columbia River estuary extending from Bonneville dam to the Pacific Ocean. The color shows the bathymetry difference between the largest CSZ earthquake scenario and contemporary condition; (b) zoom-in of the Columbia River estuary with 8 hydro-geomorphic reaches of the Columbia River Estuary Ecosystem Classification (Simenstad et al., 2011b); (c) horizontal view of unstructured grid of the lower estuary (reach A, B, and C) 72
Figure 3. 2. (a) Histograms show the distribution of salinity intrusion length (SIL) for both contemporary condition and the XXL1-CSZ scenario; (b) histogram illustrates the difference in salinity intrusion length between the XXL1-CSZ scenario and contemporary condition. The black dashed line shows the mean difference; (c) time series of salinity intrusion length for contemporary system, XXL1-CSZ, and the difference between the two.....73
Figure 3. 3. (a) Histograms show the distribution of salt volume for both contemporary condition and the XXL1-CSZ scenario; (b) histogram illustrates the difference salt volume between the XXL1-CSZ scenario and contemporary condition. The black dashed line shows the mean difference; (c) time series of salt volume for contemporary system, XXL1-CSZ, and the difference between the two.....74
Figure 3. 4. (a) Histograms show the distribution of plume volume for both contemporary condition and the XXL1-CSZ scenario; (b) histogram illustrates the difference in plume volume between the XXL1-CSZ scenario and contemporary condition. The black dashed line shows the mean difference; (c) time series of plume volume for contemporary system, XXL1-CSZ, and the difference between the two.....75
Figure 3. 5. (a) Histograms show the distribution of shallow water habitat (SWH) in contemporary condition and the XXL1-CSZ scenario at reach A; (b) histogram illustrates the difference in shallow water habitat between the XXL1-CSZ scenario and contemporary condition. The black dashed line shows the mean difference; (c) time series of shallow water habitat in contemporary system, XXL1-CSZ, and the difference between the two at reach A. 76
Figure 3. 6. (a) Histograms show the distribution of shallow water habitat (SWH) in contemporary condition and the XXL1-CSZ scenario at reach B; (b) histogram illustrates the difference in shallow water habitat between the XXL1-CSZ scenario and contemporary condition. The black dashed line shows the mean difference; (c)

time series of shallow water habitat in contemporary system, XXL1-CSZ, and the difference between the two at reach B.....77
Figure 3. 7. (a) Histograms show the distribution of shallow water habitat (SWH) in contemporary condition and the XXL1-CSZ scenario at reach C; (b) histogram illustrates the difference in shallow water habitat between the XXL1-CSZ scenario and contemporary condition. The black dashed line shows the mean difference; (c) time series of shallow water habitat in contemporary system, XXL1-CSZ, and the difference between the two at reach C.....78
Figure 3. 8. (a) Histogram shows the distribution of nursery habitat for emergent fry in contemporary condition and the XXL1-CSZ scenario at reach A; (b) histogram illustrates the difference in nursery habitat between the XXL1-CSZ scenario and contemporary condition. The black dashed line shows the mean difference; (c) time series of nursery habitat for emergent fry in contemporary system, XXL1-CSZ, and the difference between the two at reach A. 79
Figure 3. 9. (a) Histograms show the distribution of nursery habitat for emergent fry in contemporary condition and the XXL1-CSZ scenario at reach B; (b) histogram illustrates the difference in nursery habitat between the XXL1-CSZ scenario and contemporary condition. The black dashed line shows the mean difference; (c) time series of nursery habitat for emergent fry in contemporary system, XXL1-CSZ, and the difference between the two at reach B.....80
Figure 3. 10. (a) Histograms show the distribution of nursery habitat for emergent fry in contemporary condition and the XXL1-CSZ scenario at reach C; (b) histogram illustrates the difference in nursery habitat between the XXL1-CSZ scenario and contemporary condition. The black dashed line shows the mean difference; (c) time series of nursery habitat for emergent fry in contemporary system, XXL1-CSZ, and the difference between the two at reach C.....81
Figure 3. 11. Percentage change in salinity intrusion length (SIL), salt volume (SV), plume volume (PV), shallow water habitat (SWH), and salmon habitat (SH) for the XXL1-CSZ scenario relative to the contemporary condition. Mean percentage change is expressed as black circles; dark lines show maximum and minimum percentage change; light lines show 25th and 75th percentile percent changes.....82
Figure 4. 1. Top view of unstructured grid with bathymetry for Columbia River estuary and shelf, extending from Bonneville dam to the Pacific Ocean with 8 hydrogeomorphic reaches of the Columbia River Estuary Ecosystem Classification (Simenstad et al., 2011b). (a) The full extent of model domain, along the west coast of the U.S. from California to British Columbia; (b) zoom-in of the Columbia River estuary; Black circles show the NOAA tide gauge at Astoria station (Station ID: 9439040), the location of computed offshore sea level change, and Bonneville Dam. 116
Figure 4. 2. Estimated relative sea level change from 1992 to 2100 at Astoria, OR, NOAA tide gauge: 9439040, NOAA's regional rate:-0.00040 m/yr. All sea level change values are expressed in meters relative to local mean sea level.....117
Figure 4. 3. Percent changes in salinity intrusion length (SIL), salt volume (SV), plume volume (PV), shallow water habitat (SWH), and salmon habitat (SH) for six scenarios of sea level change relative to the contemporary condition. The range of color bars reflects the different scenarios. In each bar, the lighter color indicates the

maximum and minimum, the darker color indicates the 25th and 75th percentile, and the white circle indicates the average of each indicator for each scenario. 118
Figure 4. 4. Salinity intrusion length (SIL) in the Columbia River estuary for the contemporary condition (CC; year 2010) and six scenarios of sea level change. Histograms at the top panel show the distribution of SIL. The lower panel shows the timeseries of SIL. 119
Figure 4. 5. Salt volume (SV) in the Columbia River estuary for the contemporary condition (CC; year 2010) and six scenarios of sea level change. Histograms at the top panel show the distribution of SV. The lower panel shows the timeseries of SV. 120
Figure 4. 6. Isoline map of bottom salinity response to a) contemporary condition and for six scenarios of sea level change: b) -0.04 m, c) 0.27 m, d) 0.63 m, e) 0.97 m, f) 1.27 m, g) 1.77 m on September 28th in the Columbia River estuary. 121
Figure 4. 7. Plume volume (PV) in the Columbia River estuary for the contemporary condition (CC; year 2010) and six scenarios of sea level change. Histograms at the top panel show the distribution of PV. There are zoom-in views of parts of original histograms for each scenario. The lower panel shows the time series of PV. 122
Figure 4. 8. Isoline maps of surface salinity response to (a) a scenario of sea level change of 1.77 m; (b) contemporary condition (CC); (c) the difference in surface salinity between current condition and 1.77 m SLC (Surface salinity at 1.77 m scenario minus CC) on June 21th in the Columbia River estuary and the Pacific Ocean. The black contour line delineates salinity= 28 psu. 123
Figure 4. 9. Salinity intrusion length for six scenarios of sea level change as a function of river discharge at Bonneville Dam. CC: contemporary condition. 124
Figure 4. 10. Percent changes in shallow water habitat (SWH) at eight reaches for six scenarios of sea level change relative to the contemporary condition The range of color bars reflects the different scenarios. In each bar, the lighter color indicates the maximum and minimum, the darker color indicates the 25th and 75th percentile, and the white circle indicates the average of each indicator for each scenario 125
Figure 4. 11. The change in SWH (calculated for each element) with a 1.77 m sea level rise relative to the contemporary condition throughout the Columbia River estuary when the highest value of SWH was seen at most reaches on June 14th. The positive values reflect more SWH availability with a sea level rise of 1.77 m, while the negative numbers indicate less SWH availability with the same rise in sea level. . 126
Figure 4. 12. Percent changes in juvenile Chinook salmon habitat (SH) at eight reaches for six scenarios of sea level change relative to the contemporary condition The range of color bars reflects the different scenarios. In each bar, the lighter color indicates the maximum and minimum, the darker color indicates the 25th and 75th percentile, and the white circle indicates the average of each indicator for each scenario. 127

Acknowledgements

I would like to express sincere gratitude to my advisor, Professor António M. Baptista, for his guidance and support throughout this research. His immense knowledge and experience have been a continual source of inspiration.

Along with my advisor, I would like to thank the rest of my thesis committee: Dr. Tawnya Peterson, Dr. G. Curtis Roegner, Dr. Holly Simon, and Professor Richard Johnson, for their insightful comments, encouragement, and for asking questions that helped me broaden my research perspective.

I am extremely grateful for the guidance provided by Daniel L. Bottom, Dr. G. Curtis Roegner, David J. Teel, and Kurt L. Fresh from NOAA's Northwest Fisheries Science Center, as well as Charles. A. Simenstad from the University of Washington's School of Aquatic and Fishery Sciences. Their input improved my analysis of salmon habitat in the Columbia River estuary.

I would also like to thank Dr. George R. Priest from the Oregon Department of Geology and Mineral Industries for providing a post-deformation bathymetry map that reflected the results of a large Cascadia Subduction Zone earthquake.

I want to thank all past and present members of Antonio's lab: Paul Turner, Charles Seaton, Dr. Tuomas Kärnä, Dr. Jesse Lopez, Katie Morrice, Dr. Joseph Zhang, Dr. Michella Burla, and Dr. Sergey Forolov.

I would also like to thank Nancy Christie, Amy Johnson, Nievita BuenoWatts, Vanessa Green, Karen Sears, Bonnie Gibbs, Summer Steele, Jim Mohan, and Ethan Van Matre for all of their help from the day I applied to the program up to today.

And a very special thanks to my family. Words cannot express how grateful I am to my parents and my brother and sister for always believing in me and encouraging me to follow my dreams.

Finally, I would like to express my appreciation for my beloved husband, Ali Shamsa, who put up with the many hours of work required to conduct this research and was always my support in the moments when there was no one around to answer my queries.

This research was funded in part by the National Science Foundation cooperative agreement OCE-0424602, the Bonneville Power Administration (BPA 66219), and the National Oceanic & Atmospheric Administration (NOAA AB133F10SE2827). Computational resources were funded in part by the NSF XSEDE grant TG-OCE140024.

Abstract

The Columbia River estuary, the transitional zone between continental land and the ocean, is a river-dominant estuary with a large plume that supports a variety of aquatic species. In recent decades, human activities, such as hydropower generation, irrigation, fishing, and navigation, along with natural variability and climate change, have substantially altered the Columbia River to the point that multiple salmon stocks are now listed as either endangered or threatened under the Endangered Species Act. As expensive recovery efforts are being conducted, the possible implications of both sea level changes and a large Cascadia Subduction Zone (CSZ) earthquake on those efforts are pertinent but poorly understood. Because of the possible impacts of those regional events on ecosystems, understanding the variability and change in estuarine physics and plume is critical for stakeholders and decision makers to best preserve and restore salmon stocks.

In this dissertation, a refined habitat computation method was introduced that combines the skill-assessed simulation results from a 3D circulation model with the best available empirical understanding of fish response to the hydrodynamic variables found in the Columbia River, downstream from the Bonneville Dam. The methodology distinguished between nursery and migratory habitat, and for nursery habitat recognized different life stages of salmon.

This methodology was applied to characterize juvenile Chinook salmon habitat, and created a contemporary baseline of its spatial and temporal variability over a 15-year

timespan (2000–2014) in the Columbia River estuary. The results suggested that nursery habitat responds primarily to river forcing in the upper reaches of the estuary, and to tides in the lower reaches. We found that nursery habitat increases depending on shallow area extent and is typically an order of magnitude smaller than migratory habitat. We also found that at most reaches, the estuary offers more nursery habitat for fingerling than for fry, which is initially relevant to the water velocity regime in each reach.

Also, estuarine physics and habitat change in response to the largest Cascadia Subduction Zone (CSZ) earthquake and sea level changes scenarios separately were investigated. The simulations of river-to-ocean circulation were conducted by using a 3D numerical model for both the largest CSZ earthquake (as developed by the Oregon Department of Geology and Mineral Industries and collaborators) and for six scenarios of sea level changes (derived from the projection developed by the NRC, NOAA, and the USACE). Year-round habitat-relevant indicators, including salinity intrusion length, salt volume, shallow water habitat, and juvenile Chinook salmon habitat, were compared between the contemporary condition and conditions resulting from scenarios of change.

The results suggested that the largest CSZ earthquake would increase salinity propagation upstream causing a major loss of freshwater habitat during low river discharges (e.g., in September). Also, we found that plume volume increases during the freshet, which some salmon stocks could get benefit during their out-migration to the ocean.

The results for the response of the estuary to sea level rise indicated by passing specific thresholds (approximately ~1m off the coast), rising sea levels would drastically increase the extent of ocean influence on the estuary (as measured by salinity intrusion

length), and would substantially reduce the seasonal influence of freshwater on the continental shelf (as measured by plume volume during river freshets). Specifically, in response to high-end sea level rise scenario (1.77 m), the Columbia River would be deeply altered by salinity where salinity will propagate upstream to Port of Portland and plume will be disappeared during low river discharge.

In a habitat perspective, rising sea levels will alter shallow water—and specifically—salmon estuarine habitat within the estuary in complex spatial and temporal ways. There will be winners and losers in terms of reaches, stocks, and migration periods, which will be critical to consider in designing long-term plans for restoration and hatchery programs.

Although there is a degree of uncertainty about how, when and where this system will experience the impact of sea level changes, an extensive and continuous system monitoring will help to track ongoing changes, which will help to prevent permanent system damages.

Chapter 1

Introduction

1.1. The Columbia River estuarine habitat

The Columbia River basin has supported abundant runs of salmon and steelhead by providing nursery habitat, food resources, and transition zones (Bottom et al., 2005; Emmett et al., 1991; Groot and Margolis, 1991; Healey, 1992). The basin is home to five species of Pacific salmon: Chinook, sockeye, chum, and Coho salmon and steelhead that spawn and rear in the middle and upper reaches of the Columbia River Basin. They then migrate to the Columbia River estuary and lower mainstem and then to the ocean. After spending 1-5 years in the ocean, adults migrate back to their natal streams to spawn spawn (Bottom et al., 2005; Emmett et al., 1991).

Salmon have served as the dietary foundation for the region's Native American tribes for thousands of years and continue to provide a critical food source for at least 137 different animal species (Cederholm et al., 2000; Dalton et al., 2013; NRC, 2004b). The existence of salmon is a sign of healthy rivers in the Pacific Northwest, with biologists designating salmon as a keystone species of the region (Bottom et al., 2005).

However, the Columbia River has experienced a significant loss of habitat and with an almost 90% decline in population from historical levels (Bottom et al., 2011; Bottom et al., 2005; Dalton et al., 2013; NRC, 2004b; Pearcy, 1992; PFMC, 2011; Weitkamp et

al., 2014). This has led to 13 stocks of Pacific salmon and steelhead being listed under the U.S. Endangered Species Act (Ford, 2011; Weitkamp et al., 2014).

Natural variability in the Columbia River Basin, ocean conditions, and factors such as hatchery production, overfishing, the generation of hydroelectric power, irrigation, degradation, and climate variability and change, are each contributing to the decline in salmon (Bartz et al., 2006; Battin et al., 2007; Bottom et al., 2005; Dalton et al., 2013; ISAB, 2007; Jorgensen et al., 2009; Mantua et al., 2010; Mantua et al., 1997).

Many expensive restoration and protection efforts are being conducted to mitigate the impact of various non-climate-related stressors in the Columbia River estuary. In recent years, some improvements have been seen in adult salmon and steelhead passing through Bonneville Dam, but the majority of them are hatchery fish (NPCC, 2014; Smith, 2014).

A landmark synthesis indicates that habitat changes, and other factors affecting salmon population structure and life histories, have altered and likely reduced the estuary's capacity to support salmon species (Bottom et al., 2005). Therefore, it is important to quantify habitat variability currently occurring in the estuary as it provides a baseline for addressing the range of potential changes in estuarine habitat in future scenarios. Some forthcoming changes that will influence the Pacific Northwest include: change in hydrologic stream flow regimes, temperature, and sea level, as well as a possible major Cascadia Subduction Zone (CSZ) earthquake.

Projected climate change for the Columbia River basin suggests reductions in snow pack, more rain precipitation in winter (Elsner et al., 2010; ISAB, 2007) . These changes will create higher-than-average flows in winter, an earlier freshet, and lower

flows in the summer (Dalton et al., 2013; Elsner et al., 2010; Hamlet et al., 2010). Since river flow is one of the leading factors affecting salmon arrival time and residency in the estuary (Bottom et al., 2005), any change in the hydrologic regime, including the timing and extent of high and low river streamflow, will alter salmon habitat, population, and life cycle (Mantua et al., 2009, 2010).

Also, the Pacific Northwest has undergone an annual- average warming of 0.7 °C during the time span of 1895–2011 (Dalton et al., 2013). Current climate change projections accounts for increases in annual average temperatures of 0.1 to 0.6 °C per decade, while future average weekly stream temperatures are expected to increase from 0.5 to 2 °C relative to past and current conditions at Bonneville Dam (Mote and Salathe, 2010). Future long-term Pacific Northwest climate changes are expected to result in increasing stream temperatures (Dalton et al., 2013; IPCC, 2007, 2013; Mote et al., 2003; Mote and Salathe, 2010).

The Pacific Northwest coastal margin has also faced sea level change, which, in combination with subsidence or uplift, threatens the ecosystem (Scavia et al., 2002).

By 2100, sea level rise will most likely affect many estuarine habitats because salinity propagation into the estuary may convert freshwater marsh and swamp habitats into salt marsh (Dalton et al., 2013; Glick et al., 2007). Specifically, with 0.69 m sea level rise by 2100, it is predicted that Willapa Bay, the Columbia River, and Tillamook Bay will lose 32%, 31%, and 63% of brackish marsh, tidal swamp, and tidal flats, respectively (Glick et al., 2007).

A change in global average sea level as a result of a change in the volume of the world ocean causes an eustatic sea-level change. Recent research has forecasted ranges

of global SLC by the year 2100 between 0.2 to 2 m (IPCC, 2007, 2013; Jevrejeva et al., 2009; NRC, 2012; Parris et al., 2012; Pfeffer et al., 2008; USACE, 2013a; Vermeer and Rahmstorf, 2009). To compute relative SLC based on global SLC over the next 100 years, USACE developed the SLC Curve Calculator (USACE, 2013a). The calculator adds constant value of regional VLM (i.e., subsidence or uplift) to the different scenarios of global sea level change derived from the projections developed by NRC (2012), NOAA (Parris et al., 2012), and USACE (NRC, 1987; USACE, 2013a).

Besides climate change, documented geological records show that major earthquakes have occurred in the past and will likely occur again in the future along the Cascadia Subduction Zone (Atwater and Hemphill-Haley, 1997; Nelson et al., 1996; Savage et al., 1981). The last major earthquake on the Cascadia mega-thrust occurred on January 26, 1700 (Satake et al., 1996). Studies suggest that a future earthquake will occur in this area with a magnitude of the M_w (moment magnitude) of 8.8 to 9.2 (Hawkes et al., 2011; Satake et al., 1996). Besides tsunami and inundation impacts, this event is likely to create significant changes in the Columbia River estuary bathymetry, thus affecting the estuarine ecosystem and specifically salmon habitat.

To effectively plan for long-term ecosystem restoration and salmon recovery, quantifying the estuary's variability and anticipating future change are necessary. These characterizations require an advanced methodology such as a modeling system and observation network in order to support regional decision makers in the Columbia River estuary.

1.2. Research objectives and structure of the dissertation

This research relied on the pre-existing SATURN regional infrastructure (Baptista et al., 2015) for the Columbia River estuary, which includes integrated modeling (the Virtual Columbia River) and observation systems. This research also relied, and expanded upon, regionally accepted estuarine-related habitat indicators (Miller et al., 2014; USACE, 2012). Together, these tools have the potential to inform studies of habitat variability and change, and thus support thinking on the evolving salmon usage of the estuary.

The objectives of this thesis were specifically to:

- Characterize contemporary variability of Chinook salmon habitat in a river-dominated, meso-tidal estuary.
- From a habitat perspective, determine the potential impact on the estuary of both sudden change [a large Cascadia Subduction Zone (CSZ) earthquake] and longer-term change (sea level change).

To achieve these goals, simulations of a baroclinic circulation model were used, which cover a river-to-shelf domain that ranges from the first dam (i.e., the one furthest downstream) in the Columbia River to the Pacific Northwest continental shelf. These simulations were conducted using SELFE (Zhang and Baptista, 2008). The simulations are an operational product of the SATURN collaboratory and are referred to as simulation database 33 (DB33). The settings and skill of DB33 are documented in detail in (Kärnä and Baptista, 2016a), with additional discussion in (Kärnä et al., 2015).

Model outputs (water depth and the 3D fields of velocity, salinity, and temperature) were filtered to compute regionally accepted habitat-relevant indicators. These indicators included modified juvenile Chinook salmon habitat shallow water habitat, plume volume, and salinity intrusion length.

To compute the variability of salmon habitat within the Columbia River system, we used DB 33 circulation simulations for 2000-2014. To predict future changes, we conducted simulations for a) six regionally accepted scenarios for future of sea level change (-0.04 m, 0.27 m, 0.63 m, 0.97 m, 1.27 m, 1.77 m) with values derived from the projection developed by the National Research Council (NRC, 2012), National Oceanic and Atmospheric Administration (Parris et al., 2012), and the U.S. Army Corps of Engineers (USACE, 2013a); and b) the largest CSZ earthquake scenario as developed by the Oregon Department of Geology and Mineral Industries and collaborators.

Beyond this introduction, the dissertation is divided into chapters. In chapter 2, a refined version of the methodology for habitat computation is proposed. The method computes both nursery and migratory habitats for four life stages of juvenile Chinook salmon. Seasonal and inter-annual variability of juvenile Chinook salmon habitat is then addressed for years 2000–2014. Chapters 3 and 4 explore the predicted Columbia River estuary response to both a large CSZ earthquake and to sea level changes respectively. Finally, Chapter 5 summarizes the research contributions, identifies main factors of uncertainty, and outlines possible areas for future research.

Chapter 2

Characterizing juvenile Chinook salmon habitat and its variability in a riverine estuary[1]

[1] I would like to thank Daniel L. Bottom, Dr. G. Curtis Roegner, David J. Teel, and Kurt L. Fresh from NOAA's Northwest Fisheries Science Center, as well as Professor Charles A. Simenstad from the University of Washington's School of Aquatic and Fishery Sciences. Their expert advice and guidance greatly improved the salmon habitat indicators for the Columbia River estuary. I also wish to thank Paul Turner for providing multi–year (2000–2014) simulations of baroclinic circulation and and Dr. Tuomas Kärnä for his modeling skill. A version of this chapter will be submitted to Estuaries and Coasts.

Abstract

Highly productive estuarine ecosystems offer critical habitats for diverse species. However, alterations in estuarine habitats have contributed to decline in fish populations. To effectively design restoration plans for preserving fish populations, habitat quantification is essential. We introduce a refined habitat computation method combining the best available empirical understanding of fish response to hydrodynamic variables, with skill-assessed, 15–year simulations of baroclinic estuarine circulation. The method classifies habitat use based on different life stages of fish, and distinguishes between estuarine habitat used for growth (nursery habitat) and those used for migration from river to ocean (migratory habitat). We then apply this method to characterize juvenile Chinook salmon habitat in the Columbia River, and create a baseline of its spatial and temporal variability. We find that habitat differs strongly among hydrogeomorphic reaches and responds primarily to river forcing in the upper reaches and to tides in the lower reaches. Temperature modulates habitat seasonally, with least habitat in summer and winter. Inter-annual variability in nursery habitat changes significantly from one reach to the other and is sensitive to the river discharge anomalies at upper reaches. Nursery habitat increases depending on shallow area extent and is typically an order of magnitude smaller than migratory habitat. In most reaches, the estuary offers more nursery habitat for fingerlings than for fry. Since habitat alone cannot explain the use of the estuary by salmon, results should be interpreted as a

conceptual model of the contemporary salmon habitat and best used to forecast habitat response to future changes.

2.1. Introduction

Estuaries provide nursery habitats, food resources, and transition zones for different life stages of fish and invertebrates (Bottom et al., 2005; Goertler et al., 2015; Sheaves et al., 2015). However, the healthy estuarine habitat has been substantially altered by natural variability, human activity, and climate change, resulting in a decline in fish populations (Bottom et al., 2005; Dalton et al., 2013; ISAB, 2007). Currently, 13 stocks of Pacific salmon and steelhead are listed under the U.S. Endangered Species Act in the Columbia River Basin (Ford, 2011; Weitkamp et al., 2014). A variety of efforts are underway to prevent further decline, as well as to recover wild stocks and increase abundance of both wild and hatchery stocks (Borde et al., 2012; Coleman et al., 2013; Miller and Simenstad, 1997; Sagar, 2012; Thom et al., 2013). It is increasingly recognized that these efforts would benefit from improved understanding of the continuum of influence of ocean, river and estuarine conditions on the salmon life history (Battin et al., 2007; Bottom et al., 2011; Bottom et al., 2005; Burla, 2009; Burla et al., 2010; Mantua et al., 2010; Mantua et al., 1997).

A landmark synthesis (Bottom et al., 2005) indicates that habitat changes, and other factors affecting salmon population structure and life histories, have altered and likely reduced the estuary's capacity to support salmon species. The loss of habitat due to ongoing and future threats highlights the urgent need to characterize and quantify the estuarine habitat in order to effectively carry out restoration efforts to protect threatened

species and stocks. However, quantifying the estuarine habitat for different salmon species is challenging because the length of salmon residence time varies in their natal stream and estuary and is influenced by their life history and ecological characteristics of the specific stock (Bottom et al., 2005; Burke, 2004; Gleason et al., 2011).

Using the member/vagrant hypothesis of Sinclair (1988) as reference, Bottom et al. (2005) developed a conceptual model of estuarine rearing conditions for ocean–type salmon, and its dependency on external physical forcing (Fig. 2.1). The model assumes that salmon performance depends on (a) population structure and life history, (b) habitat opportunity (access), and (c) habitat capacity (quality). An historical and evolutionary context for estuarine habitat is thus necessary (although insufficient) for an historical and evolutionary view of salmon performance.

Habitat opportunity, although still complex, is the most predictable element of the conceptual model. Furthermore, while opportunity depends on multiple physical, biogeochemical and ecological factors, hydrodynamic-related factors are the most predictable. This recognition led to a first effort to predict "physical habitat opportunity," based on the best available circulation models for the Columbia River estuary. To enable these efforts, Bottom et al. (2005) introduced criteria for favorable physical habitat opportunity, in the form of thresholds for water depth ($0.1 \leq D \leq 2$ m) and for depth–averaged velocity (≤ 0.3 m/s). These criteria were later adjusted and extended to also include thresholds for temperature and salinity (Burla, 2009), and have over time informed regional thinking on major Columbia River decisions (e.g. Columbia River Treaty Review project and Columbia River Channel Improvement Project.

The power of the physical habitat opportunity criteria is that, while relevant to salmon, they are predicated exclusively on hydrodynamic variables that are predictable for a broad range of historical and future scenarios. The major conceptual limitations of these criteria are that they only partially explain salmon performance (Fig. 2.1), and are empirically based (see Methods). They also depend on the skill of the circulation simulations, but that is a lesser limitation, as errors in existing simulation databases (Kärnä and Baptista, 2016a) are well within the range of the uncertainties that are traditionally associated with fisheries science.

In this study, we have expanded on past efforts in habitat quantification (Bottom et al., 2005; Burla, 2009) and introduce a refined method for computing habitat in the Columbia River estuary. While this methodology is more generally applicable, we focus on juvenile Chinook salmon (*Oncorhynchus tshawytscha*) because they use the estuary as a rearing habitat more than species such as chum salmon and steelhead, and because five Columbia River Chinook salmon are currently listed under the Endangered Species Act (Ford, 2011; NMFS, 1999; Teel et al., 2014).

The new methodology is still based on hydrodynamic variables, but differs from Bottom et al. (2005) and its extensions (Bottom et al., 2011; Burla, 2009) in five major ways:

(1) Recognizing that juvenile salmon use vertical mobility for their benefit, we define salmon habitat on a *volumetric* rather than *surface* basis.

(2) Recognizing that the estuary serves two functions relative to juvenile salmon, we distinguish between nursery habitat (which supports fish growth) and migratory habitat (which transports fish to sea).

(3) Recognizing that fish at different life stages have different swimming skill, we distinguish among nursery habitat criteria for emerging fry (<45 mm), resident fry (45–60 mm), fingerling A (61–80 mm) and fingerling B (>80 mm).

(4) Recognizing that temperature and salinity influence (or serve as surrogates for ecological variables that influence) both habitat access and quality, we replace binary thresholds (either 0 or 1) for these variables by "penalty functions" (between 0 and 1).

(5) Recognizing that salmon might be negatively affected by low dissolved oxygen concentrations, we add a penalty for low dissolved oxygen throughout the upwelling season to account for biological stress on juvenile Chinook salmon in the brackish waters of migratory habitat.

Because of the fifth of the above differences, we will refer to what we compute simply as salmon habitat, rather than as salmon habitat opportunity or physical habitat opportunity.

We applied this methodology to characterize juvenile Chinook salmon habitat variability and create a contemporary baseline of its spatial and temporal variability over a 15-year timespan (2000–2014) across eight hydrogeomorphic reaches (Simenstad et al., 2011a) of the Columbia River estuary (Fig. 2.2). We also investigated how variability in river and ocean forcing influence salmon habitat in the Columbia River estuary.

2.2. Method

2.2.1. Circulation simulations

The implementation of our methodology is enabled by multi–year (2000–2014) simulations of baroclinic circulation for the Columbia River–to–shelf domain shown in Fig. 2. 2. These simulations were conducted with the finite element unstructured–grid code, SELFE (Zhang and Baptista, 2008), version 4.0.1. Simulations are an operational product of the SATURN collaboratory (Baptista et al. 2015), and are referred to as simulation database 33 (DB33). The settings and skill of DB33 are documented in detail in (Kärnä and Baptista, 2016a) with additional discussion in (Kärnä et al., 2015).

Simulation results provide free–surface elevation, 3D velocity, salinity, and temperature of water at each node of the grid, every 15 minutes. The domain of computation extends from the Bonneville Dam (near rkm 230) to the continental shelf (Fig. 2. 2), but the analysis of habitat is focused on the estuary, and distinguishes among the 8 hydrogeomorphic estuarine reaches identified by (Simenstad et al., 2011b). While DB33 simulations start in 1999, we started the analysis of habitat only in 2000, considering 1999 a warm-up year. This long warm-up period is not necessary for most other estuarine applications, because the residence times in the Columbia River estuary are on the order of a few days (Kärnä and Baptista, 2016b). However, we found that allowing shallow areas in the upper reaches (reaches C, D, E, and F) to naturally inundate through a full year of seasonal variability of tides and flows is essential for calculations of the quantity of suitable habitat.

2.2.2. Review of the calculation of Physical Habitat Opportunity

We review here the calculation of physical habitat opportunity (PHO), as it evolved from (Bottom et al., 2005) and was applied in (Bottom et al., 2011; Burla, 2009). Criteria for favorable PHO with empirical thresholds are:

$0.5 \leq$ Depth (D) ≤ 2 m Velocity (V) ≤ 0.25 m/s

Temperature (T) ≤ 19 °C Salinity (S) ≤ 5 practical salinity units (psu)

Local application of these criteria leads to setting an auxiliary variable, c, to either 0 (criteria not met) or 1 (criteria met), per time step, at each node of the horizontal grid (Fig. 2. 2) from Bonneville Dam to the mouth of the estuary. Integration over an entire reach and period of reference, followed by temporal average, transforms the results into total area of favorable PHO. PHO calculations based on velocity, salinity and temperature are based upon depth–averaged values of each variable.

Mathematically:

$$\mathrm{PHO} = \frac{\sum_{E_{c,ts}} \sum_{ts=1}^{n} \mathrm{Area}(E_{c,ts}) \times \mathrm{time\ span(ts)}}{\mathrm{time\ span\ of\ reference}} \quad (1)$$

$E_{c,ts}$ is an element satisfying an individual habitat criterion x at a particular time step (ts); n is the number of time steps analyzed. A brief explanation follows in the sections below.

2.2.2.1. Depth criterion

Juvenile salmon preferentially occupy shallow waters, while larger sizes move into deeper estuary channels and then migrate to the ocean (Bottom et al., 2005; Groot and Margolis, 1991). Subyearling Chinook may remain in estuarine marshes and other shallow–water habitats until they reach sizes larger than 100 mm fork length (FL) (Bottom et al., 2005; Healey et al., 1982; Levy and Northcote, 1982). Based on several field studies, the depth threshold for subyearling Chinook salmon was determined to be between 0.5 m and 2 m (Bottom et al., 2011; Bottom et al., 2005; Burla, 2009) and is the first criterion used in determining physical habitat opportunity (PHO).

2.2.2.2. Velocity criterion

Favorable habitat for juvenile Chinook is also determined by swimming performance and the salmon's ability to maintain position against tidal or river currents (Bottom et al., 2005; Davis et al., 1963; Tiffan et al., 2002). Results from lab experiments indicated that Chinook salmon between 81–126 mm FL in length, move through water by sustaining swimming speeds of 0.23–0.67 m/s at an acclimation temperature of 11.5 °C; smaller salmon (51–73 mm FL) have maximum sustained swimming speeds ranging from 0.29 to 0.53 m/s at an acclimated temperature of 15 °C (Davis et al., 1963). Based on these results, Bottom et al. (2005) defined water velocity as a second criterion for determining juvenile habitat opportunity. A velocity of less than 0.30 m/s established as the threshold velocity for computing PHO for juvenile Chinook within the Columbia River estuary.

2.2.2.3. Temperature criterion

Salmon migration timing, overall health, and general performance, are all influenced by temperature (Bottom et al., 2011; Brett et al., 1982; Fresh, 2006; McCullough, 1999). Higher and sustained stream temperatures will increase thermal migration barriers for salmon migrating to and from the ocean (Bottom et al., 2011; McCullough, 1999). Juvenile Chinook salmon leave shallow waters when temperatures rise to more than 19 °C; because of this, their numbers decline after July in the Columbia River (Bottom et al., 2011; Roegner and Teel, 2014). Temperature, with an upper limit of 19 ºC, was added as the third criterion for computing PHO (Bottom et al., 2011; Burla, 2009).

2.2.2.4. Salinity criterion

In addition, a salinity criterion with a range between 0 and 5 Practical Salinity Unit (psu) was added to the PHO calculation to highlight habitat availability for those salmon that might need to gradually acclimate first to lower salinities before moving into higher salinity areas within the habitat (Bottom et al., 2011; Burla, 2009).

2.2.3. New calculation of salmon habitat

The physical habitat opportunity indicator provides a quantification of habitat potentially used by juvenile Chinook salmon. However, it is not life–stage–specific and relies on the binary (presence or absence) application of thresholds for favorable water depth, velocity, and salinity and temperature conditions and it ignores the fact that certain variables (such as temperature) influence salmon more subtly. In addition, threshold values have typically been interpreted as averages over the water column, without explicit recognition that salmon are not restricted to a particular depth within

the water column, but may be found anywhere in the vertical dimension.

This research builds upon previous studies and proposes a refined method of salmon habitat computation that represents the habitat used by various sizes of juvenile Chinook salmon. An auxiliary variable (f) is used to multiply by volume of each element (Fig. 2. 2). The auxiliary variable (f) is considered 0 if the criteria are not met and is 1 if criteria are met, then it multiply by penalties (Fig. 2. 3).

Fig. 3 outlines the methodology. The first screening for favorable habitat is by depth and temperature thresholds. A minimum depth of 0.5 m (Bottom et al., 2011) and an upper incipient lethal temperature of 25 ºC (Brett et al., 1982; McCullough, 1999; Roegner and Teel, 2014) are set as rigid limits for favorable habitats, for all sizes and stocks of Chinook salmon (Fig. 2. 3).

Although juvenile salmon can withstand temperatures up to a threshold of 25 ºC, their survival and growth rates are not constant and change by temperature. The optimal rearing temperature range for growth and normal response is 10–16 ºC. The growth rate starts decreasing at temperatures below 10 ºC (McCullough, 1999; Richter and Kolmes, 2005; Roegner and Teel, 2014; US EPA 2003), temperatures in the range of 16 to 19 ºC add to the risk of disease, and temperatures above 19 ºC are stressful for juveniles (McCullough, 1999; Roegner and Teel, 2014). Based on these literature values, we address temperature influence on habitat use by introducing a penalty (θ), which changes as a function of temperature based on bioenergetics model results. The temperature penalty is then applied to the variable f (Fig. 2. 3, temperature penalty box). Using a temperature penalty introduces the notion of habitat capacity, thus extending beyond the habitat opportunity concept. As a result, this study uses the term “salmon

habitat" instead of "salmon habitat opportunity."

We distinguish between nursery habitat, with depths less than 2 m, and migratory habitat, where the water depth can be more than 2 m but the useful part of the water column is up to ~3m (Groot and Margolis, 1991; Healey et al., 1982; Mains and Smith, 1964) (Fig. 2. 3).

Chinook salmon size is positively correlated with water velocity, reflecting the fact that smaller sized individuals tend to stay in low-velocity, shallow areas, and larger sizes choose higher velocity habitats (Davis et al., 1963; Everest and Chapman, 1972; Groot and Margolis, 1991; Tiffan et al., 2002). Because of this, we only apply juvenile Chinook salmon sensitivity to stream velocity for the nursery habitat computations. Based on field research and results from PHO calculations (Bottom et al., 2011; Bottom et al., 2005; Burla, 2009), favorable velocity for juvenile Chinook salmon in emerging fry (<45 mm), resident fry (45–60 mm), fingerling A (61–80 mm) and fingerling B (>80 mm) stages is defined as less than 0.4 m/s, 0.5 m/s, 0.6 m/s and, 1 m/s respectively (Fig. 2. 3, velocity threshold box).

The original salinity threshold was also modified from the original PHO formulation because field studies suggest some Chinook fry are able to migrate from the estuary to the ocean at salinities above 5 psu (Bottom et al., 2011; Volk et al., 2010). Some Chinook fry (≤60 mm FL) were found to have migrated to the lower estuary, where salinities often are ≥30 psu, before late May at the Salmon River (Volk et al., 2010). Some juvenile Chinook salmon captured in the estuary were also found in waters with salinities ranging from below 1 to 16 psu (Bottom et al., 2011; Roegner et al., 2012). Healey (1982) also reported high juvenile Chinook catches between 15 and 25 psu in

the Campbell River. However, metabolic costs for fry increase in brackish water based on data from (Morgan and Iwama, 1991)). Based on the above findings, we introduced a penalty (S=0.8) for nursery habitat in the presence of salinity. The salinity penalty doesn't apply when calculating migratory habitat because salmon that migrate to deeper areas are old enough to deal with brackish and marine salinity ranges (Fig. 2. 3, salinity penalty box).

In addition, juvenile salmon in salinity–affected areas (Reach A, and part of B) may face oxygen concentration deficiencies during upwelling season (Roegner et al., 2011). Studies indicate that salmon become metabolically weakened and stressed by being in low dissolved oxygen areas (Davis, 1975; US EPA 1986). Based on previous literature citing biological stress in salmon, Roegner et al. (2011) classified the oxygen concentration levels into three low dissolved oxygen (DO) levels: critical biological stress (hypoxia) on salmon at low (DO) concentration between 0 to 1.4 ml/l; moderate biological stress when DO >1.4 to 2.8 ml /l; and mild biological stress at DO > 2.8 through 4.2 ml/l.

To account for biological stress on juvenile Chinook salmon in the brackish waters of migratory habitat, as well as to highlight habitat availability for those salmon that might be affected by low dissolved oxygen concentrations, we introduced a low dissolved oxygen penalty (LOP). A regression model of observed dissolved oxygen (from SATURN stations) based on salinity is used to evaluate the ocean source of oxygen into the estuary. LOP is calculated as a scaling factor where salinity is greater than 32.7 psu and mild biological stress begins to be felt by salmon. The regression equation of LOP based on salinity is then used to calculate LOP with any measured salinity provided by

the SELFE model (Fig. 2. 3, low oxygen penalty box). This penalty is applied only from Jun 15 to Sep 15, to account for the seasonal patterns of upwelling and estuarine hypoxia (CMOP, 2015). In this approach, only the low oxygen concentration from the ocean is considered; therefore, LOP is not applied to the calculation of fresh water migratory habitat.

Physical variables, including water depth and the 3D fields of velocity, salinity, and temperature, are extracted from each prism and are then filtered through the above criteria and penalties. The auxiliary variable f is then multiplied by the volume of each prism, integrated over the depth and then over each reach, from the mouth of the Columbia River to the Bonneville Dam, every 15 minutes.

2.3. Results

2.3.1. Contrasting definitions of salmon habitat

Using year 2001 and Reach B as reference, we show here the evolution from an area-based definition of PHO to a volume-based definition of salmon habitat (Fig. 2. 4). The top panel (Fig. 2. 4a) contrasts area and volume-based definitions of PHO, keeping all thresholds the same. The results are internally consistent,, with the major feature in both cases being the drastically lower PHO in summer in response to the temperature criterion.

The second panel (Fig. 2. 4b) shows that while not affecting seasonal trends, the velocity thresholds significantly influence PHO except during summer. This suggests that different life stages of juvenile Chinook, characterized by different body sizes and

thus different abilities to sustain position in the presence of flow, potentially experience habitat quite differently. While we do not show an equivalent plot for other reaches, we note that this result holds for some reaches (A, B, D, G and H) while for others (C, E and F) velocities are such that size influence is minimal.

The third panel (Fig. 2. 4c) contrasts PHO and nursery habitat for emerging fry, with the velocity threshold set to $v < 0.4$ m/s in both cases. We now observe fundamental differences in pattern, in response to the more realistic approach (for nursery habitat) of using temperature thresholds that penalize sub-optimal temperature at both ends of the spectrum. While PHO drops to zero or near zero in summer, nursery habitat declines but remains substantially present in July and August, which is supported by the observation and theory presented in previous studies (Bottom et al., 2005; Burla, 2009; Roegner and Teel, 2014). Additionally, temperatures drive a decline of nursery habitat from fall to winter, which is consistent with the higher density of juvenile Chinook in the fall (Roegner and Teel, 2014).

Finally, Fig. 2. 4d shows that migratory habitat is an order of magnitude greater than nursery habitat, and thus accounts for the vast majority of available habitat. This important distinction was missing from the historical definition of PHO. Of note, both migratory and nursery habitats vary seasonally in response to river discharge and temperatures, but spring-neap variations in habitat are far more pronounced in nursery habitat.

2.3.2. Nursery habitat vs. migratory habitat

Fig. 2.5 contrasts the mean nursery (for emerging fry) and migratory habitat, defined

over 2000-2014, distinguishing among four seasons and all 8 reaches of the estuary. Because the different reaches differ in size, we standardized the results relative to the water volume of the reach. Results are similar for the other 4 life stages considered in this analysis, which is why we only show emergent fry data.

Consistently across reaches and seasons, migratory habitat is dominant. With some exceptions, nursery habitat is typically largest in spring and fall, and smallest in winter and summer. For reaches A-F, spring offers the most nursery and migratory habitat; for the two upper reaches (G-H) total habitat is similar in Spring and Fall, and nursery habitat is dominant in Fall (with Spring habitat being quite depressed, likely because the freshet flows reducing the amount of shallow water available). Reach D is essentially depleted in nursery habitat throughout the year, and reaches E and G also offer minimal nursery habitat. By contrast, reaches C and F offer the largest relative volume of nursery habitat. All reaches offer substantial amounts of migratory habitat, with minima at ~15% and maxima ranging from ~25% to ~40% of total volume.

2.3.3. Sensitivity of salmon habitat to life stage

In order to examine the difference in mean seasonal nursery habitat at each reach for every season and for each of the 4 sizes of juvenile Chinook, we used two–way analysis of variance (ANOVA). To meet the assumption of normality, the ANOVA test was done on log–transformed nursery habitat. The ANOVA comparisons were considered significant at P–values less than 0.001, and Tukey's honestly significant difference (HSD) post hoc test was used to distinguish between multiple pairs. Here too, we specifically focus on the difference between resident fry, fingerling A, and fingerling B

relative to the emergent fry in Tukey's HSD test.

Seasonal means of nursery habitat for Chinook were significantly different among size classes for each season (p <0.001, ANOVA) at all reaches, except for reaches C and F (Fig. 2. 6). We found that the seasonal mean of nursery habitat increases based upon fish size; the estuary provides more nursery habitat for fingerling rather than for emergent or resident fry at those specific reaches (Fig. 2. 6). We summarize our findings for each reach in the following sub–section:

Reaches A and B: There was significant difference among mean seasonal nursery habitats for 4 sizes of juvenile Chinook salmon (p <0.001, ANOVA and Tukey's HSD) at reaches A and B. Mean seasonal nursery habitat increased by more than 20% (but <40%) for resident fry, fingerling A, and fingerling B, relative to the emergent fry, for all seasons (Fig. 2. 6).

Reach C: There was no significant difference in mean seasonal nursery habitat among the 4 sizes of Chinook for all seasons except in spring (p <0.001, ANOVA) at reach C, which is only a 4% difference between the mean seasonal nursery habitat for fingerling B and emergent fry during the spring (p <0.001, Tukey's HSD) (Fig. 2. 6).

Reach D: There was a significant difference among mean seasonal nursery habitat for 4 sizes of juvenile Chinook (p <0.001, ANOVA and Tukey's HSD) at reach D. For fingerling A and resident fry, the mean increases by 40% relative to emergent fry, at reach D. Mean spring nursery habitat for fingerling B increases by more than 40% relative to emergent fry (Fig. 2.6).

Reach E: There is significant difference (p <0.001, ANOVA and Tukey's HSD) between fingerlings relative to emergent fry for all seasons at reach E. The mean

seasonal nursery habitat for fingerlings only increase by less than 20% relative to emergent fry. Although the ANOVA test showed significant differences between the groups (p <0.001), Tukey's HSD showed no significant difference (p >0.001) between mean seasonal nursery habitat for resident fry and emergent fry (Fig. 2. 6).

Reach F: There was no significant difference in mean seasonal nursery habitat among the 4 sizes of Chinook for all seasons (p >0.001, ANOVA) (Fig. 2. 6).

Reach G: There was a significant difference between mean seasonal nursery habitats for 4 sizes of juvenile Chinook (p *<0.001,* ANOVA and Tukey's HSD) at reach G. The mean seasonal nursery habitat for resident fry was higher than 20% (<40%) for all seasons (Fig. 2. 6). Mean winter and spring nursery habitat for fingerlings A and B; however, were higher than 63% and 102% relative to emergent fry. Mean summer and fall nursery habitat for fingerling A increased relative to emergent fry by more than 53% and 49%, respectively. Mean seasonal nursery habitat for fingerling B increases by more than 96% in summer and 74% in fall (Fig. 2. 6).

Reach H: There is significant difference between mean seasonal nursery habitats for 4 sizes of juvenile Chinook (p *<0.001,* ANOVA and Tukey's HSD) at reach H (Fig. 2. 6). The mean seasonal nursery habitat for fingerling A, fingerling B, and resident fry increases by more than 20% (<40%), relative to emergent fry, in winter, summer, and fall. In spring; however, the mean seasonal nursery habitat for fingerling A, fingerling B, and resident fry increases, relative to emergent fry, by 34%, 40%, and 23%, respectively.

Although nursery habitat increases with juvenile size, the seasonal pattern stays the same. We scale nursery habitat for fingerling A, fingerling B, and resident fry to

emergent fry because nursery habitat for this stage is also used by larger sizes of juveniles.

2.3.4. Natural variability of nursery habitat for emergent fry

2.3.4.1. Intra–annual variability

The 2000-204 climatology of nursery habitat (Fig. 2. 7a) shows strong, reach-specific, seasonal variability. This variability is best understood in the context of the variability in river discharge and temperatures at the river and end members (Fig. 2. 7b-d). For reference, we highlight in all panels of Fig. 2.7 the years of 2001 (extremely low freshet), 2011 (generally high flows, and extremely high freshet) and 2012 (moderate-to-high flows). Visually, while nursery habitat responds strongly to the spring-neap cycles at reaches A and B, it is mostly influenced by river discharge in the upper reaches. During freshet, high river discharge (Fig. 2. 7b), combined with favorable stream temperatures (10–16 °C) (Fig. 2. 7d), provide greater nursery habitat at reaches A through F. However, high river discharge decreases nursery habitat at reaches G and H. This response is mostly through the depth criterion. Shallow (0.5–2 m) waters increase during the freshet at reaches A through F and decreases at reaches G and H.

2.3.4.2. Inter–annual variability

To characterize the inter–annual variability of nursery habitat, we calculated the coefficient of variation (CV) for daily nursery habitat during a 15–year window, and then we averaged the CV over each season. Nursery habitat has high variability at reaches D (Winter: M=60.30%, Range=90.8%; Spring: M=75.5%, Range=108.1%) and E (Winter: M=82.5%, Range= 41.2%; Spring M=100.6%, Range= 82.9%). On the other

hand, reach A has the lowest variability (Spring M=12.1%, Range=18%) among all reaches (Table 2. 1). Low inter–annual variability of nursery habitat at reaches A and B during the years 2000–2014, is the result of low inter–annual variability in tidal range (Mean CV= 14.4% in summer and 17.0% in spring and fall) and in ocean temperature (Mean CV= 5.3% in winter and 7.7% in spring). In contrast, the highest inter–annual variability of nursery habitat occurs during all seasons at reach E and during the spring (freshet) at reaches D, E, and H due to the highest variability of river discharge (CV=30%) occurring in the spring (Table 2.1).

2.3.5. Nursery habitat anomalies

To quantify seasonal anomalies for nursery habitat, as well as analyze the relationship between river and ocean forcing and nursery habitat anomalies, the standard scores for average seasonal tidal range, ocean temperature, temperature and river discharge at Bonneville Dam, and nursery habitat at 8 reaches has been computed. Seasonal anomalies have been calculated based on the reference mean of 2000–2014 for consistency with the period simulation results for SELFE are available. The seasonal anomaly for each variable (log–transformed variable to meet the assumption of normality) is calculated based on the departure the variable's seasonal average from the 2000–2014 mean and then normalized by the standard deviation of 2000–2014 (equation 2).

$$VAR\ anomaly_{(year,season)} = \frac{\overline{VAR}_{year,season} - \overline{VAR}_{2000-2014,season}}{\sigma(VAR_{2000-2014,season})} \quad (2)$$

Here, we concentrate on seasonal average nursery habitat anomalies that are more than +1 (less than -1) standard deviation above (below) the 2000–2014 mean.

Reaches A and B: The nursery habitat anomaly varies by ±1σ during 2000–2014 for all seasons at reaches A and B (Fig. 2. 8; Table 2. 2). Low variability in nursery habitat seasonal mean is due to the low variability found in the mean seasonal tidal range, which ranges of ±1σ over the 2000–2014 mean. The ocean temperature anomalies found during the 2008, 2009, 2014 spring and winter, 2003 winter, and 2005 spring, range [±1σ,±2σ] above (and below) the 2000–2014 mean. Positive Pacific Decadal Oscillation (PDO) and El Niño–Southern Oscillation (ENSO) resulted in warmer ocean temperatures in winter 2003 and spring 2005 and 2009. Negative PDO and ENSO were associated with cooler ocean temperatures during 2008 and 2009 winter and spring. Although PDO was positive in winter and spring 2014, and ENSO was negative in winter, but positive in the spring, the ocean temperature was still cooler (less than 1σ) than the 2000–2014 mean. This happened because PDO was negative in 2011, 2012, and 2013, and it takes the ocean a long time to warm up. Increasing (or decreasing) ocean temperatures of between 0.62 °C to 1.24 °C (or between -0.62 °C to -1.24 °C) influences on nursery habitat, but it only increased (decreased) nursery habitat by 1σ (-1σ) at reaches A and B. In addition, change in mean ocean temperature between ±0.62 °C relative to the 2000–2014 mean, doesn't impact nursery habitat anomalies at reaches A and B.

Reaches C, D, E, and F: The impact of river discharge on nursery habitat increases when moving from reaches C to F. The spring 2011 and 2012 extreme positive nursery habitat anomalies seen at reaches C through F ([1σ, 2σ] relative to the 2000–2014 mean) indicate the combined impact of large positive river discharge anomalies ([1σ, 2σ]) and negative river temperature anomalies (<-1σ relative to the 2000–2014 mean)

(Fig. 2. 8; Table 2. 2). In the summer of 2011 and 2012, large positive river discharge anomalies [1σ, 2σ] increased the 2011 nursery habitat at reaches D and E by more than 1σ. The 2012 nursery habitat increased at reach E by [1σ, 2σ] relative to the 2000–2014 mean (Fig. 2. 8; Table 2. 2). Although the 2011 and 2012 fall river discharge anomalies were less than the spring and summer, nursery habitat anomalies still increased by [1σ, 2σ] relative to the 2000–2014 mean at reaches D and E because the higher river discharge during the two previous seasons provided favorable areas for juvenile during the following fall and winter of 2012, when river discharge decreased.

The high river discharge seen during 2011 and 2012, provided juveniles with a higher nursery habitat for most of the upper reaches during all seasons except for summer 2014. Increased stream temperatures (+0.1.53 °C) relative to the 2000–2014 mean (M=19.75 °C) prevented higher nursery habitat at all reaches, except at reach E (Fig. 2. 8; Table 2. 2).

Reaches G, H: Large negative river discharge anomalies [-1σ, -2σ] relative to the 2000–2014 mean in winter 2010 and spring 2001 increased nursery habitat at reaches G and H by more than 1σ from the 2000–2014 mean. In contrast, large negative anomalies nursery habitat at these two reaches resulted by extreme positive river discharge anomalies at 2011(Fig. 2. 8; Table 2. 2).

2.3.6. Spring–neap effects on salmon habitat

The tidal amplitudes in the estuary (measured as the difference between maximum and minimum values of elevation in a given tidal day) change between 2–3.6 m (Chawla, 2007). Tidal ranges that are less than 2 m, between 2–3.2 m and more than 3.2 m, are

considered neap, transition, and spring tides, respectively. A one–way ANOVA test was conducted to compare the seasonal mean of nursery habitat in neap, transition, and spring cycles at 8 reaches. To meet the assumption of normality, the ANOVA and the Games–Howell post hoc (because of unequal group size) tests were done on log–transformed nursery habitat. Those tests were both used (suitable for unequal group size and variances) to distinguish between multiple pairs. The ANOVA and the Games–Howell tests comparisons were considered significant at p–values less than 0.05. Among the 8 Columbia River reaches, the results indicate that the nursery habitat response to the spring–neap tide varies.

There is a significant difference between the seasonal mean of nursery habitat for juvenile Chinook in neap, transition, and spring tide (p <0.05, ANOVA & Games–Howell test) at reaches A and B. Over transition and spring tide cycles, reaches A and B provide higher nursery habitat at neap tide for all seasons (Fig. 2. 9; Table 2. 3). Mean nursery habitat for reaches A and B at spring tide, decreases relative to the neap tide maximum by 40% and 36% in winter and by a minimum of 23% and 29% in spring, respectively. The seasonal mean of nursery habitat during transition tide, decreases relative to neap tide by less than 25% for all seasons at reaches A and B.

There is no significant difference between the nursery habitat mean for spring, transition, and neap tide cycles in winter, summer and fall at reach C. The relative percent changes in the Nursery habitat mean for spring–transition tides and transition–neap tides are less than 4% and 10%, respectively, for all seasons (Fig. 2. 9; Table 2. 3).

There is significant difference between the nursery habitat mean for different tidal cycles at reach D (p <0.05, ANOVA & Games–Howell test) for all seasons. In contrast

to reaches A and B, the nursery habitat mean at spring tide has the highest value for all seasons, relative to the neap tide. The maximum percent changes in the mean for nursery habitat during spring tide, relative to the neap tide, is about 60% in fall (Fig. 2. 9; Table 2. 3).

Nursery habitat mean does not vary significantly in spring and fall at reach E; however, it changes significantly (p <0.05, ANOVA & Games–Howell test) in winter and summer. Similar to the lower reaches of A and B, reach E provides more nursery habitat at neap tide than at spring and transition tide (Fig. 2. 9; Table 2. 3). Nursery habitat mean at spring tide decreases by 26% and 30%, relative to neap tide, in winter and summer, respectively.

Spring nursery habitat mean doesn not significantly change for different tidal cycles at reach F, but it changes significantly (p <0.05, ANOVA & Games–Howell test) in winter, fall, and summer. Accordingly, the nursery habitat mean at spring tide decreases by 22%, 16%, and 31%, relative to neap tide in winter, fall and summer. But, there is no significant difference (p <0.05, Games–Howell test) between the fall nursery habitat mean during the transition and spring tidal cycles (Fig. 2. 9; Table 2. 3).

The summer nursery habitat mean varies (p <0.05, ANOVA & Games–Howell test) during different tidal cycles at reach G. The summer nursery habitat mean at transition tide decreases by 20% and at spring tide by 34%, relative to the nursery habitat mean at neap tide, for reach G. The fall Nursery habitat mean varies (p <0.05, ANOVA & Games–Howell test) between spring and neap tides in such a way that the fall nursery habitats mean decreases by 12%, relative to the neap tide. Winter and spring nursery habitat mean don't seem to change significantly for different tidal cycles (Fig. 2. 9;

Table 2. 3). There is significant difference in nursery habitat mean (p <0.05, ANOVA & Games–Howell test) during winter and summer at reach H between spring and neap tidal cycles—so much so that the nursery habitat mean decreases by 15%, relative to the neap tide, for both seasons. During different tidal cycles, there isn't any significant difference in fall and summer nursery habitat mean (p <0.05, ANOVA) (Fig. 2. 9; Table 2. 3).

2.4. Discussion

2.4.1. Methodology for salmon habitat calculation

An important first step in evaluating salmon performance in the estuary is to characterize the available habitat. In this paper, we introduce a refined method for quantifying habitat for the different life stages of juvenile Chinook salmon. This method computes habitat based on volume instead of taking depth averages for all variables and calculating habitat based on area (Bottom et al., 2005; Burla, 2009).

Habitat calculated based on binary thresholds for temperature and salinity produced almost zero habitat in summer with no seasonal variability (Fig. 2. 4c). When we instead use penalty functions for temperature and salinity, more reasonable seasonal patterns emerged. A 15–year habitat analysis indicates that not only is habitat seasonally modulated by temperature at all reaches, but that less habitat is available in the summer and winter. In reach C, these findings are also supported with a higher mean density of juveniles in optimal temperatures and a lower mean density in suboptimal and stressful temperatures (Roegner and Teel, 2014).

In addition, we also quantify juvenile migratory habitat since the estuary not only provides rearing habitat, but also a transition corridor for larger juvenile to migrate from Bonneville Dam to the ocean. In migratory habitat quantification, by adding low oxygen penalty function to our habitat computation, we consider the impact of low dissolved oxygen water levels brought in from the coastal upwelling event into the estuary. However, we don't consider low dissolved oxygen impacts from the riverside because except for some spikes, the dissolved oxygen levels are above 85% and 70% saturation at SATURN05 (46.18 N, 123.18 W, Depth= 2.5 m) and SATURN06 (45.51 N, 122.66 W, Depth= 0.5 m), respectfully, from 2009 to present, which are not stressful levels for salmon (Roegner et al., 2011).

2.4.2. Nursery and migratory habitat

Using the multi–variable metrics, we quantified juvenile Chinook salmon habitat for years 2000–2014. Our results illustrate that the estuary provides more migratory habitat than nursery habitat for 4 sizes of juvenile Chinook at all reaches. The shallows of the estuary offer critical, but limited and sensitive refuge. While reaches D, E, and G provide the least amount of nursery habitat, reaches C and F offer the most nursery habitat compared to other reaches, though the size of the habitat is relatively small: a maximum of about 7% at reach C and F in spring (Fig. 2. 5). The extent and recurrence of these refuges are controlled by depth criterion that is influenced by river discharge. The calculated shallow water ($0.5 \leq D \leq 2$ m) volume for all reaches confirms that reaches D, E, and G contain the lowest shallow water volume due to the reaches' bathymetry (Fig. 2. 5). It is important to note that all reaches provide an abundance of

migratory habitat. For example, a maximum of about 37% at reach B can be found during the spring for juveniles.

2.4.3. Sensitivity of salmon habitat to life stage

Extensive effort has gone into calculating habitat using velocity criterion (Bottom et al., 2005; Burla, 2009). In this study, we not only consider velocity criterion in nursery habitat computation, but we also classify nursery habitat for different juvenile Chinook salmon sizes based on their ability to swim at different stream flow velocities. Scientific literature indicates that larger fish tolerate high stream velocity better than smaller sizes. Based on the velocity thresholds for different sizes, the estuary provides more nursery habitat for fingerlings than it does for emergent or resident fry at specific reaches. We find that nursery habitat increases slightly in the shallow areas of reaches B, D, and H, with no change at C and F, and with significant change at reach G (Fig. 2. 6).

The difference in nursery habitat availability for various sizes of juveniles at different reaches is related to the velocity found in shallow water ($0.1 \leq D \leq 2$ m). To analyze the velocity gradient impact on nursery habitat at each reach, we calculated water volume based only on individual velocity criterion at depths between 0.5–2 m and depths greater than 2 m. We found that water volume rises when velocity increases at depths greater than 2 m; however, we found that water volume also slightly rises in the shallow areas of reaches B, D, and H, with no change at C and F, and with significant change at reach G. This means that there is more shallow water volume with a velocity <1 m/s than there is shallow water with a velocity <0.4 m/s at reach G. The shallow water has a higher velocity gradient at reach G when compared with other reaches, and it is here

that we see nursery habitat differ dramatically between juvenile sizes. The geometry and topography of each reach are the main factors that contributing to stream velocity.

2.4.4. Nursery and migratory habitat variability and anomalies

Characterizing seasonal and inter–annual variability of habitat for years 2000–2014 represents strong spatial and temporal variability in nursery habitat and reflects the prevailing dynamic balance between river and ocean influences on the estuary. In contrast, migratory habitat has almost no temporal variability over the 15 years. While nursery habitat in most of the upper reaches are most responsive to river discharge, it appears that nursery habitat at reaches A and B is more responsive to the tidal range. Nursery habitat responds positively to the freshet at reaches A through F and negatively at reaches G and H (Fig. 2. 7, 2. 9). The reason for this behavior is that nursery habitat is strongly controlled by depth criterion, which is moderated largely by river discharge at the upper reaches and by the tide at reaches A and B.

A review of seasonal nursery habitat anomalies for years 2000–2014 reveals that a high positive river discharge anomaly (more than 1σ from the 2000–2014 mean) in winter 2011 increased nursery habitat slightly only at reach D. Additionally, high positive river discharge anomalies during spring and summer 2011, as well as a relatively high and early freshet in 2012, provided juveniles with a higher nursery habitat at reaches D, E, F; in contrast less nursery habitat was available at reaches G and H during this time. In some reaches, the high river discharge from 2011 continued to provide ample nursery habitat for juveniles the following year, even when river discharge had decreased (Fig.

2. 8). In contrast, high negative river discharge anomalies during spring and summer 2001, reduced nursery habitat dropped in 2001 at reaches A through F, but increased at reaches G and H. An exception was found in fall 2004 where we didn't find any high positive or negative anomalies for ocean or river forcing that led to a high negative nursery habitat.

Inter–annual variability of ocean temperature for all seasons appears to be mostly determined by the variability in PDO and ENSO. High negative or positive winter and spring anomalies (less than -1σ or more than 1σ from the 2000–2014 mean) in ocean temperature control nursery habitat at reaches A and B—cooler ocean temperatures during 2008 and 2009, decreased nursery habitat, and warmer ocean temperatures during 2003, increased nursery habitat. Low ocean temperature variability ([-1σ, 1σ]) during summer and fall however, does not seem to have any influence on nursery habitat at reaches A and B. In addition, upwelling variability doesn't seem to impact nursery habitat.

2.4.5. Sensitivity of salmon habitat to spring–neap tide

Our analyses show that nursery habitat responds to the tidal regime differently across 8 reaches. In the lower estuary, where reaches A and B are most influenced by tidal regime, neap tide (tidal range less than 2 m) provides more nursery habitat. The rearing area decreases significantly during transition and spring tide. It appears that neap tide provides more shallow water refugee for juveniles, and with increasing in tidal range, these two reaches lose their nursery habitat in transition tide by for all seasons (Fig. 2. 9; Table 2. 3).

Nursery habitat responses to spring–neap tide with the same pattern at other reaches; however, depending on the tidal regime, the nursery habitat may decrease from neap tide significantly during some seasons or remain constant. The impact of various tidal regimes decreases in spring season at upper reaches due to freshet (Fig. 2. 9; Table 2. 3). Only at reach D, spring tide provides higher nursery habitat for all seasons. This may be due to reach D having the lowest value of nursery habitat and higher tidal ranges providing more shallow water area (Fig. 2. 9; Table 2. 3). The various regional nursery habitat responses to the tidal range are the result of the different bathymetry of each reach.

2.5. Conclusion

Quantification of habitat is critical to enhancing decision–making to preserve and recover salmon through optimization of hydropower systems and navigation channels, as well as ecosystem restoration. In this paper, we present a refined method for quantifying estuarine nursery and migratory habitat. Although we quantify habitat for juvenile Chinook salmon, the methodology can be used to compute habitat for other species that have defined thresholds in a defined reach.

We characterized 15 years (2000–2014) of quantified habitat over 8 reaches at the Columbia River estuary and investigated the seasonal and inter–annual variability and anomalies of habitat. We also acknowledge how river and ocean forcing variability can influence habitat in the Columbia River estuary. Contemporary system analyses provide a baseline for predicting the vulnerability of the system relative to future changes in climate, navigation channel bathymetry, and flow regulation.

It is important to recognize that even with an extensive methodology to identify estuarine habitat, we are unable to predict salmon performance in the estuary. Based on the member/vagrant hypothesis, biological interaction, competition, food availability, existence of prey and the prevalence of disease also influences the performance of salmon.

Tables

Table 2. 1. Seasonal mean and range of daily Coefficient of Variation in nursery habitat for emergent fry at 8 reaches, river discharge and temperature at Bonneville Dam, continental shelf temperature, and tidal range at Tongue Point (2000-2014).

		Winter		Spring		Summer		Fall	
Variable	**R**	**Mean**	**Range**	**Mean**	**Range**	**Mean**	**Range**	**Mean**	**Range**
	A	20.4	19.1	12.1	18.0	14.0	14.7	15.7	27.6
	B	23.7	22.0	10.5	16.8	20.7	21.5	17.3	32.3
	C	32.0	41.6	16.1	25.2	23.4	33.5	27.4	52.4
Nursery	D	**60.30**	90.8	**75.5**	108.1	43.7	81.2	47.1	73.8
Habitat	E	**82.5**	41.2	**100.6**	82.9	**86.0**	24.9	**80.7**	51.9
(m^3)	F	49.6	46.4	40.6	32.3	42.5	60.0	50.0	73.7
	G	31.7	26.2	47.9	31.8	33.5	44.9	19.5	26.5
	H	48.6	34.4	**87.0**	60.4	32.6	71.2	16.4	42.6
RD (m^3/s)		23.1	17.8	30.0	17.6	23.0	31.0	13.8	17.7
T (Bon) (°C)		21.1	23.0	8.7	7.7	5.5	3.4	11.6	17.4
T(Oc) (°C)		5.3	2.9	7.7	5.3	9.3	6.6	6.3	10.4
TR (m)		14.8	19.2	17.0	21.5	14.4	21	17.0	22

R - Reach
RD - River discharge at Bonneville Dam (from observations used to force simulations)
T(Bon) - Temperature at Bonneville Dam (from observations used to force simulations)
T(Oc) - Temperature at the bottom of the Pacific Ocean continental shelf, about 13 km off the mouth of the Columbia River (from simulations)
TR - Tidal Range at Tongue Point, calculated based on the difference between the maximum and minimum values of elevation within a tidal day (from simulations).

Table 2. 2. Seasonal mean and standard deviation (SD) of log-transformed nursery habitat for emergent fry at 8 reaches, river discharge at Bonneville Dam, temperature at Bonneville Dam, ocean temperature, and tidal range at Tongue point for years 2000-2014.

		Winter		Spring		Summer		Fall	
Variable	**R**	**Mean**	**SD**	**Mean**	**SD**	**Mean**	**SD**	**Mean**	**SD**
	A	7.16	0.11	7.34	0.06	7.25	0.07	7.28	0.10
	B	7.38	0.14	7.63	0.05	7.44	0.12	7.54	0.13
	C	7.25	0.23	7.54	0.08	7.37	0.15	7.36	0.25
Nursery	D	4.77	0.27	5.17	0.27	4.60	0.22	4.81	0.21
Habitat	E	5.86	0.30	6.17	0.30	6.00	0.30	6.03	0.30
(m^3)	F	7.04	0.35	7.36	0.18	7.11	0.30	7.07	0.47
	G	5.81	0.17	5.83	0.26	5.93	0.23	6.15	0.17
	H	6.26	0.26	6.10	0.33	6.40	0.25	6.63	0.17
RD (m^3/s)		3.64	0.1	3.85	0.14	3.60	0.16	3.54	0.08
T (Bon) (°C)		0.70	0.12	1.30	0.11	1.01	0.03	1.00	0.17
T(Oc) (°C)		1.05	0.03	0.97	0.03	1	0.04	0.98	0.03
TR (m)		0.42	0.07	0.42	0.08	0.43	0.07	0.43	0.08

R - Reach
RD - River discharge at Bonneville Dam (from observations used to force simulations)
T(Bon) - Temperature at Bonneville Dam (from observations used to force simulations)
T(Oc) - Temperature at the bottom of the Pacific Ocean continental shelf, about 13 km off the mouth of the Columbia River (from simulations)
TR - Tidal Range at Tongue Point, calculated based on the difference between the maximum and minimum values of elevation within a tidal day (from simulations).
SD - Standard deviation

Table 2. 3. 2000-2014 Mean nursery habitat for emergent fry for 8 hydrogeomorphic reaches of the Columbia River estuary, separated by season and tidal cycle (spring and transition). Units are percentage of the nursery habitat at neap tidal cycle at each reach.

		Winter		**Spring**		**Summer**		**Fall**	
Variable	**R**	**T**	**S**	**T**	**S**	**T**	**S**	**T**	**S**
	A	-21.1	**-35.7**	-16.8	-28.8	-17.0	**-30.7**	-18.7	**-32.6**
	B	-24.6	**-39.5**	-15.1	-23.4	-24.3	**-37.2**	-18.6	**-31.6**
	C	-4.3	-10.8	3.8	8.6	-1.3	-4.6	3.1	3.8
Nursery	D	12.5	**-35.0**	16.7	**46.6**	-6.6	24.6	22.0	**60.0**
Habitat	E	-16.2	-26.1	-1.2	0.7	-15.8	-29.8	1.3	-0.4
(m^3)	F	-13.0	-22.4	-5.0	-6.3	-14.8	-31.1	-6.7	-16.8
	G	-5.2	-5.9	0.7	-1.3	-19.7	-33.6	-3.6	-12.4
	H	-11.6	-15.4	-2.9	-4.6	-1.4	-15.3	-0.7	-1.9

R - Reach

T - (nursery habitat at transition tidal cycle- nursery habitat at neap tidal cycle)/ nursery habitat at neap tidal cycle)*100

S - (nursery habitat at spring tidal cycle- nursery habitat at neap tidal cycle)/ nursery habitat at neap tidal cycle) *100

Figures

Figure 2. 1. Juvenile Chinook salmon performance depends on criteria that include population structure and life history, habitat opportunity (access), and habitat capacity (quality and quantity) criteria, all of which are influenced by regional physical factors (adapted from Bottom et al. 2005).

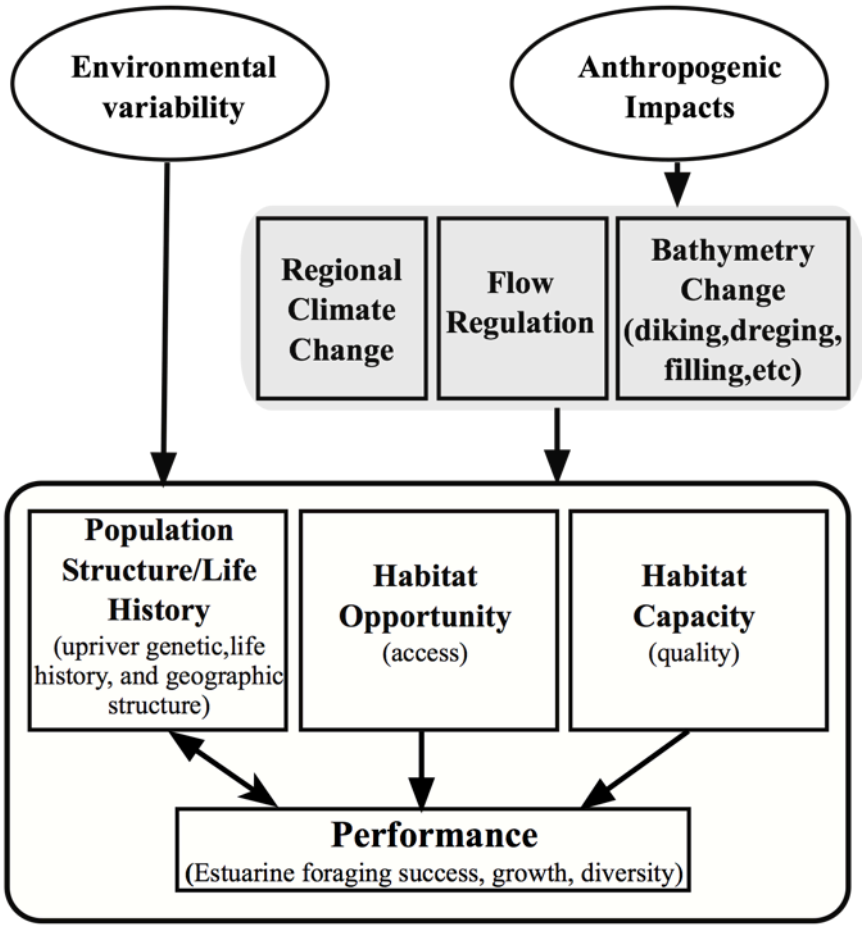

Figure 2. 2. Horizontal view of unstructured grid for Columbia River estuary and shelf, extending from Bonneville dam to the Pacific Ocean with 8 hydrogeomorphic reaches of the Columbia River Estuary Ecosystem Classification (Simenstad et al., 2011b). (a) The full extent of the model domain, from California to British Columbia; (b) zoom-in of the Columbia River estuary; (c) coastal lowlands entrance mixing and coastal uplands salinity gradient; (d) volcanic current reversal, Western Cascades tributary confluences, and tidal flood plain basin constriction; (e) middle tidal flood plain basin; (f) upper tidal flood plain basin and Western Gorge.

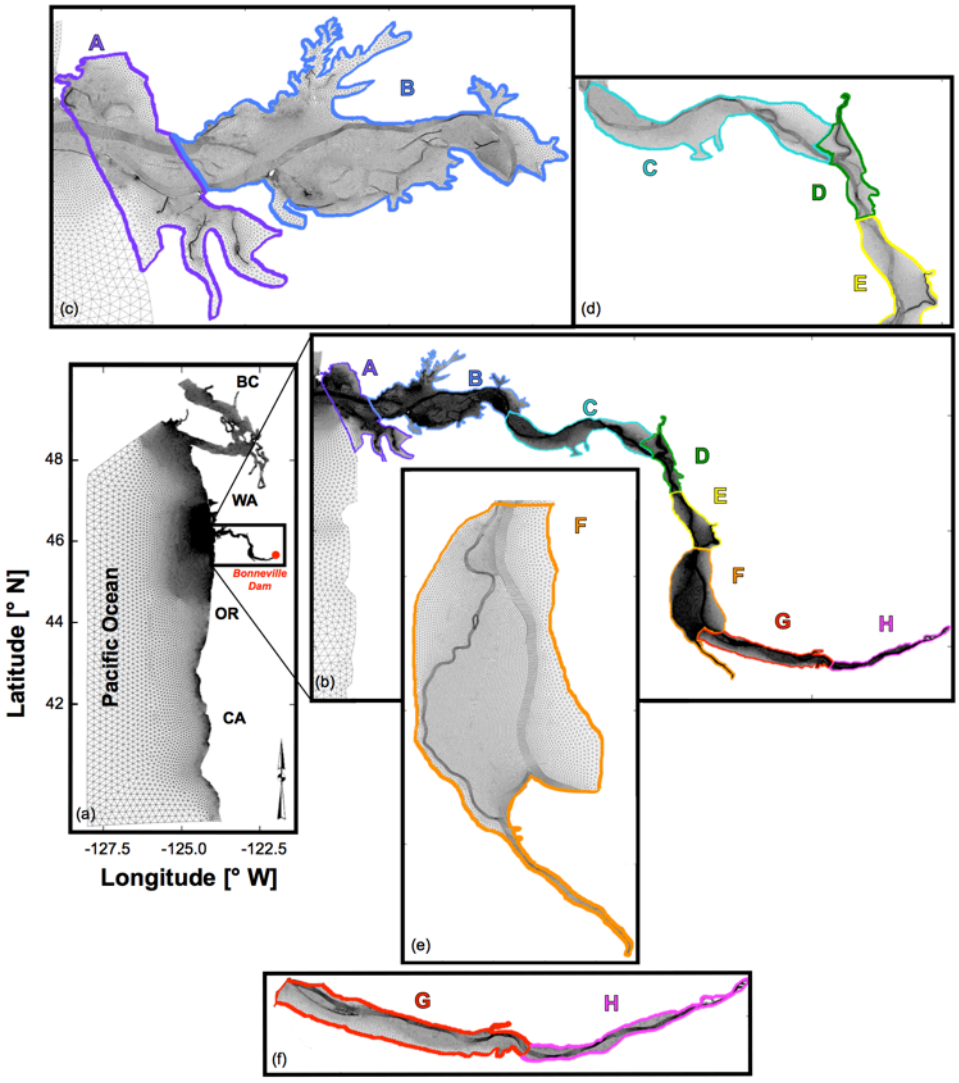

Figure 2. 3. Schematic representation of the method used to determine juvenile Chinook salmon habitat. The method distinguishes between (a) nursery and (b) migratory habitat, and operates through a combination of thresholds and penalty functions. For nursery habitat, the method distinguishes between four life stages through the velocity threshold

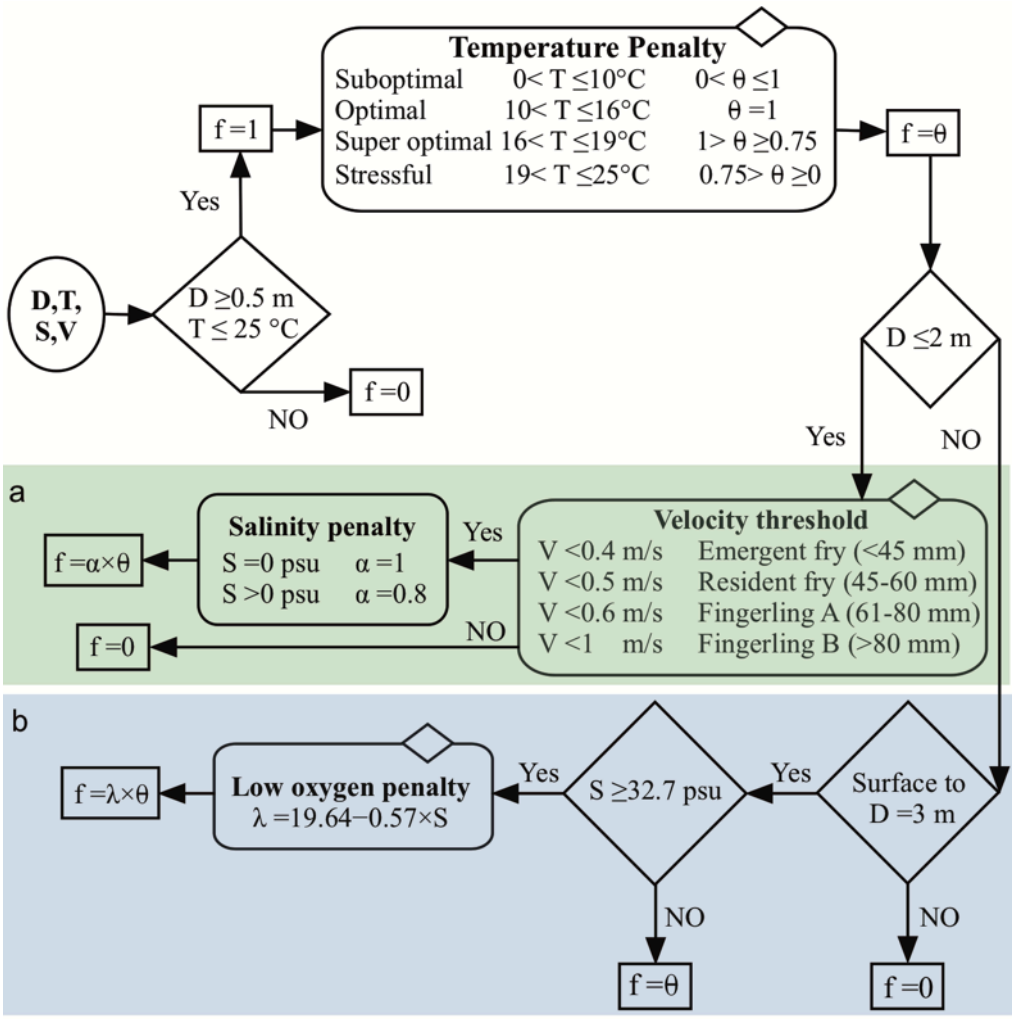

Figure 2. 4. Illustration of the effect of the changes introduced in the habitat criteria, for 2011 time series of daily averaged values of either PHO (Bottom et al., 2005) or salmon habitat (as in this work). (a) Contrast between area- (blue) and volume-based (orange) calculations of PHO. (b) Effect of using different threshold velocities on the calculation of volume-based PHO. (c) Contrast between volume-based PHO and nursery habitat tailored for emerging fry (v<0.4m/s). (d) Comparison of nursery habitat for emerging fry, migratory habitat, and total habitat.

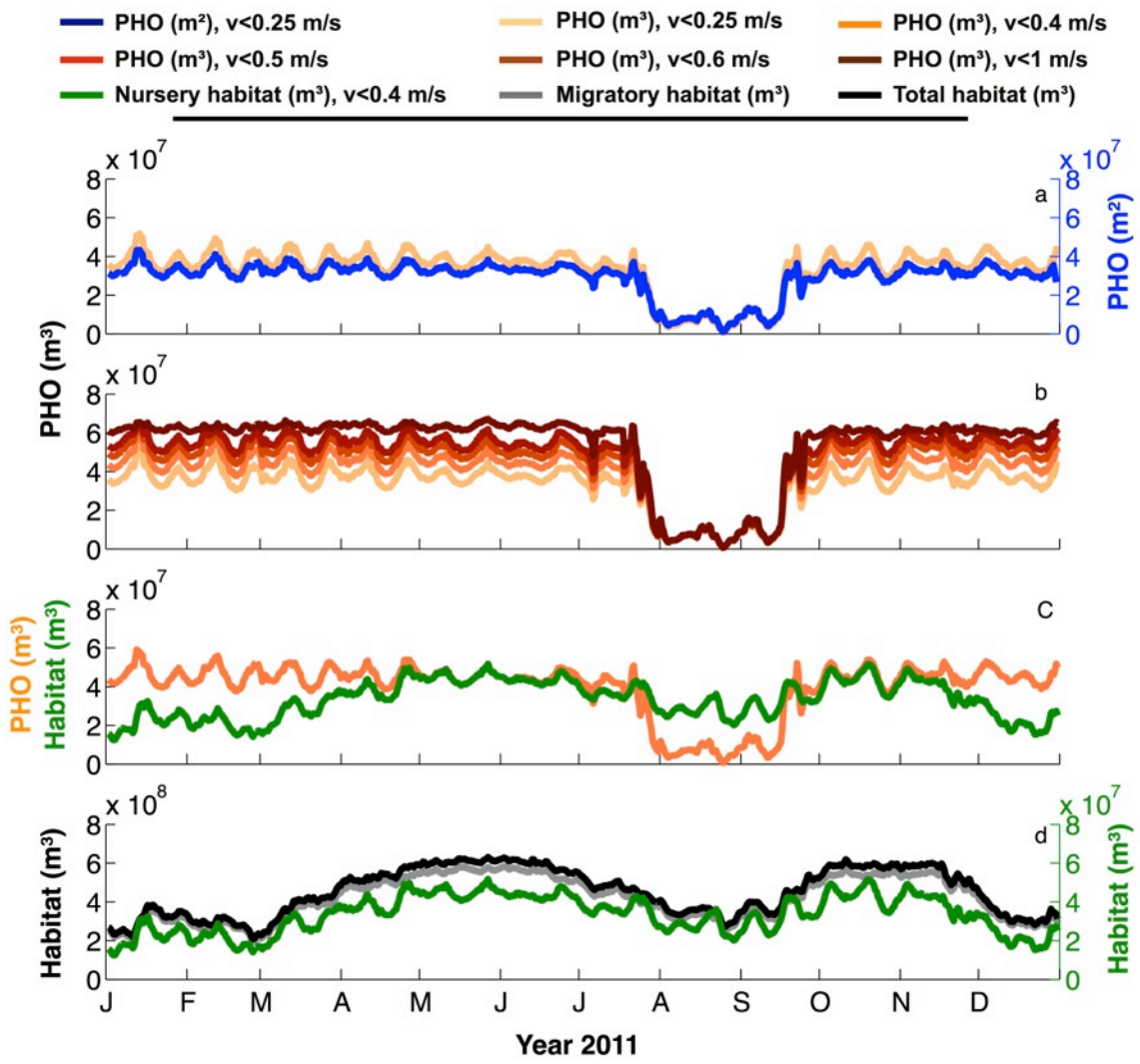

Figure 2. 5. 2000-2014 Mean habitat for each of the 8 reaches of the estuary, separated by season and habitat type (migratory versus nursing habitat for emerging fry). Units are percentage of the total volume of the reach. Here and in other figures, seasons are defined as follows: Seasons: W = winter (Jan, Feb, Mar); Sp = spring (Apr, May, Jun); Su = summer (Jul, Aug, Sep); F = fall (Oct, Nov, Dec)

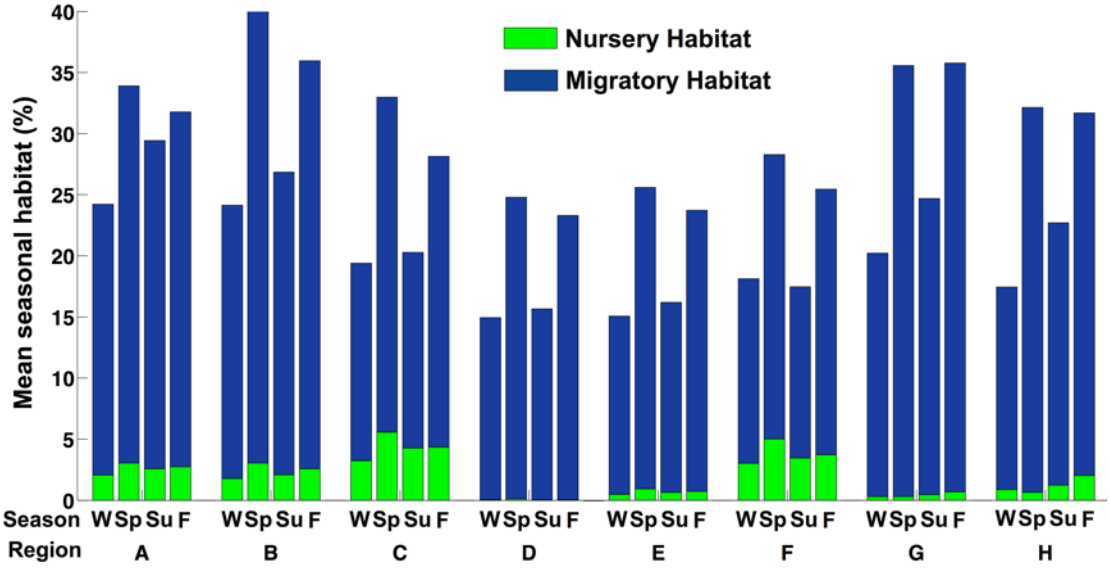

Figure 2. 6. 2000-2014 Mean habitat for each of the 8 reaches of the estuary, separated by season and life stage (resident fry, fingerling A, and fingerling B). Colored by percentage change of the nursery habitat for emergent fry of the reach. X-axis: 1: ((Resident fry-emergent fry)/emergent fry)*100; 2: ((Fingerling A-emergent fry)/emergent fry*100; 3: (Fingerling B-emergent fry)/emergent fry)*100.

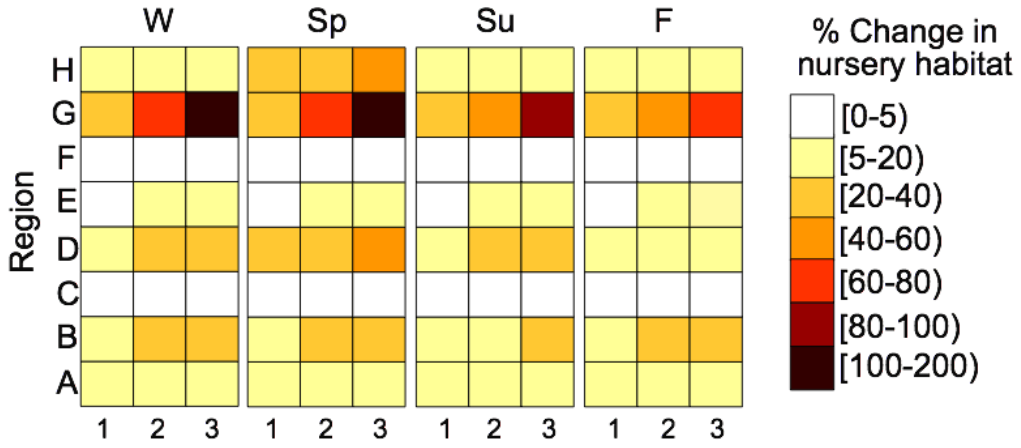

Figure 2. 7. Climatology of: (a) nursery habitat for emergent fry at each reach; (b) river; (c) water temperature at Bonneville Dam; (d) ocean temperature; (e) nursery habitat for resident fry at each reach; (f) nursery habitat for fingerling A at each reach; and (g) nursery habitat for fingerling B at each reach. The statistics are computed for 2000-2014**.** Individual years referred in text are displayed as colored lines.

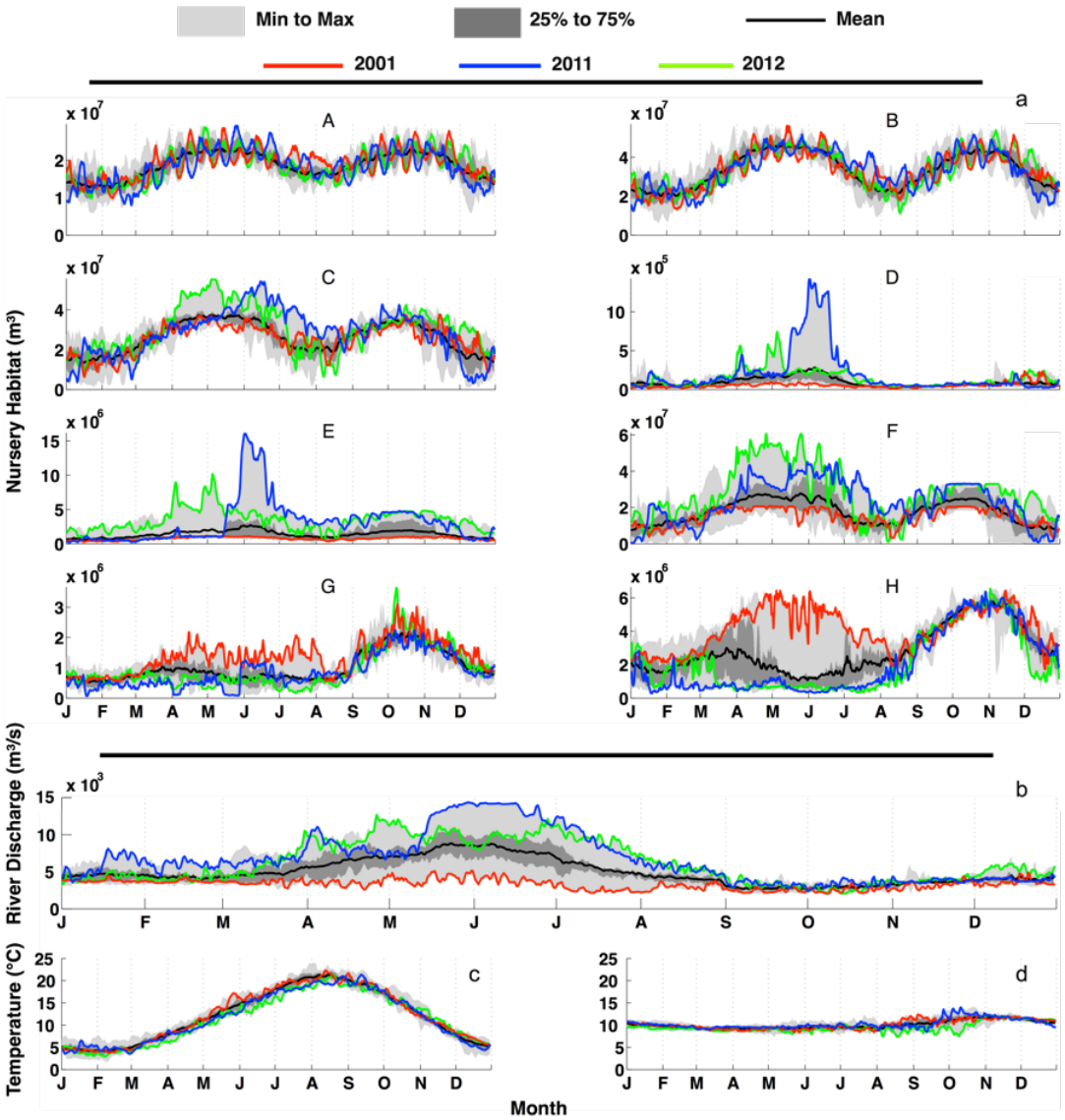

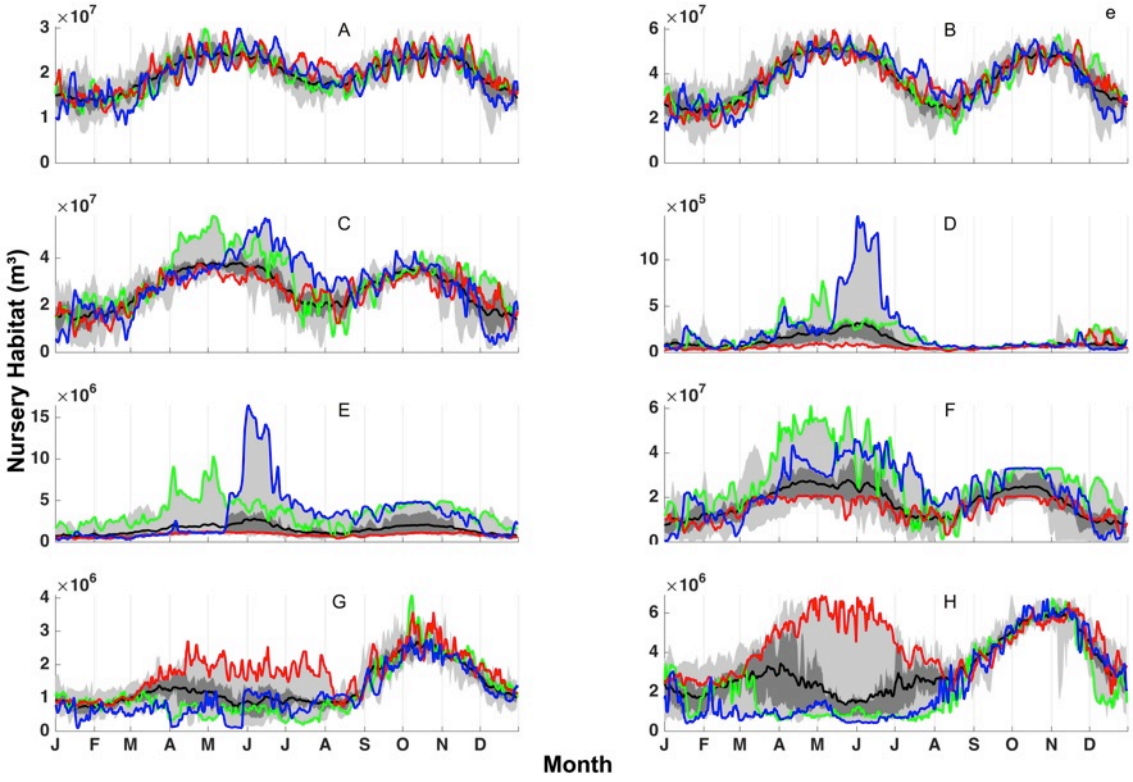
A
B
C
D
E
F
G
H
e
Nursery Habitat (m³)
Month
J F M A M J J A S O N D

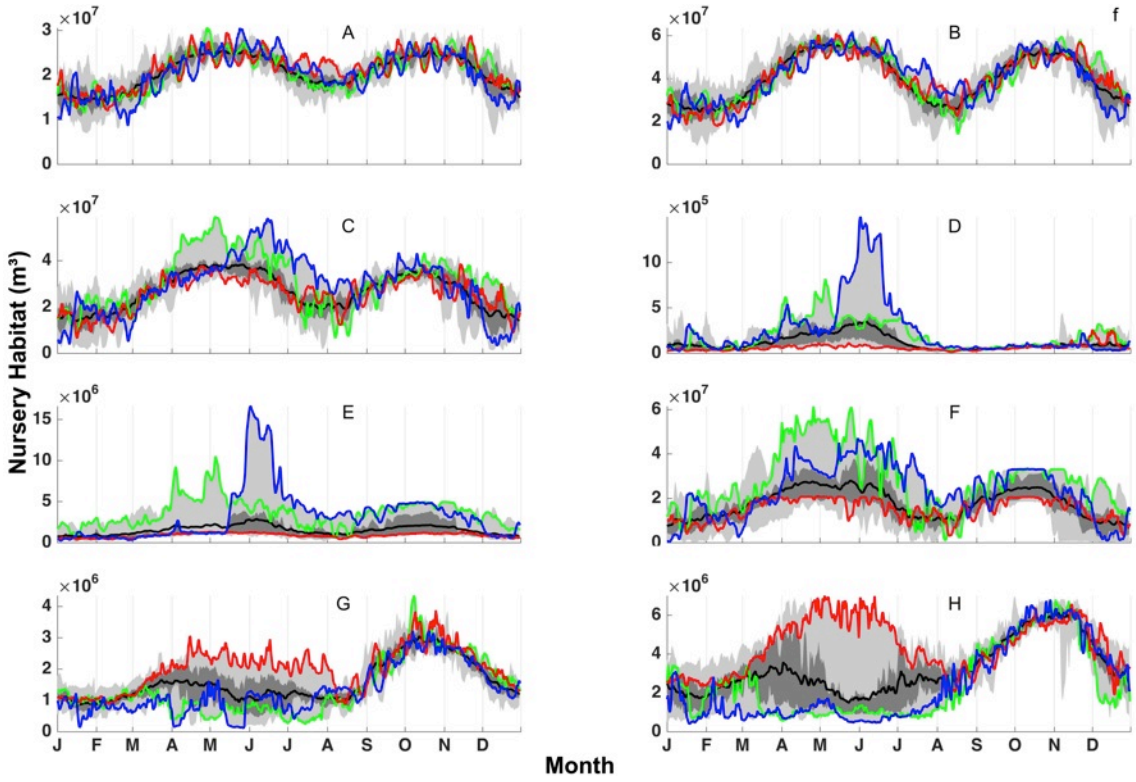
Nursery Habitat (m³)
A
B
C
D
E
F
G
H
f
×10⁷
×10⁵
×10⁶
J F M A M J J A S O N D
Month

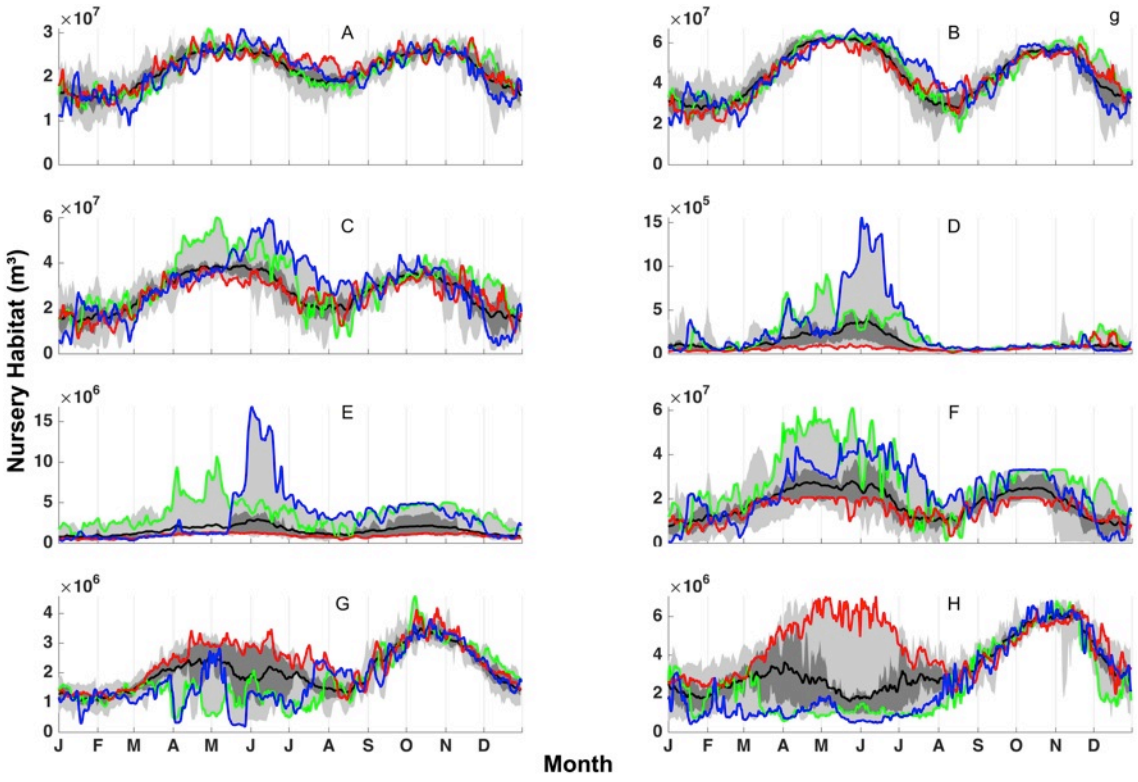
A
B
g
C
D
E
F
G
H
Nursery Habitat (m³)
Month
J F M A M J J A S O N D

Figure 2. 8. Z-scores of nursery habitat for emergent fry at all reaches of the estuary, for the four seasons and contextualized by: Z-scores of river discharge at Bonneville Dam (RD (BON)), temperature at Bonneville Dam (T (BON)), tidal range (TR) and ocean temperature (T); and values of the seasonal averages of the Cumulative Upwelling Index (CUI) divided by 100, the Pacific Decadal Oscillation (PDO), and the El Niño–Southern Oscillation (ENSO)

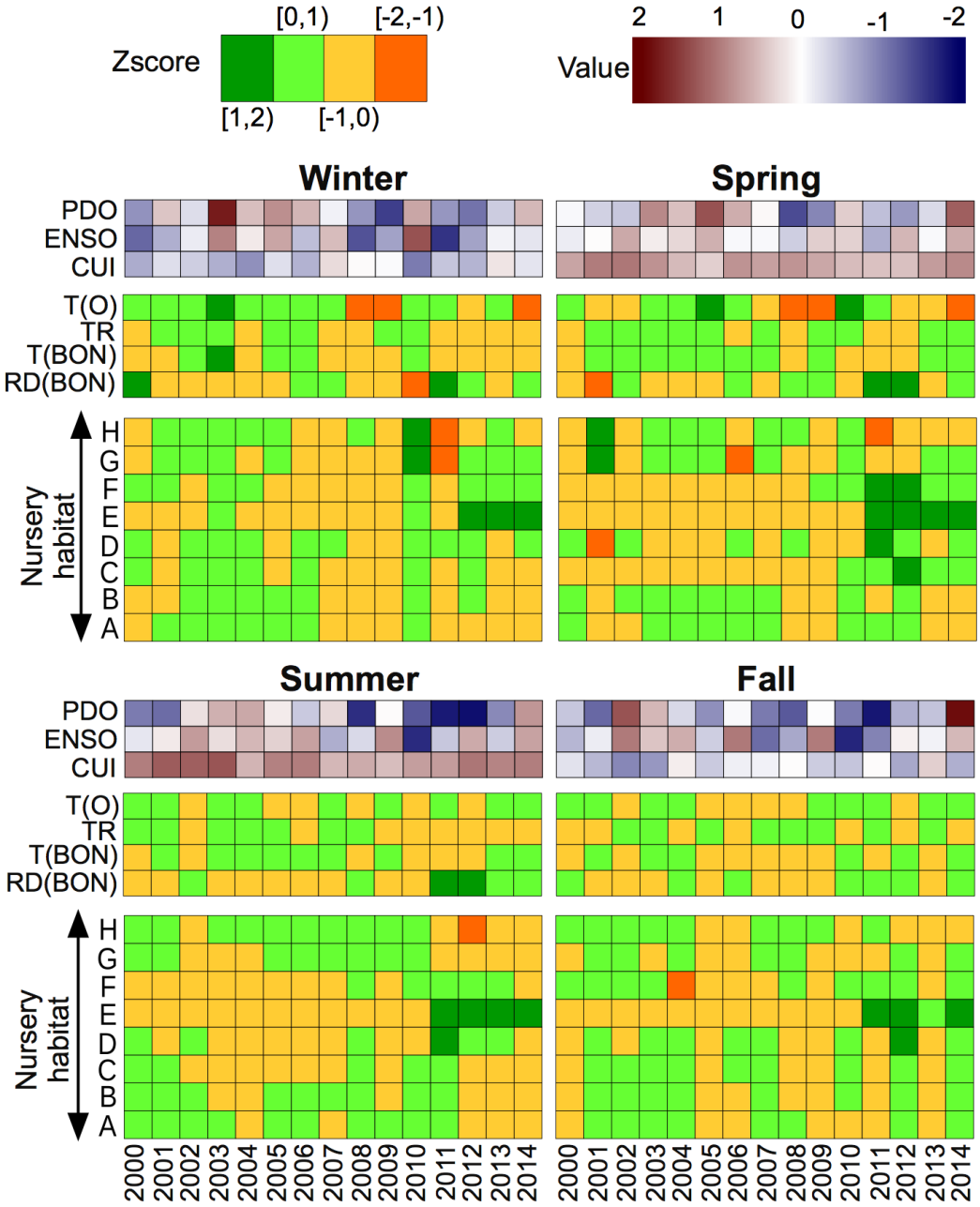

Figure 2. 9. 2000-2014 Mean nursery habitat for emergent fry for 8 reaches of the estuary, separated by season and tidal cycle (spring and transition). Colored by percentage of the nursery habitat at neap tidal cycle at each reach. X-axis: 1: ((nursery habitat at transition tidal cycle- nursery habitat at neap tidal cycle)/ nursery habitat at neap tidal cycle) *100; 2: ((nursery habitat at spring tidal cycle- nursery habitat at neap tidal cycle)/ nursery habitat at neap tidal cycle) *100.

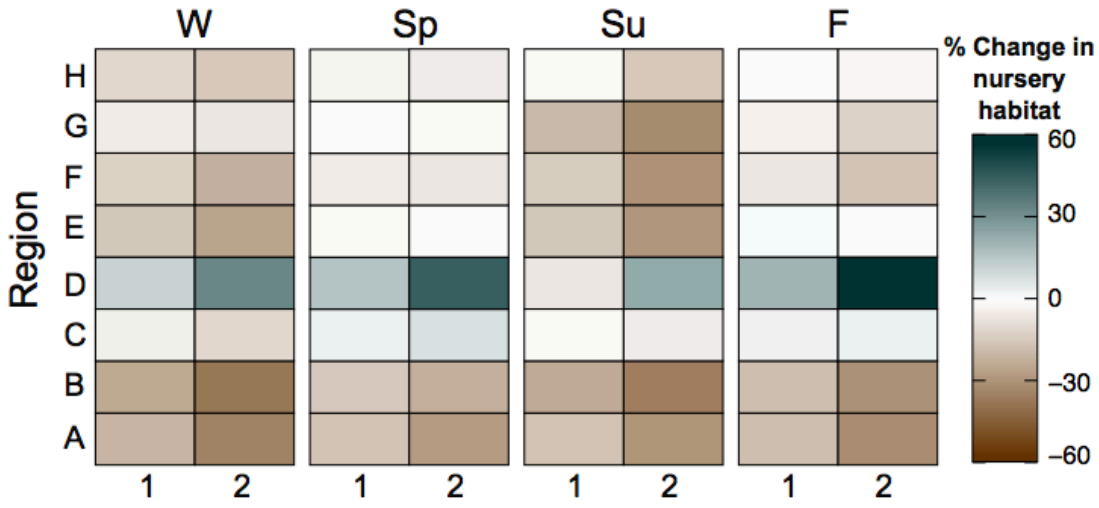

Chapter 3

Potential impacts of a large Cascadia Subduction Zone earthquake in the Columbia River estuary: a habitat perspective[2]

[2] I would like to thank Dr. George R. Priest from the Oregon Department of Geology and Mineral Industries for providing a post-deformation bathymetry map resulting from a large Cascadia Subduction Zone earthquake. I would also like to thank Paul Turner for conducting simulations needed for this research.

A version of this chapter will be submitted to Estuarine, Coastal and Shelf Science.

Abstract

The Columbia River estuary has historically provided important nursery habitat, food resources, and transition zones for salmonids. However, the structural and functional attributes of the estuary have been substantially altered by navigation improvements, hydropower operations and other regional activity, as well as by large-scale climate system and change, to the point that multiple salmon stocks are now listed as either endangered or threatened under the Endangered Species Act. As expensive recovery efforts are being conducted, the possible implications of those efforts for a large Cascadia Subduction Zone (CSZ) earthquake are pertinent, but poorly understood. To characterize estuarine physics and habitat changes in response to a CSZ event, we conduct numerical simulations of river-to-ocean circulation. From these simulations, we extracted year-round habitat indicators, including salinity intrusion length, shallow water habitat, and juvenile Chinook salmon habitat. Using these indicators, we compare contemporary conditions and a future scenario resulting from the subsidence due to a large CSZ earthquake. Results suggest the potential changes in estuarine circulation will be significant, with associated implications for aquatic species habitat. The annual mean of salinity intrusion length and plume volume increase by 50% and 38%, respectively, and the estuary loses 94% of fresh water habitat. Parts of the lower estuary lose shallow water habitat and juvenile Chinook salmon habitat by a yearly average of 42% and 34%, respectively, while further inside the estuary shallow water habitat and juvenile Chinook salmon habitat increased by as much as a yearly average of 29% and 50%. The magnitude of these changes suggests that CSZ earthquake scenarios should be

accounted for in long-term plans to restore habitat and increase the abundance, diversity and resiliency of salmon populations.

3.1. Introduction

Multiple Columbia River salmon stocks are listed as either endangered or threatened under the Endangered Species Act due to factors such as installation and operation of navigation and hydropower projects, irrigation, ocean conditions and climate change (Bottom et al., 2011; Bottom et al., 2005; Dalton et al., 2013; Ford, 2011; Mantua et al., 2010; Mantua et al., 1997). The estuary's circulation patterns, sediment transport, and habitat formations have also been affected by many jetties, pile dikes, tide gates, docks, and other structures that have been added to the system throughout the years (Bottom et al., 2005; Burla, 2009). As an example of the impact, the total area of tidal wetlands in the lower estuary has been decreased by more than 50% by diking, filing, and other development activities (Bottom et al., 2011).

While some expensive monitoring and restoration efforts have been conducted to preserve salmon habitat (Borde et al., 2012; Coleman et al., 2013; Roegner et al., 2012; Sagar, 2012; Thom et al., 2013), the possible impact of the subsidence associated with a large Cascadia Subduction Zone (CSZ) earthquake has not been considered.

Measurements of deformation and geological records show the potential of disastrous earthquakes along the CSZ area (Atwater, 1987; Atwater and Hemphill-Haley, 1997). The last major earthquake on the Cascadia mega-thrust occurred in A.D. 1700 with an estimated of M_w (moment magnitude) of 8.8-9.2, creating a coseismic subsidence of 1.67±0.75 m (mean ± standard deviation) in the Columbia River estuary (Atwater,

1988; Atwater, 1994; Leonard et al., 2004; Peterson et al., 1997; Peterson et al., 1993; Peterson and Madin, 1997; Satake et al., 1996. This type of large subsidence is likely to create significant changes in the Columbia River estuary and river mouth bathymetry, thus affecting the estuarine ecosystem and species habitat. While the subsidence will rebound over time, it took nearly a century for full rebounding from the A.D. 1700 earthquake in Tofino, British Columbia (Hughes et al., 2002)—hence effects will likely be long-lasting.

Several studies along the Oregon coast have shown sudden changes in food availability, migration, and nursing patterns that may be related to marsh subsidence resulting from the historic 18th century CSZ earthquake (Minor and Grant, 1996). Subsidence from the 1700 A.D. earthquake impacted the Coquille communities, the Tillamooks, Makahs, Yuroks, and many other native tribes and forced them to move their fishing dikes in order to adjust to the tideland changes and new fish habitat (Byram, 1999). Conversely, some research indicates that the land subsidence resulting from the 1960, M_w 9.5 Chilean earthquake provided a wetland with high biodiversity (Corti and Pablo Schlatter, 2002; Lagos et al., 2008; Reinhardt et al., 2010).

For our research, we evaluated regionally accepted indicators, including salinity intrusion length (SIL, km), plume volume (PV, m^3), shallow water habitat (SWH, m^2), and juvenile Chinook salmon habitat (SH, m^3). When accounting for a CSZ seismic subsidence, such indicators can provide proxy information on salmon relevant changes in state and variability of the estuary. We use a baroclinic circulation model, SELFE (Zhang and Baptista, 2008), to contrast contemporary estuarine conditions with conditions after a future large CSZ earthquake.

3.2. Method

3.2.1. Estuarine habitat: relevant indicators

3.2.1.1. Salinity Intrusion Length

Salinity distribution inside the estuary (which results from the interaction between tides and stream flow) influences fish distribution, estuarine vegetation, and food web (Maier and Simenstad, 2009; Sagar, 2012; Simenstad et al., 2011; Teel et al., 2014). Also, ocean-type salmon adapt to saltwater before moving from the estuary out to the ocean (Bottom et al., 2005); therefore, assessing both the maximum upriver distance of salinity intrusion in the contemporary system, as well as the response to a large CSZ earthquake, is essential. We computed SIL that shows the magnitude of ocean influences in the estuary as the maximum length of salinity at one practical salinity unit (psu) measured along the south channel relative to the mouth. We also compute salt volume (SV, m^3.psu) as the integration of salinity over the volume of estuary that is under ocean influence.

3.2.1.2. Plume Volume

Recent studies show that the Columbia River plume not only plays an important role in fish distributions in the shelf (De Robertis et al., 2005; Morgan et al., 2005), but also in the survival of salmon and steelhead during out-migration (Burla et al., 2010; Miller et al., 2013; Miller et al., 2014). Many stream type of yearling salmonids (e.g. yearling coho salmon [*Oncorhynchus kisutch*], Chinook salmon [*O. tshawytscha*], chum salmon [*O. keta*], and steelhead trout [*O. mykiss*]) start to migrate out from the estuary by taking

advantage of the high river flows during late spring and late summer and tend to stay in the low-salinity plume and frontal regions for hours to a few days (De Robertis et al., 2005). Also subyearling Chinook salmon appeared to have higher densities at the Columbia River shelf during strong ebb tide currents (Emmett et al., 2004). Smolt-to-adult returns (SARs) for steelhead positively correlate with plume volumes in May and June (Burla et al., 2010). In addition, SARs for Snake River sp/su Chinook salmon (listed as a threatened species under the Endangered Species Act in 1992) at lower Granite Dam highly correlate with plume area from April to July for years 1999 to 2008, except for years 2001 and 2005 (dry years) (Miller et al., 2014). Therefore, we computed PV in this study to characterize the Columbia River freshwater input into the Pacific Ocean and its role to salmon migration. Following Burla et al. 2010, PV was calculated as the volume of water at the Oregon and Washington continental shelf where salinity is less than 28 (psu).

3.2.1.3. Shallow Water Habitat

Juveniles except chum and some fall Chinook that leave estuary directly, tend to use shallow water areas in the lower estuary as rearing habitat until they become larger and migrate to the ocean (Bottom et al., 2005). The stomach contents of fish in the estuary reveal that they consume food resources produced in the wetland and shallow water areas (Diefenderfer HL, 2012). The loss of wetlands and related food and refuge has influenced salmon and steelhead recovery (Bottom et al., 2005; Maier and Simenstad, 2009). We chose a shallow water habitat (SWH, m^2) indicator to evaluate how changes in bathymetry, due to a large CSZ earthquake, influences shallow water areas. To capture the area of SWH (areas within water depths between 0.1 to 2 m), we used the

elevations at 65 points along the navigation channel during a tidal day. To compute the elevation for other estuary elements, we extrapolated the elevation from the navigation channel points to the nearby part of the grid and then calculated the area for each reach that met the shallow water criterion.

3.2.1.4. Salmon Habitat

Spatial and temporal patterns of juvenile Chinook salmon habitat (SH, m^3) were also quantified. We used a refined method of habitat computation (Chapter 2) that is based on a semi-empirical indicator—physical habitat opportunity—which has been used in the estuary to quantify and support regional decisions for over a decade (Bottom et al., 2005; Burla, 2009). SH was computed based on the water volume that met specific thresholds (extracted from fisheries data) for water depth and 3D fields of velocity, salinity, and temperature (Rostaminia et al., 2017). We calculated nursery habitat, where depth is less than 2 m for juvenile Chinook salmon at the emergent fry stage (<45 mm), by applying velocity thresholds for emergent fry (v <0.4 m/s). Also, to determine the dominant criterion, which causes changes to SH, SH was also computed using individual criteria.

We compute SIL, SV and PV as a single value integrated over their appropriate domains, and we computed SH and SWH at eight hydrogeomorphic reaches (Simenstad et al., 2011) (Fig. 3. 1). Indicators were calculated every 15 minutes for both the 2010 reference simulation outputs, as well as the XXL1 scenario of a CSZ earthquake simulation.

3.2.2. Cascadia earthquake scenario

Witter et al. (2013) developed idealized, deterministic Cascadia earthquake scenarios to evaluate tsunami impacts along the Oregon coast. They defined these scenarios based on knowledge of the structure of the Cascadia megathrust (Goldfinger, 1994; McCrory et al., 2004), 10,000 years of paleosiesmic records (Goldfinger et al., 2012), models of seafloor deformation during megathrust ruptures (Wang and He, 2008; Wang and Hu, 2006), and the geological record left behind by great earthquakes (Chlieh et al., 2007; Hsu et al., 2006; Ito et al., 2011; Moreno et al., 2009; Subarya et al., 2006). Coseismic deformations were calculated from a fault dislocation model—the principal input being the maximum coseismic slip deficit release— and based on representative time intervals between CSZ earthquakes inferred from turbidite deposits (Goldfinger et al., 2012). Slip deficits are the amount of slip not released (between earthquakes) when the subducting plate is locked to the overriding plate and are calculated using the representative interseismic (inter-event) time interval. This interval is then multiplied by the plate convergence rate value that varies with latitude along the ~1000 km- long Cascadia subduction zone (Wang et al., 2003).

Five size classes (SM, M, L, XL, and XXL) represent the relative amount of coseismic slip assigned to each scenario, which are calculated from inter-event times (300 yrs (the "small" or Sm scenario), 425-525 yrs (the "medium" or M scenario), 650-800 yrs (the "large" or L scenario), 1050-1200 yrs (the "extra-large" or XL scenario), and 1200 yrs (XXL scenario), respectively) and plate convergence rates.

All of the CSZ fault rupture simulations assumed a "bell shaped" slip distribution up and down the megathrust, so slip was zero at the surface trace of the fault (at the

seafloor), reached a peak several kilometers deep in the vicinity of the continental shelf-slope break, and became zero deep in the earth where rocks are too hot to store slip deficit (Witter et al., 2011). Each of the five size classes were assumed to either slip with this fault distribution on the entire megathrust, slip on the megathrust until reaching a splay fault, ramping up on the splay to the surface, or stopping slip in the vicinity of where the splay fault intersects the megathrust. These three scenarios were termed the shallow buried rupture, splay fault, and deep buried rupture, respectively, but all used the same bell-shaped slip distribution, just truncating it for the two that terminate near the splay fault (Priest et al., 2009, 2010; Witter et al., 2011). The splay fault is inclined ~30° landward and smoothly merges with the megathrust, thus, when slip is partitioned to the splay from the ~10-11°-inclined megathrust, the resulting uplift for a given slip is much amplified (Priest et al., 2009, 2010; Witter et al., 2011). Multiplying these three scenarios by the five size classes yielded 15 CSZ sources that were then used to build a logic tree with appropriate weights on each branch based on the geologic likelihood of each (from a consensus of the scientific team). The splay fault model (arbitrarily assigned the label 1 in the logic tree) had the highest logic tree weight (0.8) for the three largest scenarios, L1, XL1, and XXL1. The high weight was based on the idea that splays are more likely activated during large slip events, such as what Plafker (1972) observed from the great Alaskan earthquake of 1964. Since the splay fault rupture model created the largest tsunamis in each of the five size classes, the five splay fault scenarios were used by DOGAMI to create the tsunami inundation maps for the entire ~580-km-long Oregon coastline. With the purpose of evaluating the maximum potential impact of the vertical seafloor displacement on salmon habitat, we

used the post-deformation bathymetry map resulting from the XXL1 scenario. This scenario released slip deficit built up from 1200 years of convergence along the entire CSZ resulting in a M_w 9.1 earthquake. It should be noted that the coseismic deformations of the XL and XXL size classes for all three of the fault slip scenarios in the immediate vicinity of the Columbia River are nearly identical, although they differ offshore of the river. Thus, the XXL1 coseismic deformation within the Columbia River approximates 6 of the 15 CSZ scenarios.

The XXL1 scenario of the CSZ earthquake predicts that the land will subside at the lower Columbia River estuary by almost 3 m relative to the mean sea level. However, this subsidence is not uniform across the estuary. A maximum subsidence of ~3m occurs at the mouth of the estuary, with the subsidence by Cathlamet Bay being only ~1.8 m, and no meaningful subsidence upstream of Beaver Army (Latitude 46°10'53", Longitude 123°10'56").

3.2.3. Numerical model configuration

Underlying simulations of river-to-ocean circulation with the finite element unstructured-grid model, SELFE (Zhang and Baptista, 2008), version 4.0.1. The reference simulation (using year 2010 for atmospheric, ocean, and river boundary condition) is an operational product of the SATURN collaboratory (Baptista et al., 2015) and is referred to as simulation database 33 (DB33). The settings and skill of DB33 are documented in detail in (Kärnä and Baptista, 2016), with additional discussion in (Kärnä et al., 2015). In the simulation of the XXL1 scenario, we used the post-event bathymetry conditions that resulted from vertical coseismic deformation in the XXL1 scenario. These conditions were also used for tsunami simulations in order to

create tsunami inundation maps (Witter et al., 2011). All other input files, including river, ocean, and atmospheric forcing, were kept the same as the reference simulation. The deformation data, which was provided as point data, was triangulated and then linearly interpolated to nodes of the DB33 grid in order to generate a deformation grid with nodes co-incident to the DB33 grid. Then, the depths from the DB33 grid and the depths from the deformation grid were added to determine grids for the XXL1-CSZ scenario (Fig. 3. 1).

3.3. Results

Using the estuarine habitat-related indicators, the results indicate that the salinity regime would change substantially throughout the estuary in response to a large CSZ earthquake (Fig.2a, 3a). Although SIL and SV increase in response to XXL1-CSZ, those indicators follow the same seasonal variability as the contemporary system (Fig. 2c, 3c). SIL has seasonal variability; the lowest value of 17.2 km occurs in June because of the freshet, and the highest value of 36.8 km occurs in September during low river discharge under contemporary conditions (Fig. 2c). At the same time, these values increase up to 26.6 km and 53.3 km in the XXL1 scenario (Fig. 2c). SV shows the same variability in the contemporary system and the XXL1 scenario. In the contemporary system, during the freshet, salt volume had the lowest value at 1.63×10^{10} m^3. psu, while during the dry season (September) the estuary experiences the highest salt volume value at 4.71×10^{10} m^3. psu (Fig. 3c). At the same time, under the XXL1 scenario, the maximum and minimum salt volume values would increase up to 8.88×10^{10} m^3. psu and 3.31×10^{10} m^3. psu, respectively (Fig. 3c). The computed yearly mean for SIL and SV

would increase 50% and 94% above the contemporary condition, respectively (Fig. 3. 11, Table. 1). This means that under the influence of the largest CSZ earthquake, the average SIL would propagate into the estuary by 13.8 km and the estuary would lose 3.12×10^{10} m^3 of tidal freshwater relative to the contemporary condition (Fig. 3. 2b, 3. 3b).

The yearly mean value of PV (black dashed line in Fig. 3. 4b) increases by 5.2×10^9 m^3, which is about 38% relative to the contemporary condition (Fig. 3. 11, and Table 3. 1). Some fish out-migrating to the ocean could benefit from this as plume volume also increases during the freshet from 1.10×10^{11} m^3 in the contemporary system to 1.49×10^{11} m^3 under the largest CSZ earthquake condition (Fig. 3. 4c, 3. 11, and Table 3. 1).

Shallow water and juvenile Chinook salmon habitat responds to the XXL1-CSZ scenario at reach A through C differently. We didn't find significant differences in SH and SWH at reaches upriver from reach C to the Bonneville Dam ($p > 0.001$, ANOVA); therefore, we are only presenting results for SH and SWH at reach A, B, and C.

During a year, and within the framework of the XXL1 scenario, SWH declines by a mean value of 9.78×10^6 m^3 at reach A, which is about 17% relative to the contemporary condition. However, there are some days in July, after the freshet in June, where SWH exceptionally increases slightly relative to the contemporary condition (Fig. 3. 5b, 3. 11, and Table. 3. 1). Reach B sees a loss of SWH over the course of a year by a mean value of 2.9×10^7 m^3, which is about 25.2% relative to the contemporary condition (Fig. 3. 6b, 3. 11, and Table. 3. 1). While reaches A and B lose SWH in the XXL1 scenario relative to the contemporary condition, reach C provides greater SWH throughout the year by a mean value of 1.64×10^7 m^3, which is about 29% relative to the contemporary condition

(Fig. 3. 7b, 3. 11, and Table. 3. 1). Although SWH changes in the XXL1 scenario at reaches A, B, and C relative to the contemporary condition, it follows the same seasonal variability as the contemporary system (Fig. 3. 5c, 3. 6c, 3. 7c).

At reach A, SH decreases in the XXL1 by a mean value of 1.42×10^6 m^3 (6% relative to the contemporary condition). However, there are some days in July and August that SH increases in the XXL1 by a maximum of 27.7% and decreases by 33% in June relative to the contemporary condition (Fig. 3. 8b, 3. 11, and Table. 3. 1). At reach B, a constant decrease in SH is observed with a mean value of 9.8×10^6 m^3, which is about 28% relative to the contemporary condition (Fig. 3. 9b, 3. 11, and Table. 3. 1). Under the XXL1 scenario conditions, this reach will lose its habitat by a maximum of 52% relative to the contemporary condition (Fig. 3. 11, and Table. 3. 1). Though only part of the riverbed subsides at reach C in the XXL1 scenario, the SH increases during the year and its mean value increases by 1.27×10^7 m^3, which is 50% relative to the contemporary condition (Fig. 3. 10b, 3. 11, and Table. 3. 1).

Since SH is a complex indicator, we calculated water volume based only on depth criterion (0.5 m $\leq$ depth $\leq$ 2m) and then applied salinity penalty to identify the variable that controls SH. Within the framework of an XXL1 scenario, the results indicate that during a year, reach A and B will lose water volume on an average of 17.2% and 27.6%, respectively, for depths that fall between 0.5 m and 2 m relative to the contemporary condition. In contrast, under the XXL1 scenario, reach C gains 55.3% more water volume for depths between 0.5 m and 2 m relative to the contemporary system. By then adding salinity penalty to the depth criterion, the volume of water decreases to 17.30% and 29.43% at reach A and B, respectively. This means that adding

salinity penalty decreases SH by 0.08% and 1.8%, which is negligible. Adding salinity penalty didn't change the water volume for depths between 0.5 m and 2 m at reach C because salt water doesn't intrude up to reach C. However, the volume of salt water (salinity >0 psu) for all depths increases by 73.3% and 251.6% at reach A and B, respectively. To identify the impact of applying velocity threshold in the SH calculation, we computed the water volume for depths that fall within 0.5 m-2 m with a velocity that is less than 0.4 m/s, which is a velocity that is favorable to emergent fry. The volume of water decreases to 10.5% and 25.5% at reach A and B, respectively, and increases at reach C by 48.9%. This indicates that adding velocity threshold decreases SH by 6.7%, 2.1%, and 6.37% at reach A, B, and C, respectively.

3.4. Discussion

We developed an integrated quantitative evaluation of the effects a large CSZ earthquake scenario might have on the Columbia River estuarine habitat, relative to the contemporary system. Our results suggest substantial changes in estuarine-necessary environmental conditions for fish and other aquatic species. An increase in salt propagation suggests that the XXL1-CSZ earthquake scenario deforms the estuary bed and results in more space for salt water from the ocean.

The increasing mean of SIL and SV by 50% and 94%, would then be followed by an alteration in aquatic species and vegetation, which are sensitive to salinity. For instance, riparian wetlands belong to the freshwater tidal habitat, and when they are lost, anadromous species lose their food source because riparian wetlands provide a variety of insect species, which are food for juveniles (David et al., 2015; Simenstad et al.,

1982). SIL and SV increase throughout the year, but specifically in summer months; larger SIL and SV bring more hypoxic and acidic waters associated with the upwelling of deep oceanic waters, into the estuary (Roegner et al., 2011).

Favorable northerly winds and high stream flows (freshet) create the largest possible PV in June in the contemporary system. The XXL1- CSZ earthquake scenario also creates a maximum increase of ~ 245% in PV relative to the contemporary system during freshet. Higher salt-water volume and high stream flow increase mixing and dilution and consequently creates larger plume.

Although some prior studies show a positive correlation between SARs for steelhead and Snake River sp/su Chinook salmon at lower Granite Dam with high plume characteristics from April to July for some wet years (Burla et al., 2010; Miller et al., 2014), Brosnan et al. (2014) found that this relationship may not exist for most yearling Chinook salmon stocks. It means that having higher PV may not favor all salmon stocks.

SWH, an indicator for subyearling rearing habitat that only depends on bathymetry, stays unchanged in the upper estuary from reach D through H. The two ocean-influenced reaches, A and B, lose their shallow water habitat by ~20% (yearly mean) relative to the contemporary condition. Losing shallow water habitat for those fish (especially juveniles) that survive only in the shallow areas and use it as a nursery habitat, is critical.

Archaeological evidence from shell middens at different sites along the Oregon coast also prove that some species, like butter and littleneck clams, lost their habitat after first experiencing a subsidence event at 370± 60 BP (Minor et al., 1989). However, upstream

at reach C, there is less subsidence and a narrower channel and consequently more inundated area, thus creating more shallow water habitat, about 29% (yearly mean) relative to the contemporary condition.

SH responses to the XXL1-CSZ scenario differ across the Columbia River estuary depending on the bathymetry, geometry, and the distance from the ocean of each reach. SH response to the XXL1-CSZ scenario is similar to the trends seen in SWH changes. Yearly mean of SH decreases at reach A and B by 6% and 28%, respectively, for the XXL1-CSZ earthquake scenario relative to the contemporary system. Positive changes occur for only part of the year by 27% during the dry season and negatively by 73% at reach A; reach B experiences negative change for the whole year.

Reach A will lose habitat during May, when Spring Creek Group fall fingerling is the predominant stock (96%), and during March, when West Cascade fall and Spring Creek Group fall fry are predominant stocks (50%, 40% respectively)(Teel et al., 2014), while reach B will lose habitat throughout the year.

In contrast, the narrow channel of reach C, with its specific topography and longer distance from the ocean, would create more habitat for juvenile Chinook salmon in the XXL1-CSZ earthquake scenario relative to the contemporary system. Since there was not any subsidence at other upper reaches and the estuary hydrodynamic, we did not see any changes there. Computation of water volume, based on individual criterion, reveals that depth criterion modulates the SH changes. Although salt volume increases at reach A and B, it does not impact the areas that have depths between 0.5 m and 2 m. Thus, for juvenile Chinook salmon only, depth is a dominant factor in the changes of SH. Increased salt at all depths however, may change habitat for species sensitive to salinity.

Therefore, extensive assessment of the Columbia River estuary changes, as well as the development of indicators for other species, are essential and outcomes from these analyses can be used to guide designing optimal conservation and adaptation plans.

Our research has multiple uncertainties. There is uncertainty regarding the accuracy of the rupture model results and deformation values used to do our simulation. There are inaccuracies in the DB33 simulations, as discussed by Kärnä and Baptista (2016a). We considered only one maximum scenario to evaluate the potential impact of a CSZ earthquake on estuarine habitat. Further simulations for other CSZ earthquake scenarios will benefit decision makers in designing restoration and adaptation plans. Additionally, we limited the ocean, river, and atmospheric data used as the baseline for running the SELFE model for both the contemporary condition and the CSZ scenario to just the year 2010. We considered 2010 to be representative of a recent moderate year that balanced out any river discharge and upwelling seen during 2000-2014. Importantly, there is also uncertainty in the nature of sedimentary adjustments for a post-Cascadia Subduction Zone earthquake.

Of note, we did not include a sediment model in our analyses. In a separate study, we compared the calculated salmon habitat and salinity intrusion length based on the results using only a circulation model with the results using a sediment model plus a circulation model. Although the results showed some differences, the differences were insufficient to consider running the sediment model along with the circulation model.

3.5. Conclusion

We characterized estuary response to the largest Cascadia Subduction Zone earthquake with the M_w (moment magnitude) of 9.1 by using habitat-relevant indicators (including salinity intrusion length, salt volume, shallow water habitat, and juvenile Chinook salmon habitat). These indicators were compared between contemporary condition and conditions resulting from the largest CSZ earthquake as developed by the Oregon Department of Geology and Mineral Industries and collaborators (Witter et al., 2013).

Our results suggested that subsidence would change estuarine physics and associated fish habitat. For low river discharges (e.g., in September), the effect is particularly pronounced with salinity propagating upstream nearly 15 km, causing a major (~94%) loss of freshwater habitat.

Some fish out-migrating to the ocean could benefit from this as plume volume also increased during the freshet from 1.10×10^{11} m^3 in the contemporary system to 1.49×10^{11} m^3 under the largest CSZ earthquake condition.

Changes in shallow water and salmon habitat varied strongly across the lower estuary, and there would be winners and losers in terms of reaches, stocks, and migration timing. We didn't assess any major change in shallow water habitat and habitat for juvenile Chinook salmon where there is no subsidence at upper reaches

Table

Table 3. 1. Percentage change in six salmon-relevant indicators for the XXL1-CSZ scenario relative to the contemporary condition.

Variable	Mean	Min	Max	25 percentile	75 percentile
SIL	50.34	5.35	83.68	44.58	55.44
SV	94.30	37.19	142.29	88.32	100.46
PV	38.03	-29.26	244.75	22.03	48.65
SH[a]	-5.96	-33.10	27.68	-14.56	1.48
SH[b]	-28.16	-51.89	-13.78	-32.05	-23.30
SH[c]	49.83	8.26	121.83	40.34	58.76
SWH[a]	-16.97	-50.73	2.87	-20.89	-12.94
SWH[b]	-25.20	-41.55	-6.10	-28.60	-22.05
SWH[c]	28.90	13.78	82.70	19.40	35.33

[a] Reach A
[b] Reach B
[c] Reach C

Figure

Figure 3. 1. (a) Horizontal view of the model domain, along the west coast of the U.S. from California to British Columbia and the Columbia River estuary extending from Bonneville dam to the Pacific Ocean. The color shows the bathymetry difference between the largest CSZ earthquake scenario and contemporary condition; (b) zoom-in of the Columbia River estuary with 8 hydro-geomorphic reaches of the Columbia River Estuary Ecosystem Classification (Simenstad et al., 2011b); (c) horizontal view of unstructured grid of the lower estuary (reach A, B, and C)

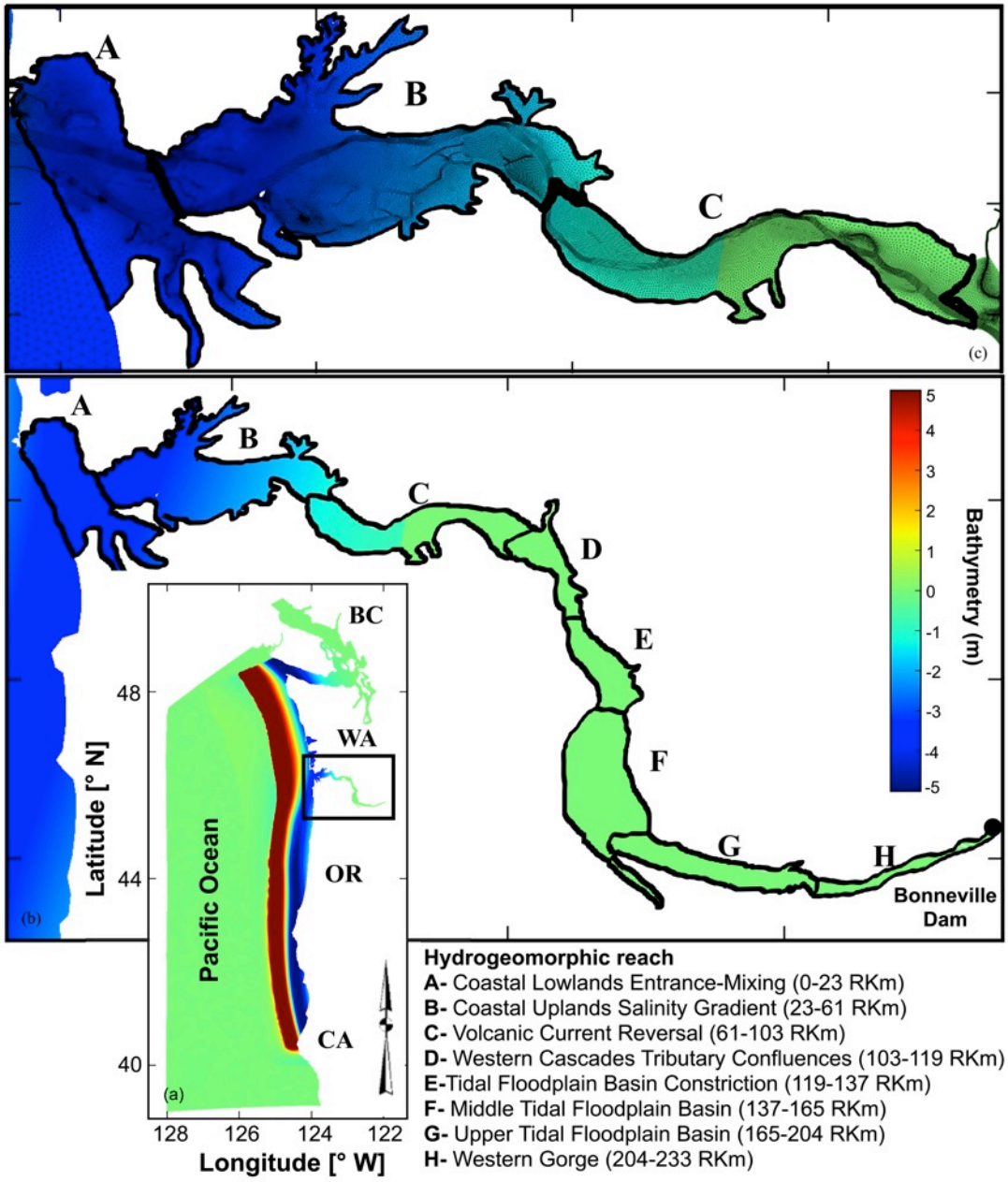

Figure 3. 2. (a) Histograms show the distribution of salinity intrusion length (SIL) for both contemporary condition and the XXL1-CSZ scenario; (b) histogram illustrates the difference in salinity intrusion length between the XXL1-CSZ scenario and contemporary condition. The black dashed line shows the mean difference; (c) time series of salinity intrusion length for contemporary system, XXL1-CSZ, and the difference between the two.

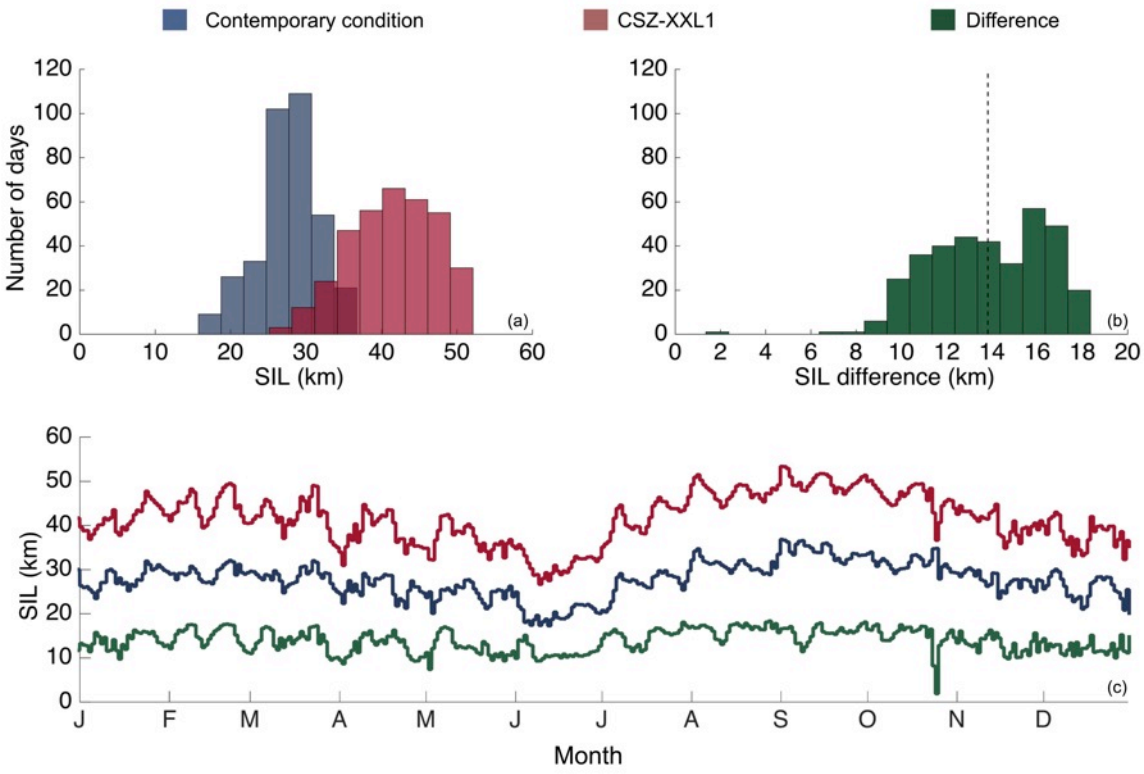

Figure 3. 3. (a) Histograms show the distribution of salt volume for both contemporary condition and the XXL1-CSZ scenario; (b) histogram illustrates the difference salt volume between the XXL1-CSZ scenario and contemporary condition. The black dashed line shows the mean difference; (c) time series of salt volume for contemporary system, XXL1-CSZ, and the difference between the two.

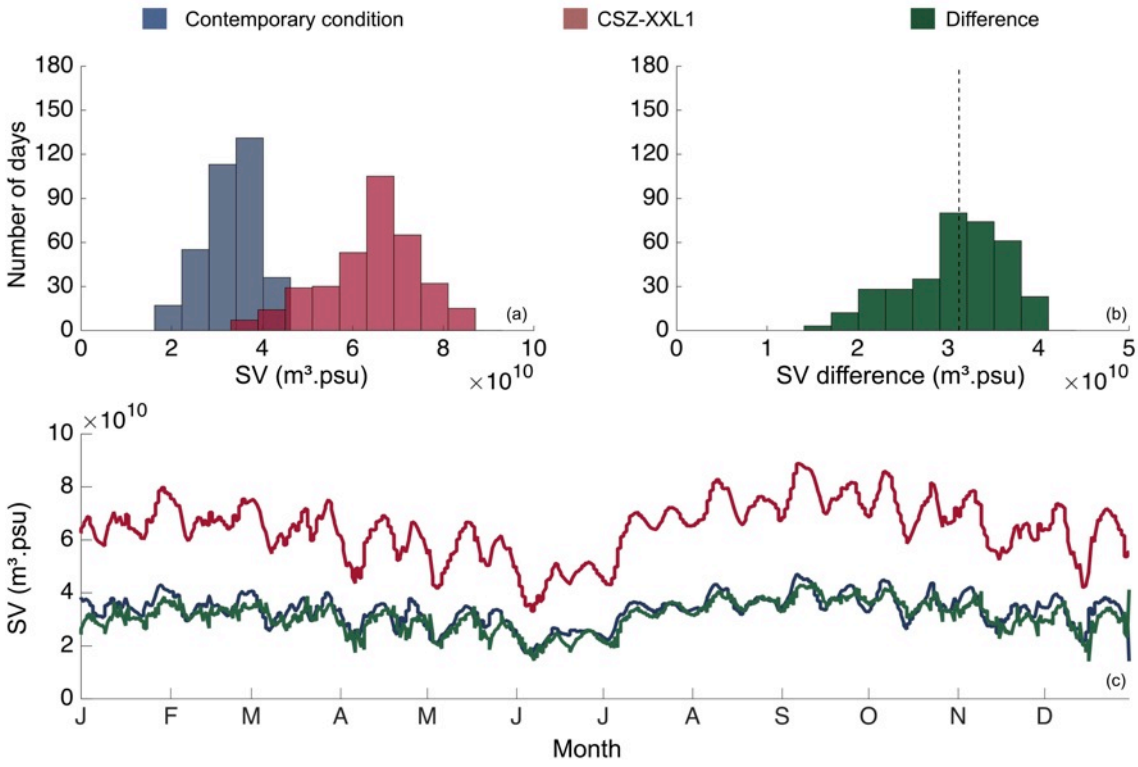

Figure 3. 4. (a) Histograms show the distribution of plume volume for both contemporary condition and the XXL1-CSZ scenario; (b) histogram illustrates the difference in plume volume between the XXL1-CSZ scenario and contemporary condition. The black dashed line shows the mean difference; (c) time series of plume volume for contemporary system, XXL1-CSZ, and the difference between the two.

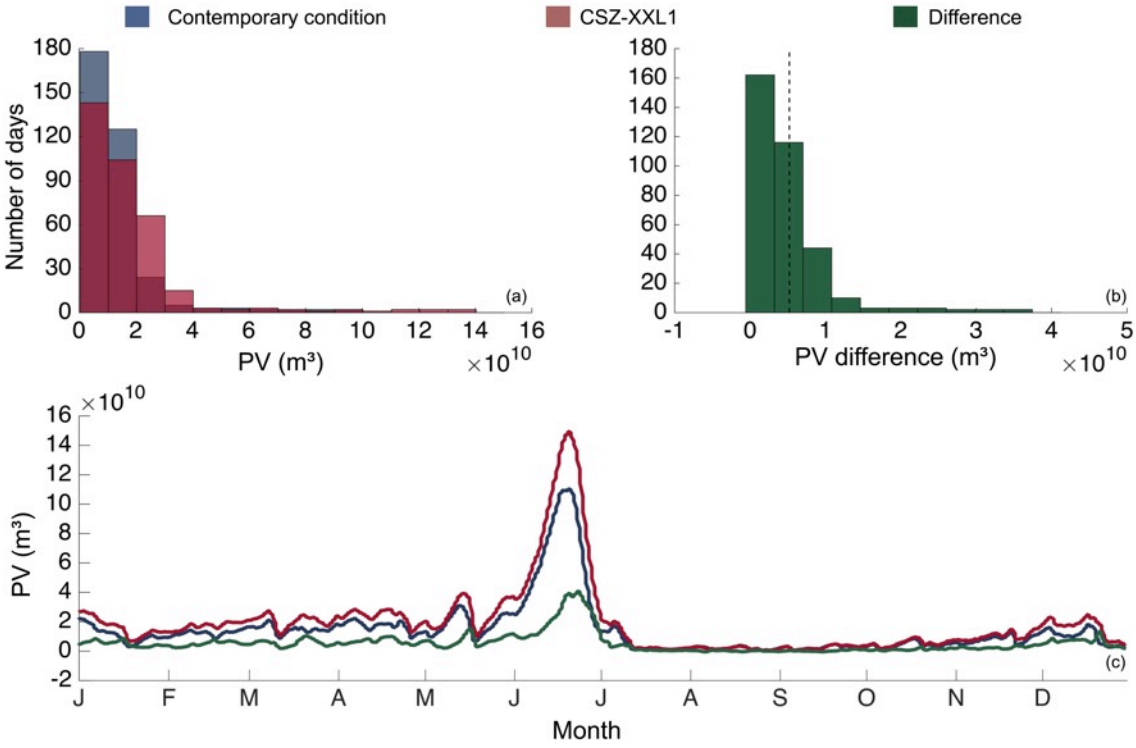

Figure 3. 5. (a) Histograms show the distribution of shallow water habitat (SWH) in contemporary condition and the XXL1-CSZ scenario at reach A; (b) histogram illustrates the difference in shallow water habitat between the XXL1-CSZ scenario and contemporary condition. The black dashed line shows the mean difference; (c) time series of shallow water habitat in contemporary system, XXL1-CSZ, and the difference between the two at reach A.

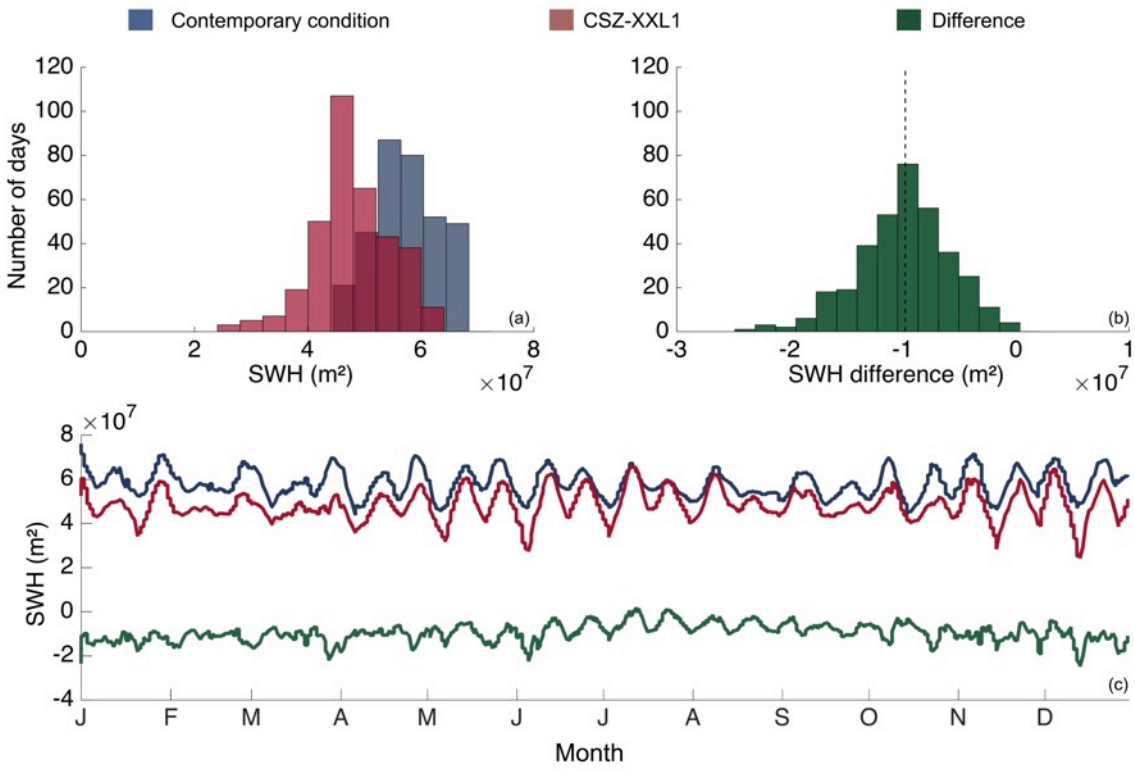

Figure 3. 6. (a) Histograms show the distribution of shallow water habitat (SWH) in contemporary condition and the XXL1-CSZ scenario at reach B; (b) histogram illustrates the difference in shallow water habitat between the XXL1-CSZ scenario and contemporary condition. The black dashed line shows the mean difference; (c) time series of shallow water habitat in contemporary system, XXL1-CSZ, and the difference between the two at reach B.

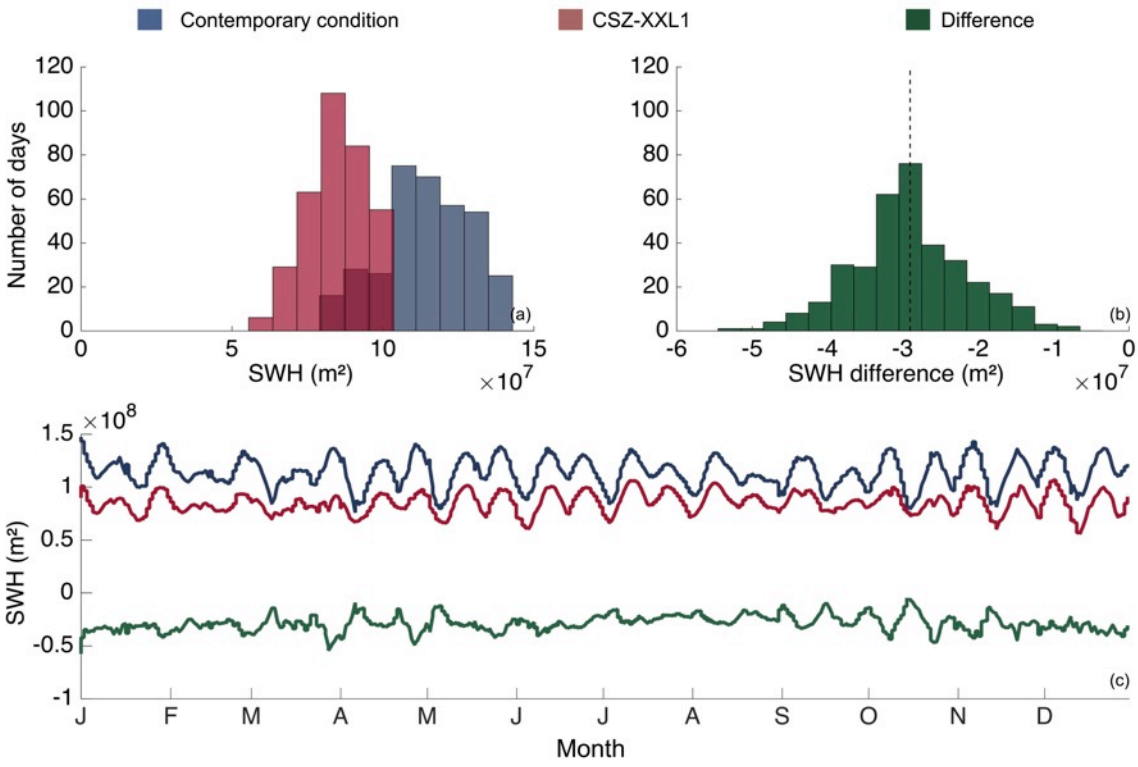

Figure 3. 7. (a) Histograms show the distribution of shallow water habitat (SWH) in contemporary condition and the XXL1-CSZ scenario at reach C; (b) histogram illustrates the difference in shallow water habitat between the XXL1-CSZ scenario and contemporary condition. The black dashed line shows the mean difference; (c) time series of shallow water habitat in contemporary system, XXL1-CSZ, and the difference between the two at reach C.

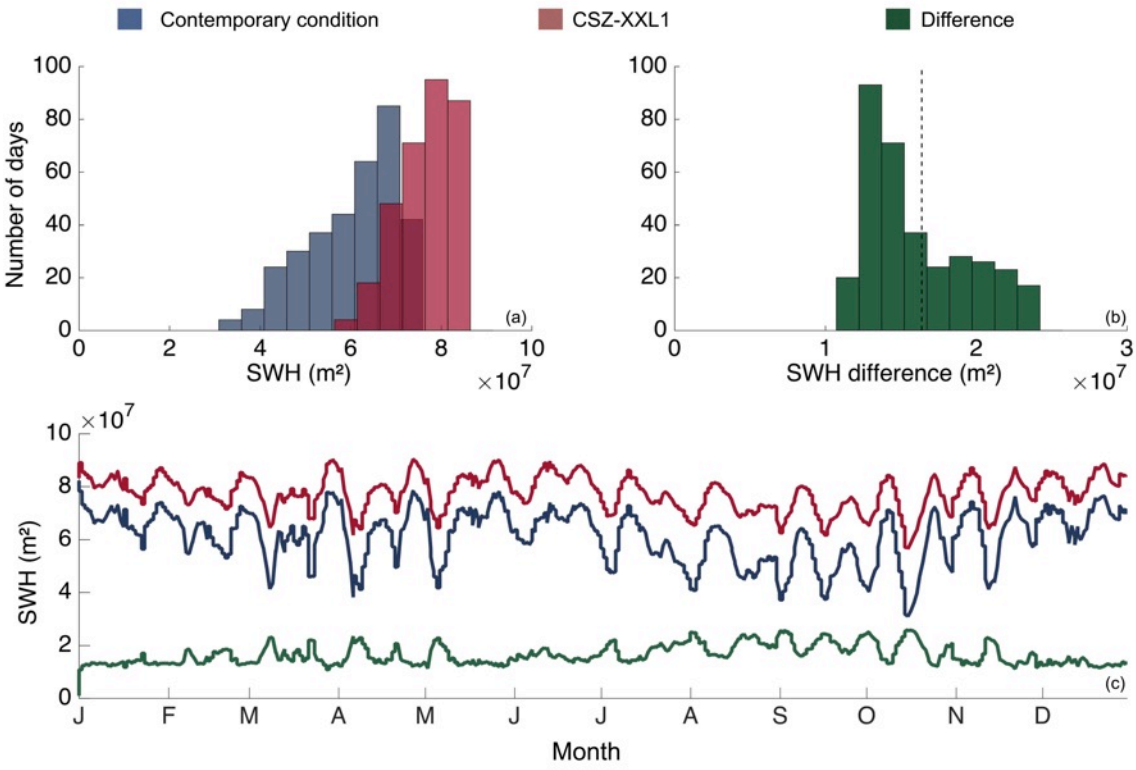

Figure 3. 8. (a) Histogram shows the distribution of nursery habitat for emergent fry in contemporary condition and the XXL1-CSZ scenario at reach A; (b) histogram illustrates the difference in nursery habitat between the XXL1-CSZ scenario and contemporary condition. The black dashed line shows the mean difference; (c) time series of nursery habitat for emergent fry in contemporary system, XXL1-CSZ, and the difference between the two at reach A.

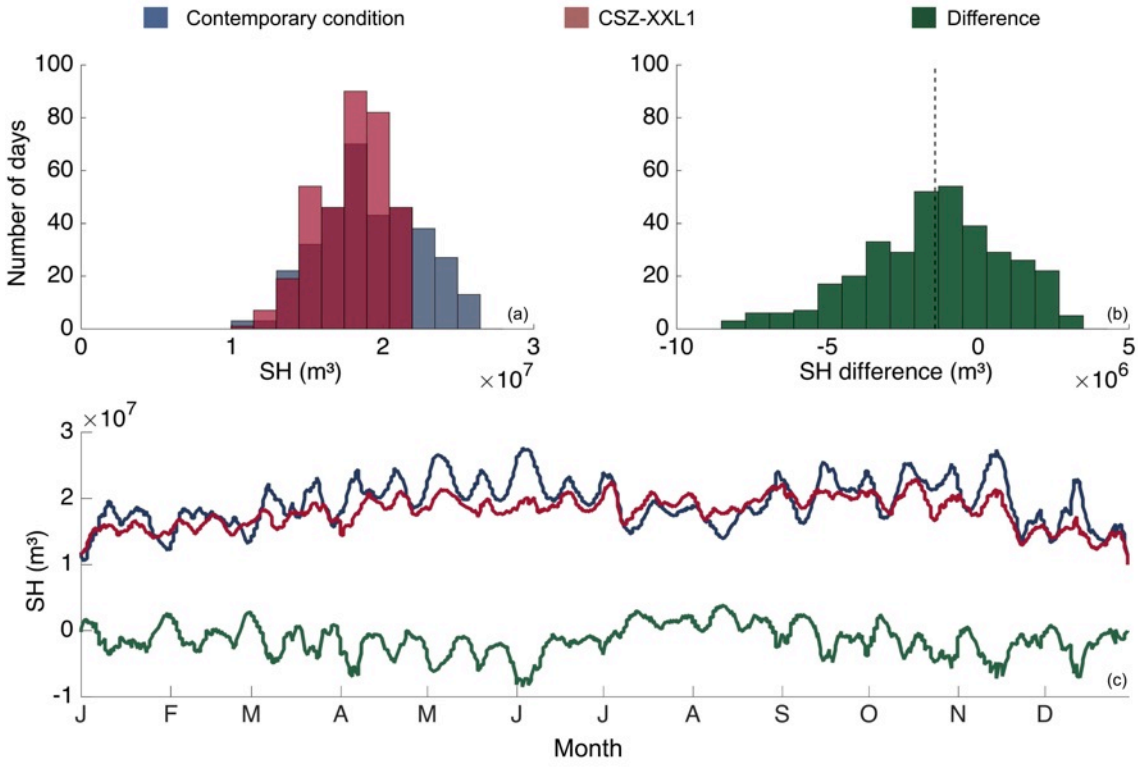

Figure 3. 9. (a) Histograms show the distribution of nursery habitat for emergent fry in contemporary condition and the XXL1-CSZ scenario at reach B; (b) histogram illustrates the difference in nursery habitat between the XXL1-CSZ scenario and contemporary condition. The black dashed line shows the mean difference; (c) time series of nursery habitat for emergent fry in contemporary system, XXL1-CSZ, and the difference between the two at reach B.

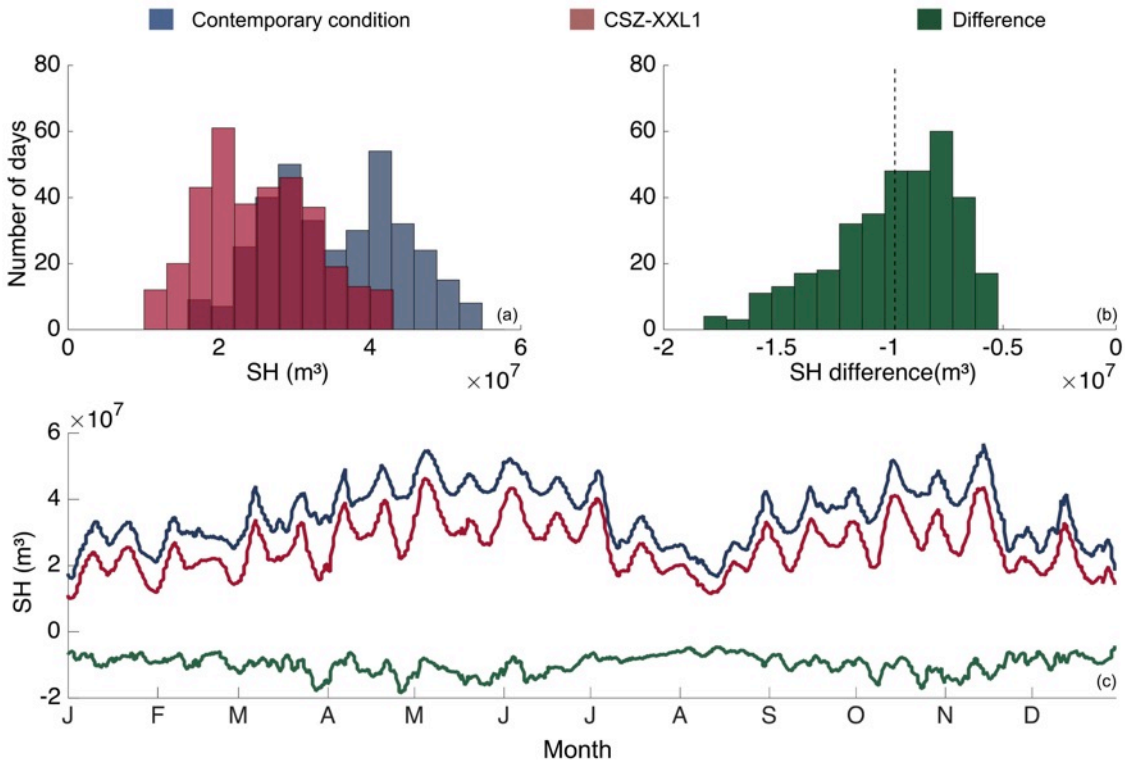

Figure 3. 10. (a) Histograms show the distribution of nursery habitat for emergent fry in contemporary condition and the XXL1-CSZ scenario at reach C; (b) histogram illustrates the difference in nursery habitat between the XXL1-CSZ scenario and contemporary condition. The black dashed line shows the mean difference; (c) time series of nursery habitat for emergent fry in contemporary system, XXL1-CSZ, and the difference between the two at reach C.

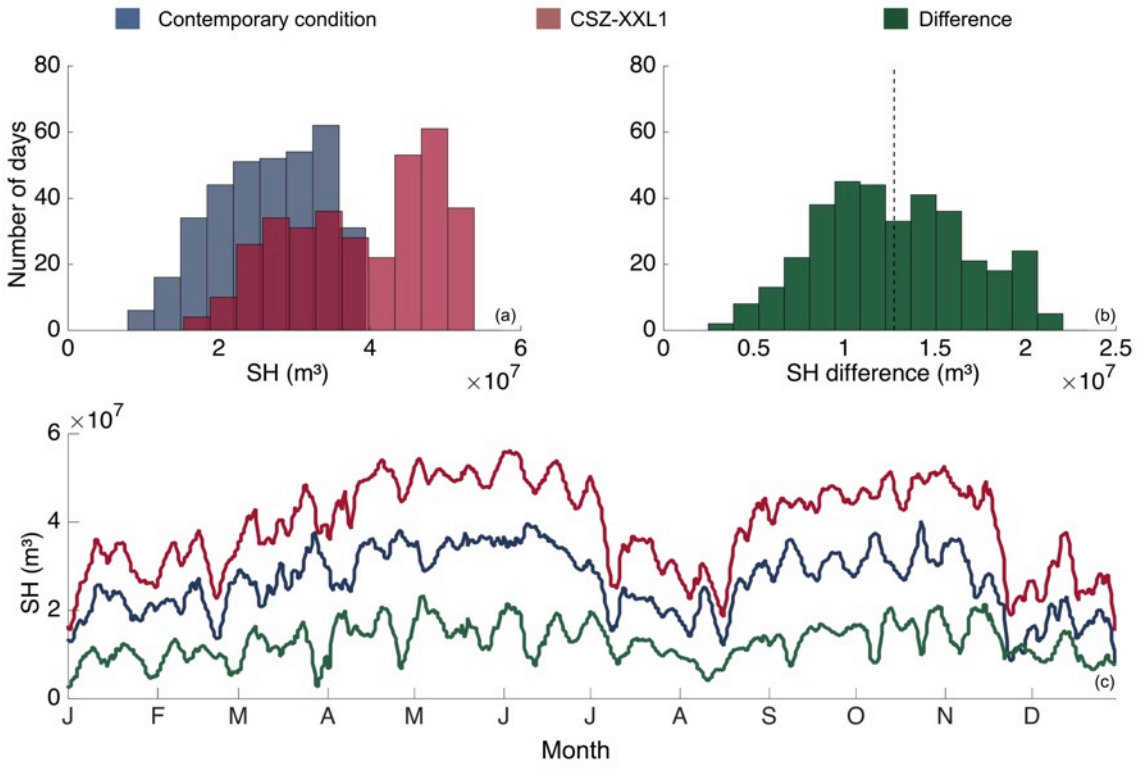

Figure 3. 11. Percentage change in salinity intrusion length (SIL), salt volume (SV), plume volume (PV), shallow water habitat (SWH), and salmon habitat (SH) for the XXL1-CSZ scenario relative to the contemporary condition. Mean percentage change is expressed as black circles; dark lines show maximum and minimum percentage change; light lines show 25th and 75th percentile percent changes.

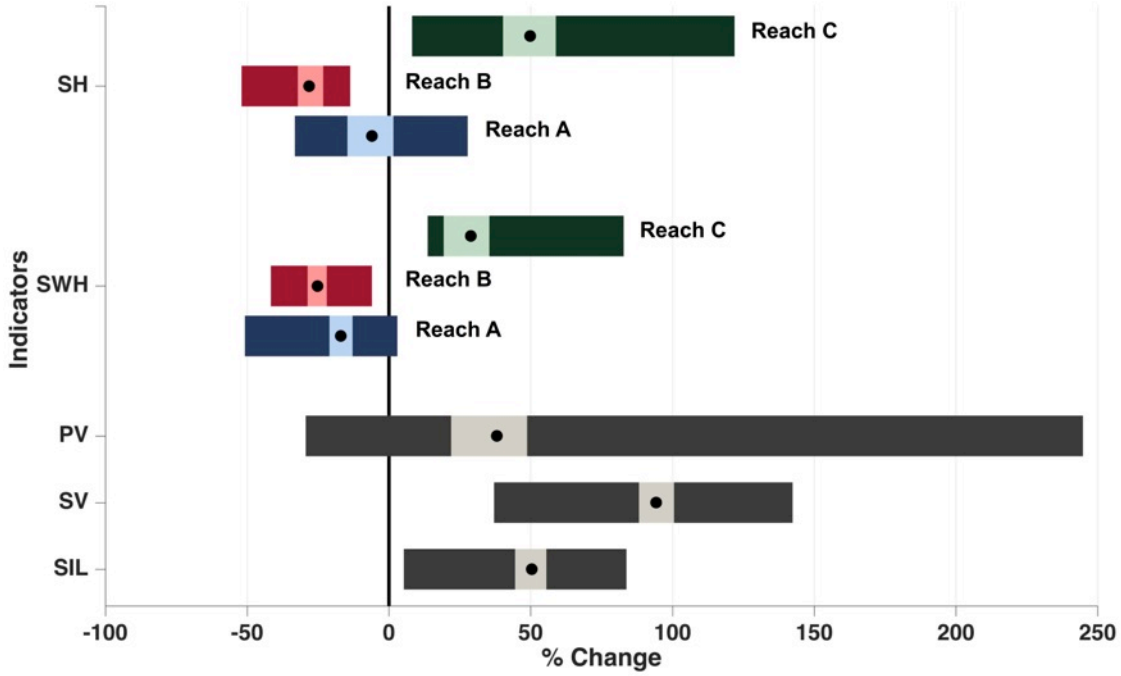

Chapter 4

Impact of sea level changes on salmon habitat in the Columbia River estuary[3]

M. Rostaminia[1], A. M. Baptista[1], P. J. Turner[1], C. A. Seaton[1]

[1] Center for Coastal Margin Observation & Prediction, Oregon Health & Science University, 3181 SW Sam Jackson Park Road, Portland, Oregon 97239, USA

[3] I want to thank Paul Turner for providing a simulation for the contemporary system. A version of this chapter will be submitted to Advances in Modeling Earth Systems.

Abstract

As transitional systems between land and ocean, estuaries are sensitive to many aspects of a changing climate. Here, we use a numerical circulation model to examine the response of the Columbia River estuary to sea level rise. This mid-latitude mesotidal estuary is home to many salmonid stocks, whose habitat is responsive to a complex physics controlled primarily by tides and river discharge. Across multiple physical metrics of ecological significance, we find the response of the estuary to sea level rise to be non-linear. Past specific thresholds (approximately 1 m off the coast), rising sea levels will drastically increase the extent of ocean influence on the estuary (as measured by salinity intrusion length), and will substantially reduce the seasonal influence of freshwater on the continental shelf (as measured by plume volume during river freshets). Rising sea levels will also alter shallow water and specifically salmon estuarine habitat within the estuary in complex spatial and temporal ways, likely leading to winners and losers among salmon stocks. These results, if combined with long-term monitoring of actual sea level rise off the coast, could guide regional mitigation strategies. An important caveat is that this study considers sea level rise in isolation, thus neglecting potentially important interactions with other climate and in-basin changes.

4.1. Introduction

The Columbia River estuary provides a variety of rearing habitats and transitional zones for anadromous fish (Bottom et al., 2005; Emmett et al., 2004; Healey, 1992; Simenstad et al., 1982). However, under multiple local stressors (in particular navigation, hydropower and irrigation) and large-scale changes in climate, the estuary has experienced significant loss of habitat with an almost 90% decline in population from historical levels (Bottom et al., 2011; Bottom et al., 2005; Dalton et al., 2013; Mantua et al., 1997; NRC, 2004b; Pearcy, 1992; PFMC, 2011; Weitkamp et al., 2014). This has led to 13 species of Pacific salmon and steelhead, being listed under the U.S. Endangered Species Act (Ford, 2011; Weitkamp et al., 2014). Although many expensive recovery efforts are being conducted, many future impacts of climate change on the estuary have not been quantitatively assessed in ways that enable them to be accounted for in long-term planning.

Changes in hydrologic stream flow regimes, increasing temperature, and sea level change are three regionally impacts of climate change that will affect the Pacific Northwest (Dalton et al., 2013). Higher stream temperatures are expected to alter freshwater habitat quality for salmon (ISAB, 2007). Adding to that, a reduced snow pack will cause earlier freshet and less stream flow in summer, thus posing significant threats to salmon life cycle and their migration pattern, as well as other aquatic species (Beechie et al., 2006; Mantua et al., 2010). Sea level change (SLC) will most likely affect the Pacific Northwest coastal margin habitats as salinity propagation into the estuary may shift freshwater marsh and swamp habitats into the salt marsh (Dalton et al., 2013; Glick et al., 2007). Specifically, by 2100, (Glick et al., 2007) predict that

Willapa Bay, the Columbia River, and Tillamook Bay will lose 32%, 31%, and 63% of brackish marsh, tidal swamp, and tidal flats, respectively.

Climate change may influence estuarine habitat in complex ways and abrupt changes may occur as thresholds are crossed. Identifying thresholds of behavior, ecological tipping points, and other singularities or non-linear behaviors in response to anticipated stressors will aid managers in designing adaptive plans that address the risks involved when a system cannot adapt to abrupt changes (Groffman et al., 2006). To ultimately facilitate the design of adaptive management plans, environmental indicators have been used to evaluate the ecosystem status in both the contemporary system and in response to stressors (Bottom et al., 2011; Burla et al., 2010; Miller et al., 2013; Miller et al., 2014).

The aim of this research is to determine the estuarine habitat response to relative sea level change (RSLC). To accomplish this, we used a baroclinic circulation model, SELFE (Zhang and Baptista, 2008), to project future effects of sea level change on Columbia River estuarine habitat. Given the uncertainties surrounding both global and Pacific Northwest rates of future sea level change, we explored a wide range of RSLC scenarios. These scenarios were informed by projections for 2100 from NOAA (Parris et al., 2012), the U.S. Army Corps of Engineers (USACE), and the National Research Council (NRC, 2012). We specifically simulated a single year (2010) under realistic contemporary river and ocean conditions, and under the same conditions modified only by the RSLC scenarios, from the simulation outputs, we then computed physically–based indicators of estuarine behavior: Salinity intrusion length (SIL, km), plume volume (PV, m^3), shallow water habitat (SWH, m^2), and juvenile Chinook salmon

habitat (SH, m^3). We used these indicators to compare contemporary and scenario conditions, thus gaining unique insights into possible future changes in salmon-relevant estuarine behavior.

4.2. Method

4.2.1. Indicators

The indicators used in this study represent key ecosystem processes for this system. We chose the salinity intrusion length (SIL, km) indicator as a surrogate for ocean influences in the estuary because increases in salinity intrusion distance may bring hypoxic water into the estuary during summer (upwelling season) and shift freshwater habitat and food availability further upstream or even eliminate it. It is, therefore, useful for decision makers to have information about how far salinity propagates into the upper Columbia River when designing adaptation and mitigation plans for different species. We computed SIL to be the distance from the river mouth to a location upstream along the south channel with a cross–section salinity of one practical salinity unit (psu).

We quantified plume volume (PV, m^3) as a proxy for freshwater influence in the continental shelf and its important role in out–migration of some salmon and steelhead. Recent studies suggest that the Columbia River plume not only plays an important role in shellfish distribution (De Robertis et al., 2005; Morgan et al., 2005), but also in the survival of steelhead during out-migration (Burla et al., 2010; Miller et al., 2013; Miller et al., 2014). Scheuerell et al. (2009) stated that the survival rate for juvenile Chinook and steelhead is 4 to 50 times greater when they out–migrate from early to mid–May

instead of mid-June. In the contemporary system, Burla et al. (2010) found a positive correlation between smolt-to-adult returns (SARs) for steelhead with plume volumes in May and June. Additionally, SARs for Snake River spring/summer Chinook salmon (listed as a threatened species under the Endangered Species Act since 1992) at Lower Granite Dam on the Snake River, highly correlate with plume area from April-July for years 1999–2008 (excluding the dry years of 2001 and 2005) (Miller et al., 2014). We computed PV as the volume of water at the Oregon and Washington continental shelf where salinity is less than 28 (psu); this is also the definition that fisheries biologists have used (Burla et al., 2010; Miller et al., 2013; Miller et al., 2014).

We selected shallow water habitat (SWH, m^2) as an indicator because shallow regions are preferential rearing habitat for juvenile salmon. Juvenile salmon generally rear in shallow water habitat, before they are ready to out–migrate to the ocean (Bottom et al., 2005; McCabe Jr et al., 1983; Roegner et al., 2010; Roegner et al., 2012). We calculated SWH as areas with water depths between 0.1-2.0 m in the Columbia River estuary. We used the elevations at 65 points along the navigation channel during a tidal day and extrapolated to the nearest part of the grid. We then calculated the area for each reach (Fig. 4. 1) that met the shallow water criterion.

Finally, we quantified juvenile ocean–type Chinook nursery salmon habitat (SH, m^3) using a refined method of habitat computation (Chapter 2). SH was computed based on the water volume that met specific thresholds (extracted from fisheries data) for water depth and 3D fields of velocity, salinity, and temperature (Chapter 2). We calculated nursery habitat, where depth is less than 2 m for juvenile Chinook salmon at the emergent fry stage (<45 mm), by applying velocity thresholds for emergent fry (v

<0.4 m/s). Also, to determine the dominant criterion, which causes changes to SH, it was also computed using individual criteria.

We compute SIL, SV and PV as a single value integrated over their appropriate domains, and we computed SH and SWH at eight hydrogeomorphic reaches (Simenstad et al., 2011) including, A: Coastal Lowlands Entrance-Mixing (0-23 river kilometer (RKm)), B: Coastal Uplands Salinity Gradient (23-61 RKm), C: Volcanic Current Reversal (61-103 RKm), D: Western Cascades Tributary Confluences (103-119 RKm), E: Tidal Floodplain Basin Constriction (119-137 RKm), F: Middle Tidal Floodplain Basin (137-165 RKm), G: Upper Tidal Floodplain Basin (165-204 RKm), and H: Western Gorge (204-233 RKm) (Fig. 4. 1). Indicators were calculated every 15 minutes for both the 2010 reference simulation outputs, as well as the scenarios of SLC.

4.2.2. Numerical model

Supporting simulations of river-to-ocean circulation were conducted using the finite element unstructured-grid model, SELFE (Zhang and Baptista, 2008), version 4.0.1. For the contemporary conditions, we used pre-existing simulations, conducted as an operational product of the Virtual Columbia River modeling system (Baptista et al. 2015). Specifically, we used the circulation simulation database DB33, which settings and skill are documented in detail in (Kärnä and Baptista, 2016a), with additional discussion in (Kärnä et al., 2015). This simulation database currently covers years 1999-2015, of which we chose 2010 as our contemporary reference because it was a moderate year regarding atmospheric, ocean, and river forcing. For RSLC scenarios, we use the same grid, parameters and forcing as for the reference, except for the sea level forcing.

4.2.3. Sea level change scenarios

4.2.3.1. Global sea level change

Global SLC is the result of the alteration in the mass of water in the oceans, a change in the shape of ocean basins, and changes in water density (Intergovernmental Panel on Climate Change's AR4 (IPCC, 2007). Ocean thermal expansion, exchange water with glaciers and ice caps, glaciers in Greenland, Antarctic and Greenland ice sheets, and change in terrestrial storage of water are factors affecting the present day global SLC (IPCC, 2007, 2013). A change in global average sea level as a result of a change in the volume of the world ocean causes a eustatic sea-level change. Recent research has forecasted ranges of global SLC by the year 2100 (IPCC, 2007, 2013; Jevrejeva et al., 2009; NRC, 2012; Parris et al., 2012; Pfeffer et al., 2008; USACE, 2013a; Vermeer and Rahmstorf, 2009). The projections for the 21st century, 2081–2100, forecasted an increase of 0.26–0.82 m relative to the reference period of 1986–2005 (IPCC, 2013). However, the IPCC projection did not consider the loss of both the Greenland and Antarctic ice sheets as potentially causing a global mean sea level rise greater than the reported range (IPCC, 2001, 2007, 2013).

The National Research Council (NRC, 1987) developed three global eustatic sea level rise scenarios to the year 2100 (0.5 m, 1.0 m, and 1.5 m) by considering high probability of accelerating global mean sea level rise In addition to a linear term, a quadratic term was included to the prediction of Eustatic sea level (Equation 1).

$$E(t) = 0.0017t + bt^2 \quad (1)$$

Where *t* represents years, starting in 1992, *b* is a constant value to fit the curve begun mid–year of 1992 from National Tidal Datum Epoch of 1983–2001. The values for coefficient being equal to 2.71E-5 for low (modified NRC Curve I), 7.00E-5 for intermediate (modified NRC Curve II), and 1.13E-4 for high (modified NRC Curve III) scenarios (NRC, 1987; USACE, 2013a, 2014).

The U.S. Army Corps of Engineers (USACE) adjusted the historical global mean sea level rate, from 0.0012 m/yr to 0.0017 m/yr from the NRC (1987). *E(t)* is the eustatic sea level change, in meters, as a function of *t* (USACE, 2013a). By using Equation 1, global sea level would rise in an intermediate scenario up to 0.5 m and in a high scenario up to 1.5 m by 2100.

The most recent NRC report (NRC, 2012) projected that global sea level would rise 0.5 m to 1.4 m based on B1 and A1FI (low and high emission in the IPCC(2007)) by the year 2100 relative to the year 2000. The thermal expansion of the ocean which was taken from the global climate models used in the IPCC (2007) as well as the impact of rapid dynamic changes in ice flow, each contributed to the Council's projections.

The 2012 report by National Oceanic and Atmospheric Administration (NOAA) indicated (with very high confidence; >9 in 10 chance) that the global mean sea level will rise in a range of 0.2 m to 2.0 m by 2100 (Parris et al., 2012). The report provided four scenarios for eustatic sea level rise to the year 2100: a) NOAA Low = 0.2 that is based on a linear extrapolation of the historical sea level change rate derived from tide gauge records beginning in 1900. b) NOAA Intermediate Low = 0.5 m that is based on the high-end scenarios from climate models using the B1 scenario in the (IPCC, 2007), which considers the risk regarding ocean warming. c) NOAA Intermediate High = 1.2

m that is based on an average of upper–end results from the semi-empirical forecast that considers observed global sea level change with the recent loss of ice sheet and air temperature. d) NOAA High = 2 m that is derived from the combination of estimated ocean warming predictions from the IPCC (2007) and maximum glacier and ice sheet loss by 2100.

4.2.3.2. Relative sea level changes

Relative SLC is the local sea level change relative to the land elevation at a specific location. Relative SLC is a combination of global and local sea level changes driven by the change in atmospheric circulation, hydrological cycle, and local vertical land movement (VLM) (Dalton et al., 2013; Mote et al., 2008; NRC, 2012). The VLM is not uniform along the coastal margin; land subsidence as a result of compaction of sediments, or extraction of groundwater, oil, and gas may cause sea level to rise more in some areas, while land uplift as a result of postglacial isostatic rebound or tectonic processes may decrease sea level rise in other areas (Mote et al., 2008; NOAA, 2010a; NRC, 2012; USACE, 2014; Zervas, 2009). Relative SLC can be measured using tide gauge data, repeat land leveling or GPS survey techniques, and InSAR remote sensing (NRC, 1987; Parris et al., 2012).

4.2.3.3. Relative SLC scenarios

Changes in shoreline erosion, inundation of low-lying areas, alteration in salinity intrusion, which causes a shift in vegetation cover and habitat are all recognized as a number of impacts that has threatened coastal and estuarine area (Glick et al., 2007) . To optimize the resilience and the performance of the coastal and estuarine projects, USACE policy required considering relative SLC effects in managing, planning,

designing, constructing, operating, and maintaining of the projects (USACE, 2013a, 2014). As part of these efforts, USACE developed a SLC Curve Calculator to compute relative SLC based on global SLC up to the year 2100 (USACE, 2013a). The calculator adds constant value of regional VLM (i.e., subsidence or uplift) to the different scenarios of global sea level change derived from the projections developed by NRC (2012), NOAA (Parris et al., 2012), and USACE (NRC, 1987; USACE, 2013a) by computing the following equation:

$$RE(t) = (E + VLM)t + b \quad (2)$$

Where *RE(t)* is relative SLC, *t* is the time from 1992–2100, *E* is eustatic sea level rise rate 0.0017 m/yr,. For the USACE's low, intermediate, and high scenarios, *b* is 0, 2.71E-05 and 1.13E-04, respectively and *b* is 2.71E-05, 8.71E-05, and 1.56E-04, respectively, for NOAA's intermediate–low, intermediate–high, and high scenarios.

While the first part of the equation (2) shows the linearity of the eustatic SLC, The term bt^2 represents the quadratic acceleration of eustatic seal level change as introduced by NRC.

We customized equation (2) to compute the relative SLC in Astoria station (Station ID: 9439040; Fig. 4. 1; Table 4. 1) in response to NOAA, NRC, and USACE scenarios. The eustatic sea level rise is 0.0017 m/yr and the VLM (subsidence rate) at Astoria is estimated at -0.0021 m/yr (NOAA, 2013b). The lowest NOAA and USACE scenario is defined based on a linear extrapolation of the historical relative mean sea level trend. There are two options for computing the relative mean sea level trend. The first is a relative mean sea level trend obtained from a linear regression of observed monthly sea levels from 1925–2006, which is -0.00031± 0.0004 m/yr (Zervas, 2009). The second

option uses the regionally corrected VLM estimate (-0.0021 m/yr) and adds it to the global sea level trend (0.0017 m/yr), thus providing a more technically accurate relative mean sea level trend (Parris et al., 2012; Zervas, 2013). Based on the latter approach, the lowest value for relative SLC in 2100 would be -0.04 (0.0017 (m/yr) – 0.0021(m/yr)*100 (yr)= -0.04 m). We chose the second computational approach to define the lowest NOAA and USACE scenario (Fig. 4. 4. 2, light blue line).

The historical trend in relative SLC provides a minimum baseline for future scenarios of relative SLC and information about past issues in the estuary. The relative SLC in response to NOAA intermediate low, intermediate high, and high global SLC was calculated by equation (2). Light blue, yellow, red, and mahogany curves (Fig. 4. 2) shows the relative SLC under NOAA low, intermediate low, intermediate high, and high from 1992 to 2100 respectively (Table 4. 1). The low, intermediate, and high scenario (USACE, 2013a) are shown with a light blue, yellow, and garnet line respectively (Fig. 4. 2). NRC Low and High scenarios are shown with a green line and purple bar respectively (Fig. 4. 2).

Though we computed relative SLC in Astoria, we needed to apply sea level change at the ocean boundary, ~300 km from the Columbia River mouth (Fig. 4. 1, black circle). We used the results of previous set of simulations for sea level rise studies, and created a linear regression model of ocean boundary elevation, based on elevation in Astoria (Equation (2)). Differences in elevation were extracted from the model result at Astoria and the ocean boundary for a whole year for each scenario relative to the reference. We then removed tide and averaged over the year.

$$Y = 1.0895X - 0.0060847 \quad (2)$$

Where y is the mean de-tide of elevation at ocean boundary and x is the mean de-tide of elevation at Astoria (R-square= 0.99). Our results for the new set of simulation also confirm the accuracy of the equation (2).

We added relative SLC to the non-tidal elevations applied at ocean boundaries to the U.S. Navy Coastal Ocean Model's (NCOM) daily sea surface height values. All other input files, including river, ocean, and atmospheric forcing, were kept the same as the reference simulation.

Multiple exploratory future scenarios and specifically extreme low and high scenarios would help decision makers assess the range of future climate change impact, vulnerability of the system, and a possible system threshold; therefore, design adaptation and mitigation plans accordingly (IPCC, 2013; Parris et al., 2012; USACE, 2013a). Although scientific consensus regarding global sea level rise exists, the accuracy of the sea level change projections regarding magnitude and timing are met with a range of uncertainty. While we acknowledge these uncertainties, the importance of identifying potential regions of change cannot be overlooked. For example, dismissing thresholds or tipping points could cause massive and irreversible regional damages (e.g. extinction of species).

4.3. Results

Our results indicated that larger change in sea level led to a significant impact on the extension of both saltwater inside the estuary and freshwater flushing out of the estuary; these changes were reflected in mean and in distribution by 2100 (Fig. 4. 3; 4. 4 a-b; 4. 5 a-b).

In the Columbia River estuary, in a moderate year (2010), maximum SIL extended to the river kilometer (RKm) ~37 during dry months (e.g. September) and ~17 RKm in freshet. The maximum salinity lines extended to a range of 45 to 170 km where sea level rose from 0.27 m to 1.77 m, respectively (Fig. 4. 4 a-b; Table 4. 2).

On average, almost 12% to 203% of water volume would be permanently changed to saltwater when sea level increases from 0.27 to 1.77 m, respectively, which is seen with the SV indicator (Fig. 4. 3; Table 4. 4). This represents roughly from 4.00E+09 to 6.67E+10 m^3 of freshwater at risk of changing to saline water (Fig. 4. 5 a-b; Table 4. 3). While mean SIL and SV increase with sea level rise, those decline by less than 2% with decreasing sea level (Fig. 4. 3; 4. 4 a-b and 4. 5 a-b; Table 4. 4). We also identified the bimodal distribution of salinity that happens when the estuary is in a state of low stream flow (less than ~8000 m^3/s) and is influenced by a sea level rise of more than 1 m. Changes are not linear—while the mean of SIL and SV increases with moderate sea level rise (<0.63 m) of less than 30%, there is a rapid response in SIL and SV to changes in sea level of more than ~ 1 m. Rapid changes in the future suggest that there might be an important threshold of response where sea level rises more than 1 m.

The bottom salinity map, when SIL has the highest value (September 28) also supports the change in salinity regime throughout the estuary and SIL calculation (Fig. 4. 6). The results suggest that although salinity propagates into the estuary with sea level rise up to the mouth of Grays and Cathlamet Bays (Fig. 4. 6a-d), the major change in salinity regime happens when sea level rises about 1 m (Fig. 4. 6e). With a 1 m sea level rise, Beaver Army Terminal would experience an influx of saltwater at ~ 16 psu (Fig. 4. 6e). Crossing the 1 m sea level rise threshold causes salt to propagate up to the

Port of Portland (Fig. 4. 6f). While salinity becomes more than 24 psu at the lower estuary and lateral Bays, freshwater becomes saltwater (~ 12 to 24 psu) at the Port of Longview and St. Helens (Fig. 4. 6f). The extreme sea level rise scenario (1.77 m) would cause the entire estuary, up to the Port of Portland, to experience increased salinity by more than 30 psu (Fig. 4. 6g). Even the Willamette River would see an increase in salinity of about 16 psu. Ridgefield Refuge and Multnomah Channel would lose freshwater habitat and anadromous fish would need to cope with salt level as high as ~ 137 RKm (Fig. 4. 6g).

We identified that salinity propagation inside the estuary is a nonlinear function of river flow, especially in the range of medium to large flow (~ 8000 m^3/s). With less than 8000 m^3/s river discharge at Bonneville Dam, SIL and SV will extend more than 100% with changing sea levels of more than ~1 m. Rapid changes in the future suggest that there might be an important threshold in river discharge in response of sea level rises more than 1 m (Fig. 4. 9).

Changes in salinity not only occur inside the estuary, but also in the fresh water moving out from the estuary to the ocean. Our results for PV, as a measurable indicator to evaluate river input to the ocean, show significant change under sea level rise scenarios relative to the contemporary system (Fig. 4. 7a-b).

The yearly mean value of PV decreases from 30% to 92% where sea level rose from 0.27 m to 1.77 m relative to the contemporary condition (Fig. 4. 7a-b, Table 4. 3 and 4). PV decreases throughout the seasons and on particular days with low river discharge; PV also tends to be zero when sea level rise is more than 1 m (Table 4. 2). During freshet, PV does not vanish, but it decreases by 100% when sea level rise is

more than 1 m (Fig. 4. 7a-b; Table 4. 4). In cases of declining sea level, mean PV only increases by 5%. Throughout the simulation year however, PV decreases to 15% and increases up to 27.30% (Table 4. 4).

The surface salinity map represents how the Columbia River's freshwater input to the Pacific Ocean would decline with sea level rise. The surface salinity was mapped for June 14th because on this day the estuary's freshwater volume flowing into the Pacific Ocean was at maximum levels due to high river discharge at Bonneville Dam and a favorable southward wind (Fig. 4. 8). The salinity regime for plume would change substantially with sea level rise, especially if sea levels rose above the 1 m threshold (Fig. 4. 8e-g).

We also calculated the SWH following sea level change for the entire estuary, as well as for each reach. Overall, the Columbia River estuary would provide more SWH between 6.9% up to 18.5% with a sea level rise of 0.27 to 1.77 m relative to the contemporary system (Fig. 4. 3; Table 4. 3 and 4. 4). Though the mean SWH declines by 1.8% relative to the 1.27 m sea level rise scenario, and it is minimally affected (1.22% decline) by a decreasing sea level scenario of -0.04 m (Table 4. 4). Dependent upon the regional bathymetry and topography of each reach, SWH presents both positive and negative change results under sea level rise scenarios relative to the contemporary condition at each reach. Reach A and C are vulnerable to 2% SWH loss when sea level rises by 1.77 m relative to the 1.27 m scenario, while reach B would experience a decrease in mean SWH by 3.4% and 4.5% when sea level rises by 1.27 m and 1.77 m relative to a 0.97 m sea level rise scenario (Fig. 4.10; Table 4. 5 and 4. 6).

Conversely, mean SWH increases with sea level rise at reach D, E, F, and G by more than 100%, while reach H loses SWH by 12% relative to the contemporary system

To show the spatial pattern of SWH, we present SWH values for each element (from June 14th when there was a peak in SWH) instead of as an integrated value for each region in the Columbia River estuary. The resulting values indicate that SWH does not necessarily change only positively or negatively. In fact, SWH may increase in some areas, while decreasing in other areas of the same reach (Fig. 4. 11; Table 4. 7). For instance, part of Cathlamet Bay experiences increased SWH near Marsh Island (green color area), while at the same time loses SWH at the mouth of Gray's Bay and near Sauvie Island (yellow color area) when sea level rises by 1.77 m relative to the contemporary condition (Fig. 4. 11).

While the SWH indicator is a general indicator and could be used for all species sensitive to depth, we computed habitat specifically for juvenile Chinook salmon habitat (SH). Although there is a shift in salinity-influenced areas in the estuary, habitat becomes more favorable for juvenile Chinook salmon depending on how salmon habitat indicators are defined. Mean SH declines by less than 1% (6.39E+05) when sea level decreases by -0.04 m and increases between 3.48% to 13.62% with sea level rise scenarios of 0.27 m, and 1.77 m relative to the contemporary system. Interestingly, mean SH further declines by 4.5 % (5.62E+06) with a sea level rise of 1.77 m relative to the 1.27 m scenario (Fig. 4. 3; Table 4. 3 and 4. 4).

Sea level rise scenarios change SH at each reach depending on geometry, bathymetry, distance from the ocean, and distance from the Bonneville Dam. Mean SH increases by 45.27% (reach A) and 35.40% (reach C) with a sea level rise of 1.27 m

relative to the contemporary system; however, with a sea level rise of 1.77 m, both reaches lose their SH by 0.75% (reach A) and 8.1% (reach C) relative to the 1.27 m scenario (Fig. 4. 12; Table 4. 9). While sea level rise by 1 m doesn't impact SH at reach B, it loses habitat by 3.65% and 13.42% with a sea level rise scenario of 1.27 m and 1.77 m, respectively (Fig. 4. 12; Table 4. 9). Of all of the reaches, reach D and E are very sensitive to sea level changes. Mean SH increases by 880% (reach D) and 174% (reach E) when sea level rise scenarios are extreme (Fig. 4. 12; Table 4. 9) but there is also an increase in SH during June when river discharge has the highest value and causes an increase of up to 4150% (reach D) and 561% (reach E) relative to the contemporary condition (Fig. 4. 12; Table 4. 9). The impacts of sea level rise appear to lessen moving closer to the upper reaches of F, G, and H. Mean SH increases with sea level rise at reach G and H and overall changes are less than 11%; however, the changes are not consistent throughout the seasons and SH both increases and decreases with sea level rise scenarios relative to the contemporary system. Mean SH decreases by maximum 7.51% at reach H and suggests that this reach would lose habitat (Fig. 4. 11; Table 4. 9).

Our sensitivity analysis, which is the computation of water volume based on an individual criterion (not shown), indicates that depth criterion modulates SH changes. For juvenile Chinook salmon only, depth criterion is a dominant factor that changes SH. Although salt volume propagates into the estuary, it has less impact on areas with depths between 0.5 m and 2 m, though overall, increased salt at all depths may change habitat for species sensitive to salinity. Because of this, extensive assessment of the changes in the Columbia River estuary, as well as the development of indicators for

other species, are essential and outcomes from these analyses must be used to guide the design of optimal conservation and adaptation plans.

4.4. Discussion

Using regionally accepted habitat-relevant indicators, we anticipate that the estuary would cross thresholds and undergo drastic and irreversible changes in response to higher sea level rise scenarios (>1 m) relative to the contemporary system. Although it is known that inundation of low-lying lands is a main response to sea level rise, our results suggest that beyond the inundation impacts, sea level rise leads to substantial changes in salinity propagation in the estuary and freshwater exports through the plume spread when sea level rises by more than ~1 m. Salinity will propagate upstream from 38 Rkm in the contemporary system to the Port of Portland (extend up the Columbia River by RKm 137 and part of the Willamette River during the dry season when sea level rises by 1.77 m relative to the current mean sea level. The salt propagation to the upper reaches limits freshwater habitat area and poses severe threats to anadromous and other species depending on freshwater habitats. These findings were consistent with Glick (2007) who found that the Columbia River estuary will lose fresh water habitat due to salt water propagation by sea level rise. Among the salmon species that rear in freshwater habitat more than one year, sockeye, stream–type Chinook and coho salmon, and steelhead would potentially be affected by altered salinity regime. It would likely bring more hypoxic water, especially in spring and summer, with coastal upwelling (Roegner et al., 2011) causing the water chemistry to change up to the Port of Portland. There would also be potential changes in fish food distribution and availability since

food webs differ in saltwater and freshwater. The tidal freshwater marshes and riparian wetlands providing anadromous species with habitat, food (insects), and refuge (Simenstad et al., 1982) would vanish and change into saltwater vegetation. Water column stratification would also change with the propagation of more saltwater from the ocean. Since anadromous fish change behaviorally and physiologically when moving from freshwater to saltwater and vice versa, they must stay along the boundary line between fresh and saltwater for up to a week in order to adapt to their new environment. If sea level was to rise 1.77 m, juvenile salmon would have to adapt to saltwater earlier in their journey to the ocean (about 97 km earlier) and do so in narrower channels at reach G and H, rather than reach C and part of reach B, where they currently adapt to saltwater in the contemporary system. Some species would be threatened by altered salinity regime while others would adapt well to the new environment; these shifts will make habitats more favorable for some species and less for others.

As saltwater moves inland with sea level rise, it limits freshwater plume by 100% when sea level rise by 1 m relative to the contemporary system. The Pacific Ocean would lose the Columbia River freshwater input, which is about 77% of the total drainage along the US west coast, from San Francisco Bay to Juan de Fuca (Barnes et al., 1972). The plume front, with a 4 to 47 times higher biomass of plankton than adjacent water (Morgan et al., 2005), would vanish. Because the plume is a primary mechanism for salmon to migrate to the ocean, such drastic changes in plume volume would likely alter salmon distribution, growth, and survival rate since each depends upon plume

characteristics (Burla et al., 2010; De Robertis et al., 2005; Hickey et al., 2010; Scheuerell and Williams, 2005).

While SWH and SH for the entire estuary increase with sea level rise due to more area being inundated, the yearly mean habitat for both shallow water and juvenile Chinook salmon decreases as the 1.27 m sea level rise threshold is crossed. Depending on the topography and bathymetry of each reach, our findings suggest that the effects of SLC on SWH and SH will be localized and not homogenous throughout the estuary and there will be winners and losers in terms of stocks, regions and periods. Because of more inundated area, reach D, E, F, and G provide more shallow water habitat and habitat for juvenile Chinook salmon under the scenarios of sea level rise relative to the current system. In contrast, with SLR more than 1 m, reach B and H will lose habitat during May, when the Upper Columbia River summer/fall fry and Spring Creek Group fall fingerling are predominant stocks (60%, 90% respectively). When SLR is more than 1.27 m, reach C also loses habitat during May, when West Cascade fall fry, West Cascade fall, and Spring Creek Group fall fingerling are predominant stocks (96%, 40%, 50% respectively).

We found that critical sea level rise thresholds have specific values ranging from 0.97-1.27 m for indicators. We suggested considering the lower value of this range, 1 m, as a critical threshold for sea level rise. We also assessed the river discharge threshold to be about 8000 m^3/s at Bonneville Dam. We discovered that once the critical threshold for sea level rise (~1 m) is crossed, only river discharge more than 8000 m^3/s may prevent salt propagation into the estuary. However, it is only during the freshet, Bonneville Dam could afford sending that amount of water to the estuary.

4.4.1. Uncertainty and limitations of the study

The uncertain and potential effects of sea level change cause great challenges for stakeholders and decision makers. We used a circulation model to calculate the defined indicators in the Columbia River estuary for the contemporary system and future scenarios of sea level change. However, sea level change influences sediment transport in such a way that non-linear and non-reversible changes may happen as thresholds are crossed (IPCC, 2007). If accretion rate becomes less than sea level rise rate, then the potential for submergence is high. To determine the actual elevation changes in response to SLC scenarios, the sediment model needs to be coupled with the circulation model to sufficiently calculate sediment deposition and erosion. We ran both a sediment model and a circulation model and compared the models' estimated accretion and erosion rates with some of the observed rates noted by Borde et al. (2012). This was done to ensure that the sediment model captured the sediment dynamic inside the estuary. Although the estimated rates were not the same as observed rates, the differences did not vary greatly. We compared the calculated salmon habitat based on the results using only a circulation model with the results using a sediment model plus a circulation model. Though the outcome showed some differences in salmon habitat, the differences were not sufficient enough to consider the impacts of sediment transport in salmon habitat analyses. The differences are acknowledged as part of the uncertainty of not considering a sediment model in the salmon habitat analyses.

In addition to that, there are multiple factors of uncertainty ranging from the defined projected sea level changes scenarios, both in global and regional scale, to hydrodynamic model output errors and hydrodynamic model input errors, as well as

uncertainty regarding atmospheric forcing, river and ocean forcing data, and grid resolution. These forces are kept the same for sea level change scenarios and the contemporary condition; however, river and ocean conditions will change by 2100. Though we only evaluated the impact of sea level change, it should be noted that climate change has a combined impact on the Columbia River, consisting of rising temperatures and changes in hydrologic stream flow regimes, which will influence the response of the system to sea level changes.

Based on our definition of defined thresholds for juvenile Chinook salmon, the species looks to benefit from sea level rise. However, our method, which computes habitat regardless of food availability and vegetation, is simple and must be considered with caution. Even though the integrated SWH for each reach responded to the sea level rise positively or negatively relative to the contemporary system, the map for SWH reveals that the sea level change response is not homogenous throughout each reach. Thus, defining appropriate regions, which may be smaller than the actual geomorphological reaches, may be needed in order to design more effective restoration plans aimed at preserving fish habitat.

4.5. Conclusion

Analyzing the environmental indicators quantitatively and identifying the system's threshold response to sea level rise are both powerful approaches to understanding the complex effects of change on the estuarine ecosystem. They are also useful in informing managers and decision makers on how to make environmentally sound management and policy decisions. Notably, we quantified fish habitat–relevant

indicators and identified the sea level rise threshold as ~1 m. Our indicator analyses suggest that the sea level changes (when increased by more than 1 m) would substantially alter estuarine salinity regime in such a way that the saltwater would propagate up to the Willamette River and freshwater plume would disappear when sea level rise by 1.77 m. Such changes in the estuary would alter the freshwater ecosystem significantly. Though regional topography and bathymetry influences estuarine shallow water habitat and juvenile Chinook salmon habitat response to sea level change, the estuary overall, will lose habitat once the extreme sea level rise (1.27 m) has been crossed.

While there are considerable uncertainties with the regional sea level change scenarios, our results reveal that at certain sea level thresholds, the potential for massive change in the Columbia River (CR) estuary is too important to be ignored. In fact, decisions about mitigation and adaption plans cannot be postponed until more accurate future scenarios become available. Just because we don't know precisely when and where we will experience the impacts, doesn't mean that we shouldn't attempt to prevent any permanent damage (e.g. species extinction) that might arise due to future changes in the CR estuary. Regardless of the degree of uncertainty, specifically for the socio-ecological impacts, considering the high-end sea level rise scenario would identify the intensification of estuarine hazard and risk. There is always a degree of uncertainty about how, when, and where this system will experience the impact of sea level changes. However, an extensive and continuous monitoring system will help track ongoing changes and therefore, prevent permanent system damages.

Tables

Table 4. 1. Relative sea level change projection for year 2100. Gauge: 9439040, Astoria, OR. NOAA's regional rate: -0.00040 m/yr. All values are expressed in meters relative to the local mean sea level.

Scenario	Global Sea Level Change (m)	Sea Level Change Astoria (m)	Sea Level Change Ocean Boundary (m)
USACE low & NOAA low	0.2	-0.04	-0.05
USACE intermediate & NOAA intermediate	0.5	0.27	0.29
NOAA intermediate high	1.2	0.97	1.05
USACE high	1.5	1.27	1.38
NOAA high	2	1.77	1.92
NRC, 2012	1.4	0.63	0.68

Table 4. 2. Yearly minimum, mean, and maximum of daily (tidally averaged) values for the indicators: salinity intrusion length (SIL), salt volume (SV), plume volume (PV), shallow water habitat (SWH), and salmon habitat (SH) for the contemporary condition and six scenarios of sea level change.

		SLC (m)[a]						
		0 [b]	**-0.04**	**0.27**	**0.63**	**0.97**	**1.27**	**1.77**
SIL (km)	**Min**	17.01	16.96	18.28	19.89	21.64	24.05	26.80
	Mean	27.74	27.28	30.60	35.61	45.43	71.34	128.57
	Max	36.82	36.03	45.00	51.90	96.80	166.80	170.06
SV (m^3)	**Min**	1.63E+10	1.60E+10	1.78E+10	2.03E+10	2.35E+10	2.68E+10	3.42E+10
	Mean	3.33E+10	3.27E+10	3.73E+10	4.45E+10	5.50E+10	7.03E+10	1.00E+11
	Max	4.70E+10	4.62E+10	5.31E+10	6.50E+10	8.60E+10	1.12E+11	1.26E+11
PV (m^3)	**Min**	3.80E+08	3.60E+08	2.06E+08	1.03E+07	0	0	0
	Mean	1.40E+10	1.45E+10	1.08E+10	6.92E+09	4.15E+09	2.63E+09	9.05E+08
	Max	1.11E+11	1.13E+11	9.88E+10	8.12E+10	6.21E+10	4.92E+10	2.58E+10
SWH (m^2)	**Min**	1.70E+8	1.67E+8	1.87E+8	2.19E+8	2.50E+8	2.54E+8	2.26E+8
	Mean	2.73E+8	2.70E+8	2.91E+8	3.11E+8	3.22E+8	3.25E+8	3.20E+8
	Max	3.46E+8	3.43E+08	3.62E+8	3.68E+8	3.75E+8	3.76E+8	3.74E+8
SH (m^3)	**Min**	4.37E+7	4.33E+7	4.59E+7	4.92E+7	5.14E+7	5.29E+7	5.29E+7
	Mean	1.11E+8	1.10E+8	1.15E+8	1.20E+8	1.25E+8	1.31E+8	1.25E+8
	Max	1.58E+8	1.56E+8	1.69E+8	1.86E+8	1.92E+8	1.98E+8	1.69E+8

[a] Sea level change in meters
[b] Mean sea level for the contemporary condition (year 2010)

Table 4. 3. Yearly minimum, mean, and maximum of difference values for the indicators: salinity intrusion length (SIL), salt volume (SV), plume volume (PV), shallow water habitat (SWH), and salmon habitat (SH) for six scenarios of sea level change minus the contemporary condition.

		Sea level change scenarios minus the contemporary system					
		-0.04	**0.27**	**0.63**	**0.97**	**1.27**	**1.77**
	Min	-7.30	-3.85	-2.02	1.09	4.69	7.34
SIL	**Mean**	-0.47	2.86	7.86	17.69	43.64	100.73
(km)	**Max**	4.31	8.55	17.07	63.15	134.82	141.36
	Min	-7.35E+9	-4.70E+9	-7.10E+8	4.93E+9	1.06E+10	1.80E+10
SV	**Mean**	-6.47E+8	3.92E+9	1.11E+10	2.15E+10	3.69E+10	6.74E+10
(m^3)	**Max**	-2.33E+8	7.22E+9	2.10E+10	4.21E+10	7.32E+11	9.37E+11
	Min	-5.54E+8	-1.39E+10	-3.31E+10	-5.04E+10	-6.79E+10	-1.04E+11
PV	**Mean**	5.44E+8	-3.11E+9	-7.07E+09	-1.02E+10	-1.36E+10	-2.35E+10
(m^3)	**Max**	2.27E+9	-1.13E+8	-2.75E+8	-3.49E+8	-7.20E+8	-8.16E+10
	Min	-8.32E+6	7.60E+6	1.34E+7	1.01E+7	5.16E+7	-2.20E+7
SWH	**Mean**	-3.20E+6	1.83E+7	3.80E+7	4.89E+7	5.24E+7	4.75E+7
(m^2)	**Max**	1.89E+07	3.85E+7	5.81E+7	8.23E+8	9.52E+8	1.00E+8
	Min	-2.59E+6	-7.67E+5	-2.5E+5	8.08E+4	5.82E+6	-1.54E+7
SH	**Mean**	-6.39E+5	3.79E+6	9.03E+6	1.33E+7	1.97E+7	1.41E+7
(m^3)	**Max**	8.60E+5	1.23E+7	3.03E+7	3.70E+7	4.55E+7	3.75E+7

Table 4. 4. Yearly minimum, mean, and maximum of percent changes for indicators: salinity intrusion length (SIL), salt volume (SV), plume volume (PV), shallow water habitat (SWH), and salmon habitat (SH) for six scenarios of sea level change relative to the contemporary condition.

		SLC (m)[a]					
		-0.04	**0.27**	**0.63**	**0.97**	**1.27**	**1.77**
SIL	**Min**	-21.33	-17.00	-8.90	4.81	22.14	37.67
	Mean	-1.51	10.19	27.70	60.38	147.00	356.00
	Max	18.26	35.26	61.34	193.66	500.31	640.00
SV	**Min**	-20.56	-13.16	-2.00	13.80	32.65	80.22
	Mean	-2.00	11.66	32.88	63.52	109.06	203.01
	Max	-0.76	18.15	55.72	126.35	276.94	420.22
PV	**Min**	-15.02	-90.75	-99.70	-100.00	-100.00	-100.00
	Mean	5.37	-30.04	-65.00	-84.15	-90.36	-92.43
	Max	27.30	-9.35	-22.08	-34.60	-44.11	-65.00
SWH	**Min**	-3.46	2.46	4.18	3.42	1.74	-8.84
	Mean	-1.22	6.91	14.49	18.88	20.27	18.48
	Max	6.68	15.17	30.41	47.65	53.80	58.60
SH	**Min**	-1.63	-0.66	-0.23	0.05	4.03	-9.91
	Mean	-0.58	3.48	8.28	12.37	18.13	13.62
	Max	0.67	8.74	19.48	24.14	39.00	63.28

[a] Sea level change in meters

Table 4. 5. Yearly minimum, mean, and maximum of daily (tidally averaged) values for shallow water habitat (SWH) at eight reaches in the contemporary condition and for six scenarios of sea level change.

		SLC (m)[a]						
Reach		**0**	**-0.04**	**0.27**	**0.63**	**0.97**	**1.27**	**1.77**
	Min	4.45E+7	4.40E+6	4.72E+7	5.03E+7	5.45E+7	5.17E+7	4.60E+7
A	Mean	5.80E+7	5.73E+7	6.21E+7	6.71E+7	6.98E+7	7.10E+7	7.04E+7
	Max	7.13E+7	7.11E+7	7.63E+7	7.80E+7	8.09E+7	8.30E+7	8.37E+7
	Min	7.90E+7	7.89E+7	8.39E+7	9.13E+7	9.27E+7	8.26E+7	6.84E+7
B	Mean	1.14E+8	1.13E+8	1.18E+8	1.23E+8	1.23E+8	1.19E+8	1.08E+8
	Max	1.43E+8	1.42E+8	1.46E+8	1.45E+8	1.40E+8	1.37E+8	1.30E+8
	Min	3.09E+7	2.96E+7	3.88E+7	5.24E+7	6.01E+7	5.74E+7	4.91E+7
C	Mean	6.11E+7	6.00E+7	6.74E+7	7.35E+7	7.73E+7	7.87E+7	7.70E+7
	Max	7.83E+7	7.78E+7	8.33E+7	8.62E+7	8.82E+7	9.03E+7	8.74E+7
	Min	3.50E+4	3.50E+4	4.74E+4	8.35E+4	8.35E+4	1.13E+5	5.65E+5
D	Mean	3.45E+5	3.27E+5	5.00E+5	7.26E+5	1.04E+6	1.40E+6	2.17E+6
	Max	2.37E+6	2.37E+6	2.86E+6	3.74E+6	5.33E+6	6.85E+6	8.40E+6
	Min	6.60E+5	6.60E+5	7.57E+5	8.86E+4	9.64E+4	9.35E+5	1.60E+6
E	Mean	1.60E+6	1.57E+6	1.85E+6	2.27E+6	2.87E+6	3.57E+6	5.07E+6
	Max	1.22E+7	1.20E+7	1.29E+7	1.39E+7	1.54E+7	1.65E+7	1.97E+7
	Min	7.08E+6	6.95E+6	8.48E+6	1.32E+7	2.49E+7	2.50E+7	2.48E+7
F	Mean	3.13E+7	3.08E+7	3.40E+7	3.72E+7	4.04E+7	4.38E+7	5.00E+7
	Max	5.63E+7	5.62E+7	5.67E+7	5.75E+7	5.88E+7	6.17E+7	6.61E+7
	Min	1.70E+6	1.70E+6	1.79E+6	2.03E+6	2.12E+6	2.30E+6	2.28E+6
G	Mean	2.89E+6	2.87E+6	3.13E+6	3.40E+6	3.70E+6	4.08E+6	4.76E+6
	Max	7.81E+6	7.81E+6	8.10E+6	8.15E+6	8.53E+6	8.72E+6	8.65E+6
	Min	2.07E+5	2.07E+5	2.07E+5	1.96E+5	1.85E+5	1.85E+5	1.85E+5
H	Mean	3.54E+6	3.53E+6	3.53E+6	3.50E+6	3.45E+6	3.37E+6	3.12E+6
	Max	5.43E+6	5.35E+6	5.33E+6	5.28E+6	5.27E+6	5.16E+6	5.10E+6

[a] Sea level change in meters

Table 4. 6. Yearly minimum, mean, and maximum of percent changes for shallow water habitat (SWH) at eight reaches for six scenarios of sea level change relative to the contemporary condition.

		SLC (m)[a]					
Reach		**-0.04**	**0.27**	**0.63**	**0.97**	**1.27**	**1.77**
	Min	-3.37	2.64	8.00	10.15	5.72	-5.88
A	Mean	-1.06	7.07	16.00	20.76	22.78	21.42
	Max	3.46	13.10	21.65	27.44	32.62	33.28
	Min	-3.90	-1.11	-3.92	-7.6	-12.48	-26.88
B	Mean	-0.67	4.05	8.31	8.84	5.46	-4.32
	Max	10.84	15.14	20.08	26.56	28.39	24.09
	Min	-5.56	1.00	-0.48	-4.22	-9.34	-16.60
C	Mean	-2.17	11.28	22.17	29.08	32.00	30.00
	Max	5.2	27.55	70.00	101.27	109.04	124.26
	Min	-49.21	-28.85	21.46	62.81	119.38	193.60
D	Mean	-5.00	58.41	168.00	370.50	586.86	1001.70
	Max	81.42	526.70	1182.40	2197.50	2808.10	4848.00
	Min	-23.30	-11.00	-2.51	8.51	10.70	59.66
E	Mean	-1.90	15.8	42.31	81.30	127.09	230.85
	Max	26.40	79.60	129.14	208.75	307.89	508.00
	Min	-19.84	-3.28	-6.28	-14.17	-14.80	-15.00
F	Mean	-2.14	11.17	23.51	35.28	47.23	67.56
	Max	27.83	82.26	159.29	257.15	287.00	364.60
	Min	-38.03	-27.00	-51.07	-57.18	-53.21	-52.00
G	Mean	-0.67	8.92	19.68	30.56	45.19	71.38
	Max	102.13	118.93	118.00	132.73	139.36	150.51
	Min	-58.40	-0.61	-62.78	-62.20	-62.05	-63.00
H	Mean	-0.20	-0.62	-1.66	-3.30	-5.70	-12.00
	Max	11.90	18.27	17.16	27.56	45.10	71.60

[a] Sea level change in meters

Table 4. 7. Shallow water habitat (SWH) changes for six scenarios of sea level change relative to the contemporary system. Shallow water habitat is calculated in each element on June 14th, when most reaches show the highest value of shallow water habitat.

	SLC (m)[a]					
SWH(m^2)	**-0.04**	**0.27**	**0.63**	**0.97**	**1.27**	**1.77**
Positive Change	2.21E+6	3.10E+7	5.30E+7	6.83E+7	8.22E+7	1.02E+8
Negative Change	-4.65E+6	-1.67E+7	-3.85E+7	-5.45E+7	-7.02E+7	-9.83E+7

[a] Sea level change in meters

Table 4. 8. Yearly minimum, mean, and maximum of daily (tidally averaged) values for salmon habitat (SH) at eight reaches in the contemporary condition and for six scenarios of sea level change.

		SLC (m)[a]						
Reach		**0**	**-0.04**	**0.27**	**0.63**	**0.97**	**1.27**	**1.77**
	Min	9.96E+6	9.86E+6	1.04E+7	1.12E+7	1.13E+7	1.34E+7	1.48E+7
A	Mean	1.96E+7	1.94E+7	2.07E+7	2.21E+7	2.31E+7	2.80E+7	2.77E+7
	Max	2.78E+7	2.75E+7	2.91E+7	2.95E+7	2.86E+7	3.30E+7	3.14E+7
	Min	1.59E+7	1.59E+7	1.58E+7	1.55E+7	1.50E+7	1.46E+7	1.19E+7
B	Mean	3.55E+7	3.54E+7	3.59E+7	3.58E+7	3.53E+7	3.40E+7	3.03E+7
	Max	5.66E+7	5.68E+7	5.60E+7	5.53E+7	5.55E+7	5.52E+7	4.61E+7
	Min	7.96E+6	7.72E+6	9.53E+7	1.20E+7	1.43E+7	1.60E+7	1.16E+7
C	Mean	2.91E+7	2.88E+7	3.11E+7	3.45E+7	3.73E+7	3.88E+7	3.61E+7
	Max	4.40E+7	4.33E+7	4.94E+7	5.85E+7	6.11E+7	6.54E+7	5.34E+7
	Min	1.27E+4	1.20E+4	1.82E+4	3.50E+4	5.44E+4	1.13E+5	1.48E+5
D	Mean	8.42E+4	8.06E+4	1.09E+5	1.53E+5	2.14E+5	3.46E+5	6.14E+5
	Max	5.25E+5	5.10E+5	6.50E+5	8.85E+5	1.57E+6	2.02E+6	3.37E+6
	Min	4.30E+5	4.45E+5	3.61E+5	2.54E+4	3.37E+4	5.34E+5	5.29E+5
E	Mean	9.50E+5	9.51E+5	9.96E+5	1.04E+6	1.53E+6	2.60E+6	2.63E+6
	Max	3.26E+6	3.16E+6	3.73E+6	5.18E+6	6.05E+6	1.08E+7	1.34E+7
	Min	2.39E+6	2.40E+6	2.41E+6	2.53E+6	2.56E+6	2.60E+6	2.70E+6
F	Mean	2.16E+7	2.16E+7	2.18E+7	2.22E+7	2.26E+7	2.28E+7	2.37E+7
	Max	4.50E+7	4.55E+7	4.50E+7	4.70E+7	4.51E+7	4.53E+7	4.72E+7
	Min	1.01E+5	1.01E+5	1.05E+5	1.09E+5	1.07E+5	1.07E+5	1.03E+5
G	Mean	1.14E+6	1.14E+6	1.13E+6	1.13E+6	1.14E+6	1.15E+6	1.18E+6
	Max	2.29E+6	2.30E+6	2.20E+6	2.13E+6	2.07E+6	2.04E+6	2.10E+6
	Min	4.81E+5	4.82E+5	4.86E+5	5.01E+5	5.00E+5	4.85E+5	4.68E+5
H	Mean	3.47E+6	3.46E+6	3.47E+6	3.48E+6	3.49E+6	3.46E+6	3.27E+6
	Max	6.50E+6	6.49E+6	6.50E+6	6.54E+6	6.60E+6	6.52E+6	6.68E+6

[a] Sea level change in meters

Table 4. 9. Yearly minimum, mean, and maximum of percent changes for salmon habitat (SH) at eight reaches for six scenarios of sea level change relative to the contemporary condition.

		SLC (m)[a]					
Reach		**-0.04**	**0.27**	**0.63**	**0.97**	**1.27**	**1.77**
	Min	-2.75	-0.48	-5.73	-5.72	5.70	4.74
A	Mean	-1.02	5.91	14.00	19.76	45.27	44.52
	Max	0.20	16.10	39.05	54.64	104.53	108.80
	Min	-1.83	-7.28	-14.20	-19.06	-24.48	-41.26
B	Mean	-0.34	1.02	1.00	-0.25	-3.64	-13.42
	Max	1.50	6.19	11.02	17.27	43.77	62.61
	Min	-5.20	-4.67	-6.12	-10.00	-6.60	-32.80
C	Mean	-1.06	7.62	19.40	30.40	35.40	27.30
	Max	2.43	37.40	93.00	139.44	130.00	118.21
	Min	-14.06	-5.26	34.00	64.28	87.30	107.02
D	Mean	-4.10	31.45	89.26	164.57	396.42	880.65
	Max	4.00	83.27	184.32	350.02	1574.80	4150.75
	Min	-7.02	-26.00	-47.94	-30.91	-10.57	-8.15
E	Mean	0.35	4.15	7.00	60.36	174.10	174.00
	Max	3.91	28.56	68.80	159.44	481.17	561.22
	Min	-3.15	-14.23	-19.25	-19.43	-18.60	-21.11
F	Mean	-0.06	0.66	2.95	4.67	5.78	10.55
	Max	4.63	8.64	23.29	26.00	31.58	45.36
	Min	-1.33	-13.05	-27.30	-35.44	-41.67	-52.33
G	Mean	0.06	-0.12	0.41	1.30	2.52	5.31
	Max	3.10	8.40	13.08	22.00	26.88	47.32
	Min	-1.26	-6.40	-13.90	-20.00	-26.00	-35.22
H	Mean	-0.00	-0.17	-0.42	-0.84	-2.08	-7.51
	Max	1.52	7.00	8.66	12.70	18.40	29.04

[a] Sea level change in meters

Figures

Figure 4. 1. Top view of unstructured grid with bathymetry for Columbia River estuary and shelf, extending from Bonneville dam to the Pacific Ocean with 8 hydrogeomorphic reaches of the Columbia River Estuary Ecosystem Classification (Simenstad et al., 2011b). (a) The full extent of model domain, along the west coast of the U.S. from California to British Columbia; (b) zoom-in of the Columbia River estuary; Black circles show the NOAA tide gauge at Astoria station (Station ID: 9439040), the location of computed offshore sea level change, and Bonneville Dam.

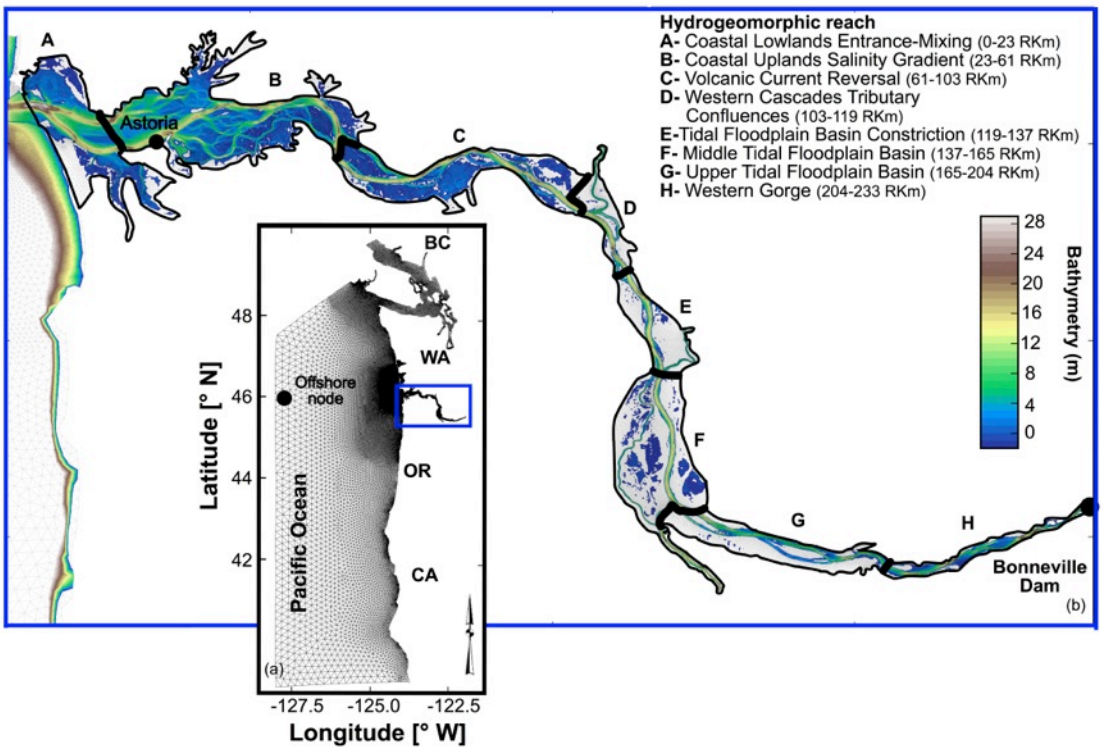

Figure 4. 2. Estimated relative sea level change from 1992 to 2100 at Astoria, OR, NOAA tide gauge: 9439040, NOAA's regional rate:-0.00040 m/yr. All sea level change values are expressed in meters relative to local mean sea level.

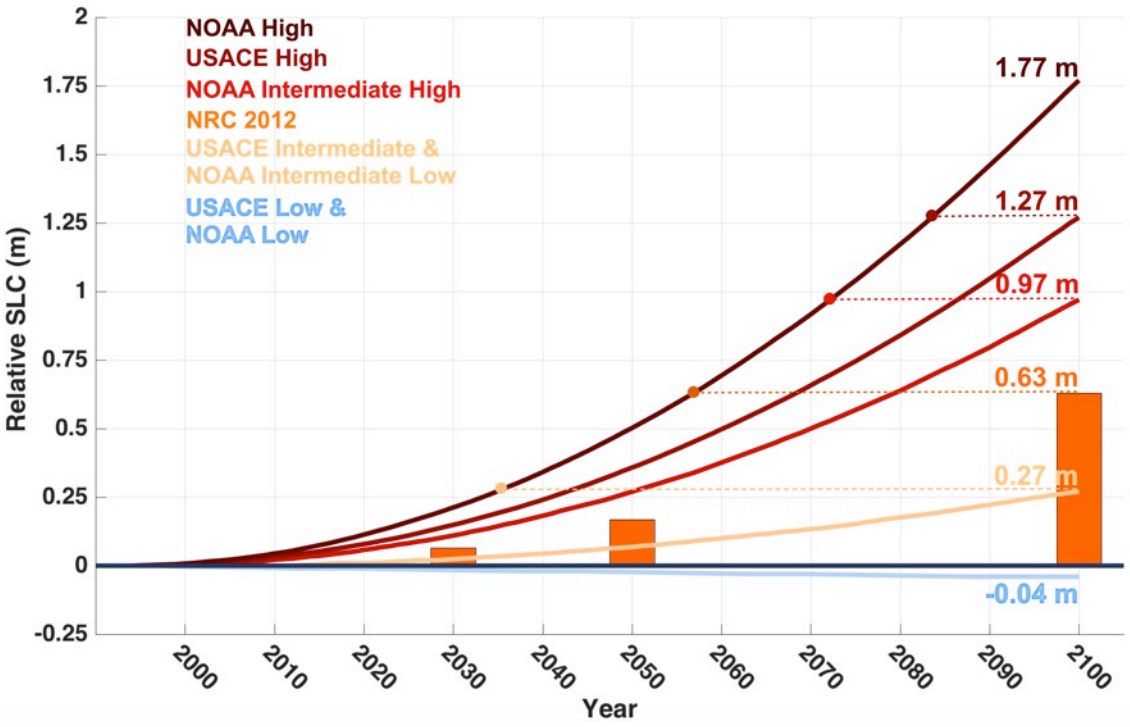

Figure 4. 3. Percent changes in salinity intrusion length (SIL), salt volume (SV), plume volume (PV), shallow water habitat (SWH), and salmon habitat (SH) for six scenarios of sea level change relative to the contemporary condition. The range of color bars reflects the different scenarios. In each bar, the lighter color indicates the maximum and minimum, the darker color indicates the 25th and 75th percentile, and the white circle indicates the average of each indicator for each scenario.

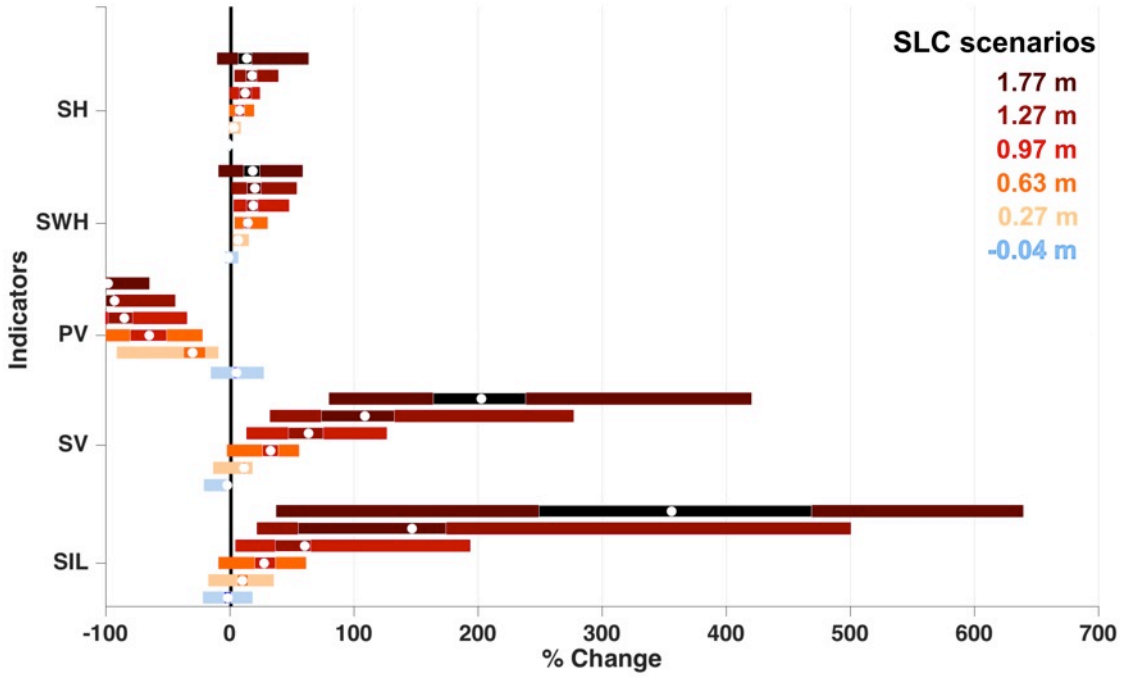

Figure 4. 4. Salinity intrusion length (SIL) in the Columbia River estuary for the contemporary condition (CC; year 2010) and six scenarios of sea level change. Histograms at the top panel show the distribution of SIL. The lower panel shows the timeseries of SIL.

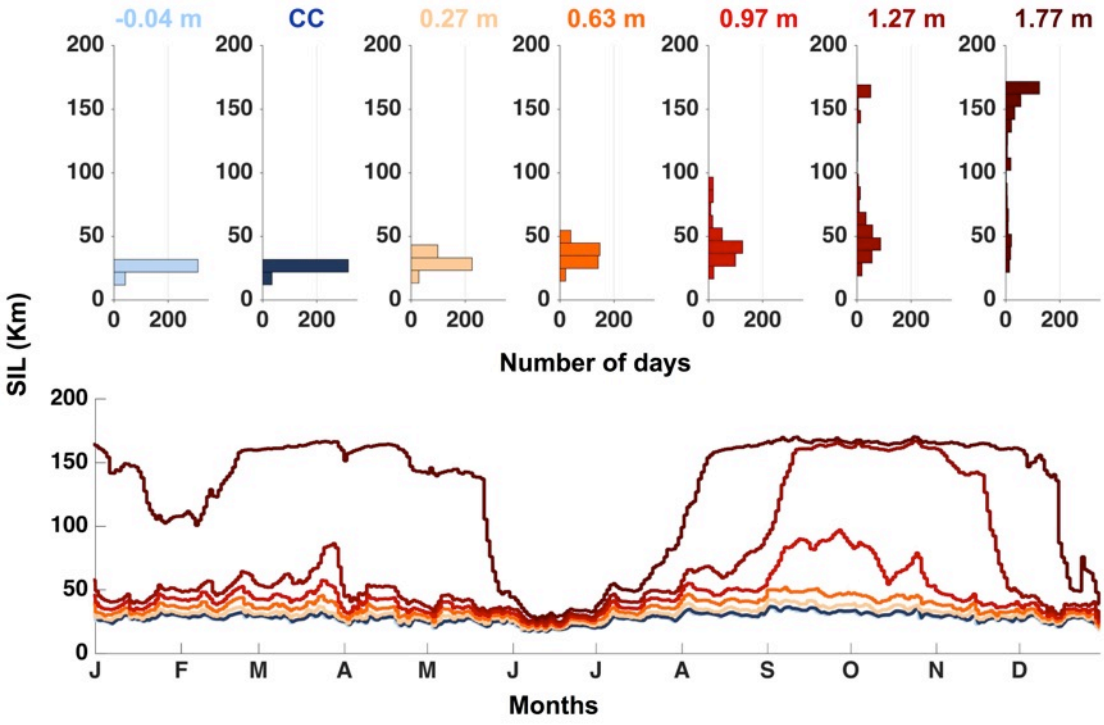

Figure 4. 5. Salt volume (SV) in the Columbia River estuary for the contemporary condition (CC; year 2010) and six scenarios of sea level change. Histograms at the top panel show the distribution of SV. The lower panel shows the timeseries of SV.

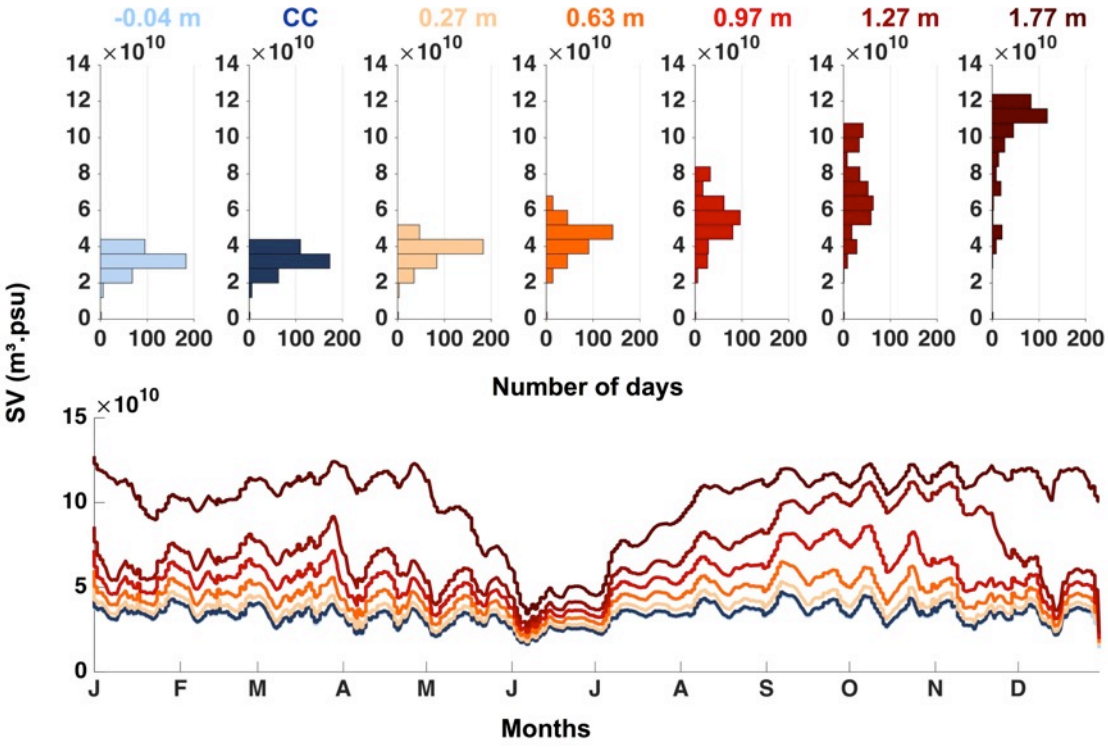

Figure 4. 6. Isoline map of bottom salinity response to a) contemporary condition and for six scenarios of sea level change: b) -0.04 m, c) 0.27 m, d) 0.63 m, e) 0.97 m, f) 1.27 m, g) 1.77 m on September 28th in the Columbia River estuary.

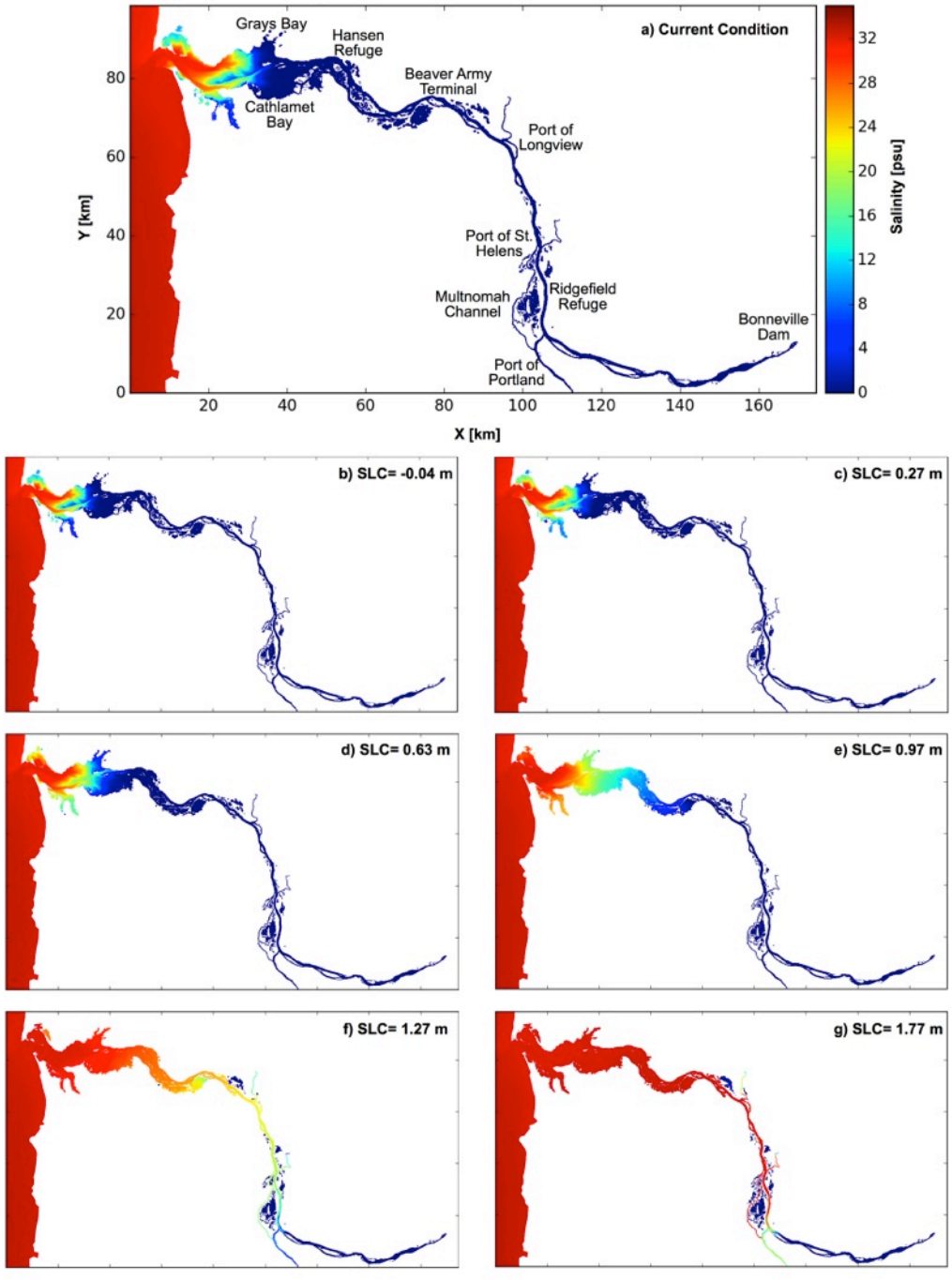

Figure 4. 7. Plume volume (PV) in the Columbia River estuary for the contemporary condition (CC; year 2010) and six scenarios of sea level change. Histograms at the top panel show the distribution of PV. There are zoom-in views of parts of original histograms for each scenario. The lower panel shows the time series of PV.

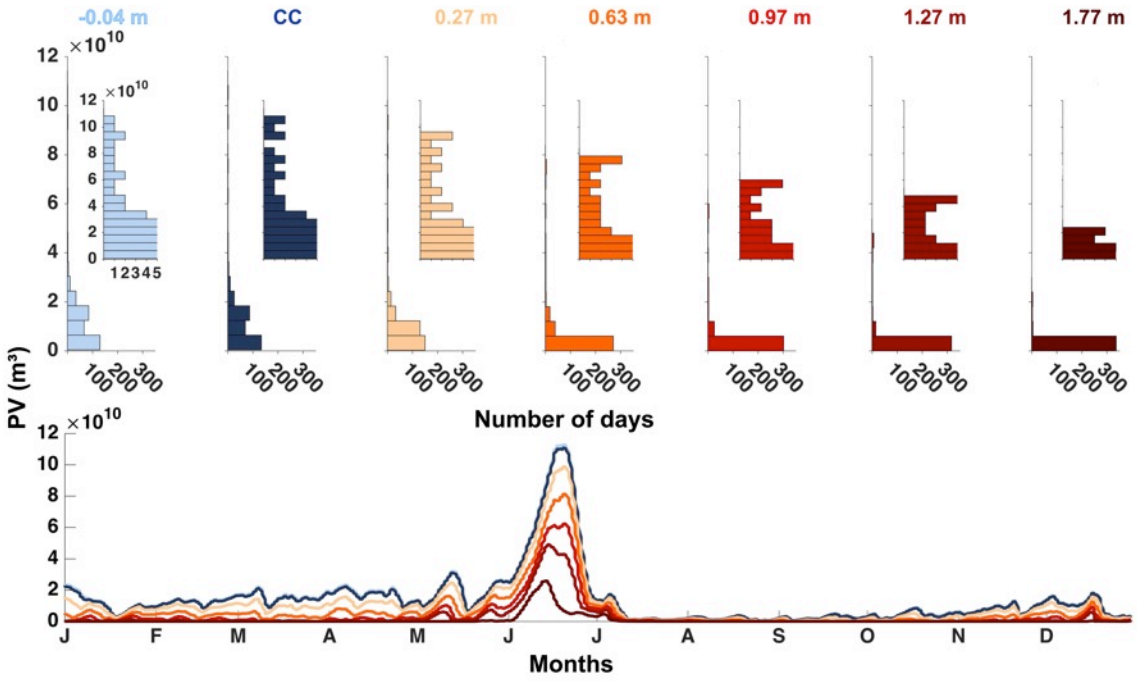

Figure 4. 8. Isoline maps of surface salinity response to (a) a scenario of sea level change of 1.77 m; (b) contemporary condition (CC); (c) the difference in surface salinity between current condition and 1.77 m SLC (Surface salinity at 1.77 m scenario minus CC) on June 21th in the Columbia River estuary and the Pacific Ocean. The black contour line delineates salinity= 28 psu.

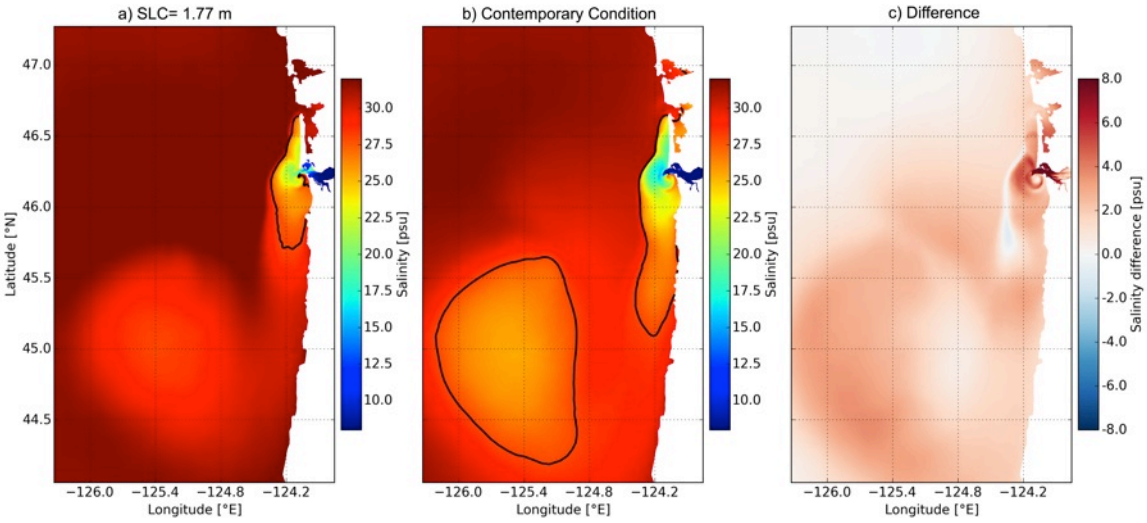

Figure 4. 9. Salinity intrusion length for six scenarios of sea level change as a function of river discharge at Bonneville Dam. CC: contemporary condition.

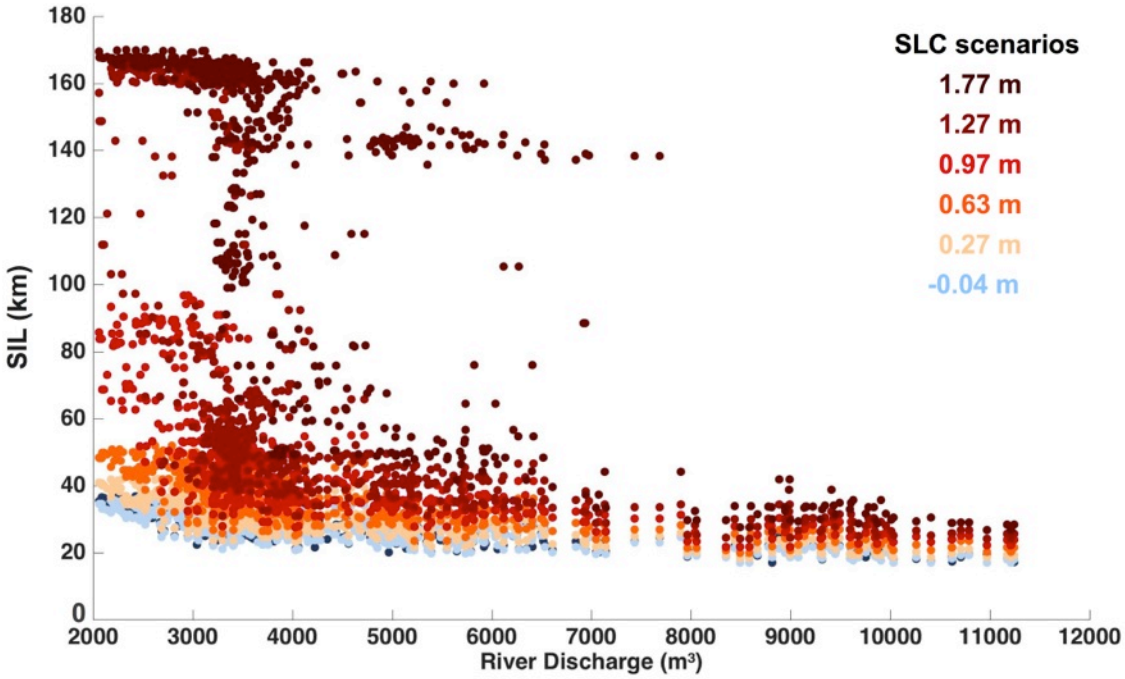

Figure 4. 10. Percent changes in shallow water habitat (SWH) at eight reaches for six scenarios of sea level change relative to the contemporary condition The range of color bars reflects the different scenarios. In each bar, the lighter color indicates the maximum and minimum, the darker color indicates the 25th and 75th percentile, and the white circle indicates the average of each indicator for each scenario

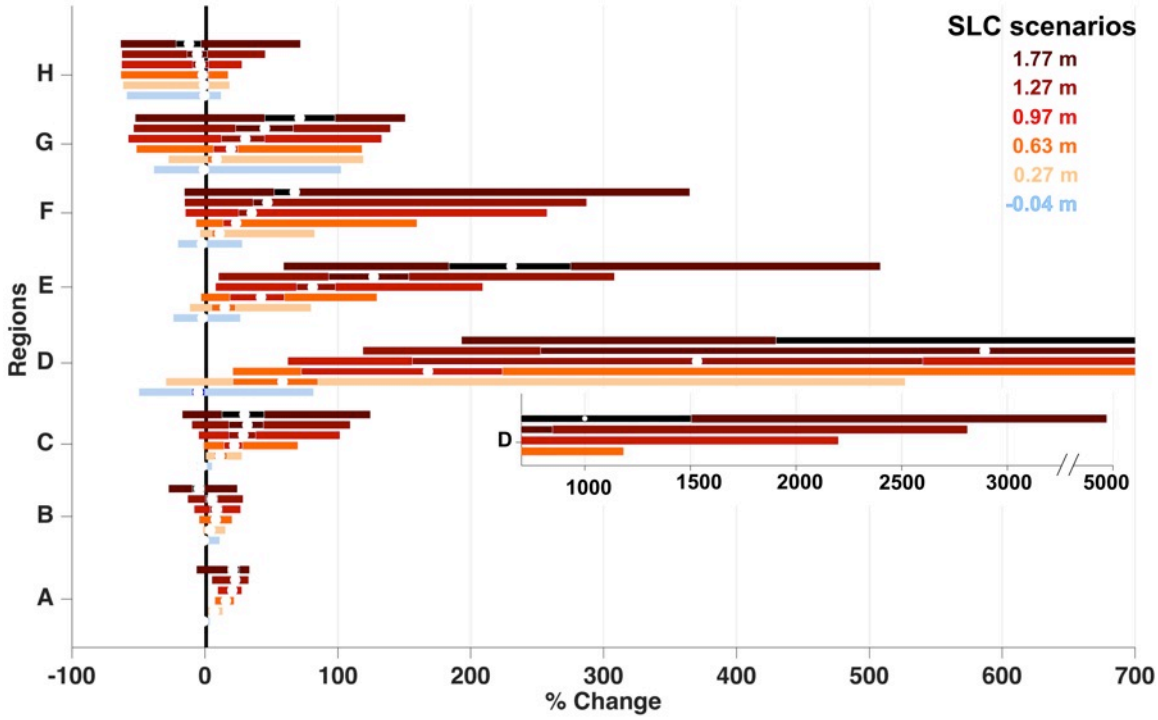

Figure 4. 11. The change in SWH (calculated for each element) with a 1.77 m sea level rise relative to the contemporary condition throughout the Columbia River estuary when the highest value of SWH was seen at most reaches on June 14th. The positive values reflect more SWH availability with a sea level rise of 1.77 m, while the negative numbers indicate less SWH availability with the same rise in sea level.

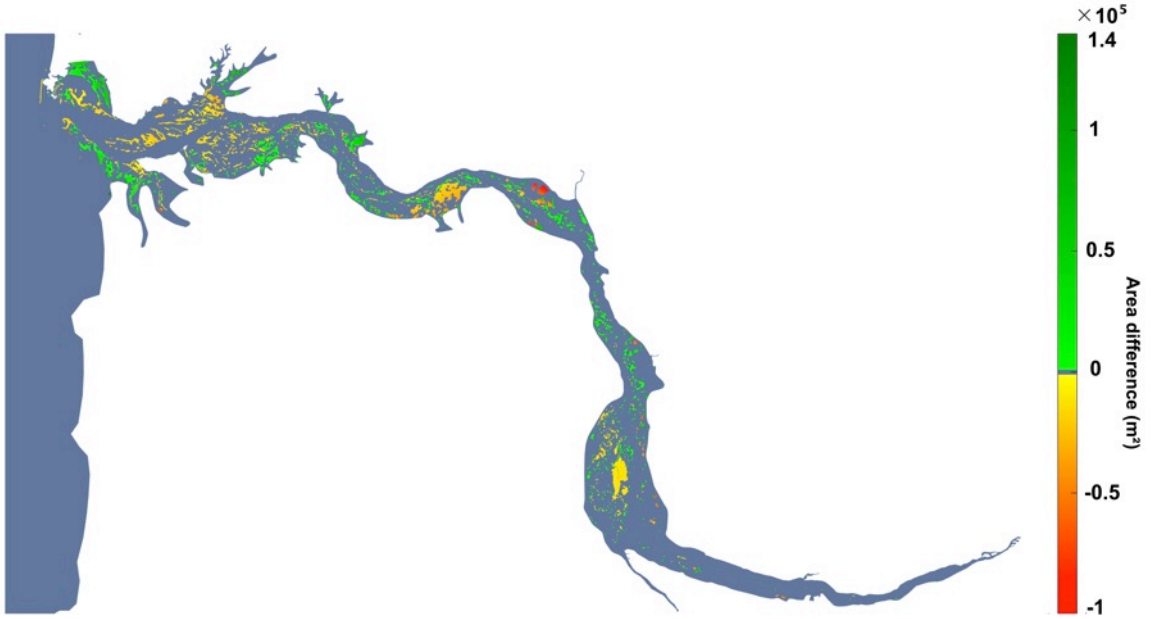

Figure 4. 12. Percent changes in juvenile Chinook salmon habitat (SH) at eight reaches for six scenarios of sea level change relative to the contemporary condition The range of color bars reflects the different scenarios. In each bar, the lighter color indicates the maximum and minimum, the darker color indicates the 25th and 75th percentile, and the white circle indicates the average of each indicator for each scenario.

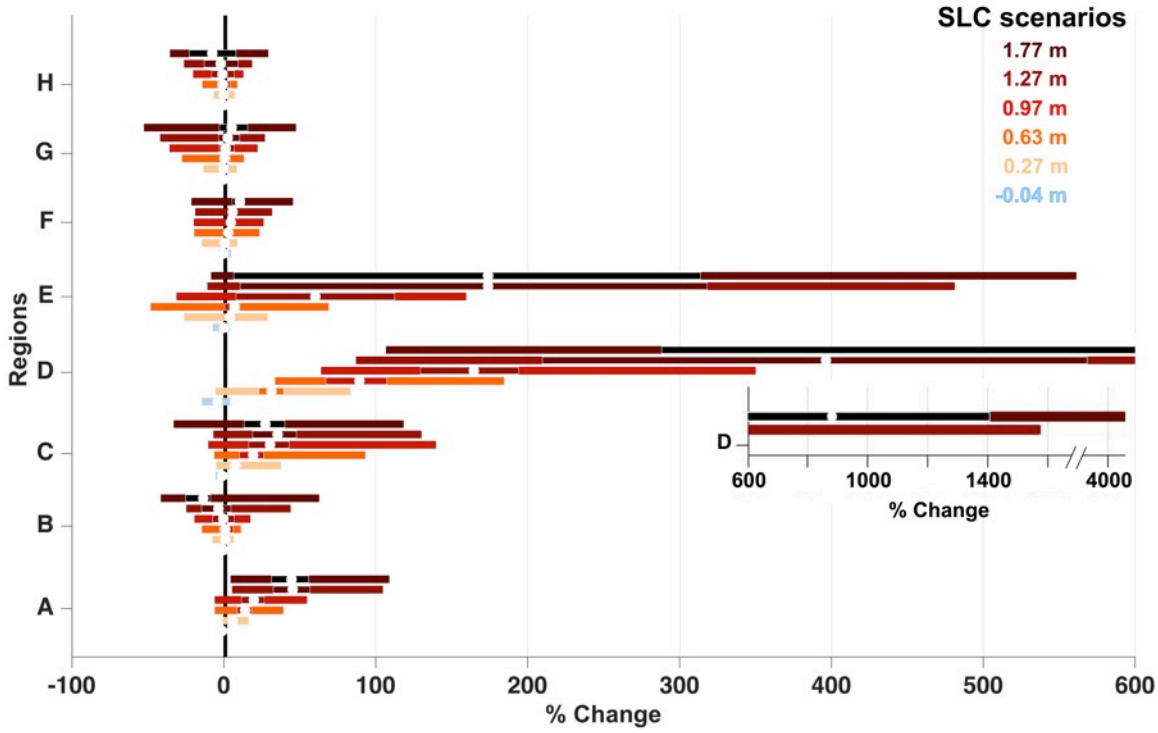

Chapter 5

Conclusions and future work

5.1. Contributions

The river-dominated, mesotidal Columbia River estuary under the influence of nutrient-rich upwelled coastal water with a highly regulated flow has served salmonids in their journey by providing nursery and migratory habitats and food resources (Bottom et al., 2005). However, the structural and functional attributes of the Columbia River estuary have long been influenced by human activity and environmental variability (Dalton et al., 2013; Mantua et al., 1997; NRC, 2004b). This has led to 13 species of Pacific salmon and steelhead, being listed under the U.S. Endangered Species Act (Ford, 2011; Weitkamp et al., 2014). Variability and changes in salmon habitat-supporting system affect the status and trends of specific stocks. Therefore, evaluation of the system's variability in the contemporary state, as well as predicting the system changes under future scenarios, are essential to design restoration plans and to enhance management-level decision-making processes for optimizing hydropower systems and navigation channel to preserve future salmon habitat.

The research presented in this dissertation provides new information about the variability and change of the Columbia River's habitat-relevant estuarine physics response to both sea level changes and a seismic subsidence by using a pre-existing

modeling and monitoring infrastructure (SATURN; Baptista et al. 2015), and newly refined definitions of regionally accepted indicators. The main research accomplishments of this dissertation are presented in the following subsections.

5.1.1. Refined set of criteria to characterize juvenile Chinook salmon habitat as a function of predictable physical factors

We introduced a refined habitat computation method which was defined initially by Bottom et al. (2005) and later modified by Burla (2009) and Bottom et al.(2011). This method combined 15 years (2000–2014) of skill-assessed simulation results from a 3D circulation model with the best available empirical understanding of juvenile Chinook salmon response to hydrodynamic variables (including depth, temperature, velocity, salinity, and dissolved oxygen levels) found in the Columbia River downstream from the first dam (Bonneville Dam). This methodology was still based on hydrodynamic variables, but differed from the previous methods in five major ways: 1) We defined salmon habitat on a *volumetric* rather than *surface* basis by recognizing that juvenile salmon use vertical mobility for their benefit. 2) The methodology distinguished between nursery habitat (where depth is less than 2 m) and migratory habitat (where depth is more than 2 m). 3) It also classified nursery habitat based on different life stages of juvenile Chinook salmon, by applying stage-specific velocity thresholds. 4) We replaced binary thresholds (either 0 or 1) for these variables by penalty functions (between 0 and 1) to quantify the optimal habitat for juveniles by recognizing that temperature and salinity influence both habitat access and quality. 5) We introduced the effects of ocean-derived hypoxia by adding low dissolved oxygen penalty throughout the upwelling season to account for biological stress on juvenile Chinook salmon in the

brackish waters of migratory habitat, as well as to highlight habitat availability for those salmon that might be affected by low dissolved oxygen concentrations.

5.1.2. Characterized temporal and spatial variability of salmon habitat over a 15 year period (2000-2014)

We characterized the seasonal and inter-annual variability of juvenile Chinook salmon habitat by filtering high-resolution, 15–year simulations of baroclinic circulation in the estuary through our refined habitat criteria.

Our results indicated that nursery habitat increases is typically an order of magnitude smaller than migratory habitat. Most available nursery habitat concentrated in specific geomorphic reaches (reaches C and F in the USGS 2011 classification) with extended shallow regions. We found that not only is habitat seasonally modulated by temperature at all reaches, but that less habitat is available in the summer and winter. In reach C, these findings are also supported with a higher mean density of juveniles in optimal temperatures (10–16 ºC) and a lower mean density in suboptimal (less than 10 ºC) and stressful temperatures (more than 19 ºC) (Roegner and Teel, 2014).. We also found that at most reaches, the estuary offers more nursery habitat for fingerling than for fry, which is initially relevant to the water velocity regime in each reach.

For years 2000–2014, we found that the temporal variability in migratory habitat to be minor. This is in contrast with the temporal variability in nursery habitat, which we found to be strong and region specific. Nursery habitat responds primarily to river forcing in the upper reaches and to tides in the lower reaches of the estuary. As a consequence, the inter–annual variability of nursery habitat is lower in the lower

estuary, where tides are dominant, and higher in the upper reaches where river discharges are dominant.

For example, higher river discharge during spring and summer 2011, as well as a relatively high and early freshet in 2012 (relative to the 2000–2014 mean river discharge), drastically increase nursery habitat at the upper reaches. Conversely, lower river discharge during spring and summer 2001 (relative to the 2000–2014 mean river discharge) reduces nursery habitat at these reaches.

Our analysis of the contemporary variability of the estuarine habitat provided a valuable baseline for assessing future changes due to climate, navigation channel, seismic subsidence, and flow regulation.

5.1.3. Determined the effect of a large CSZ subduction on the estuary and its ability to provide estuarine salmon habitat

We characterized estuary response to the largest Cascadia Subduction Zone earthquake with the M_w (moment magnitude) of 9.1 by using habitat-relevant indicators (including salinity intrusion length, salt volume, shallow water habitat, and juvenile Chinook salmon habitat). These indicators were compared between contemporary condition and conditions resulting from the largest CSZ earthquake as developed by the Oregon Department of Geology and Mineral Industries and collaborators (Witter et al., 2013).

Our results suggested that subsidence would change estuarine physics and associated fish habitat. For low river discharges (e.g., in September), the effect is particularly pronounced with salinity propagating upstream nearly 15 km, causing a major (~94%) loss of freshwater habitat.

Some fish out-migrating to the ocean could benefit from this as plume volume also increased during the freshet from 1.10×10^{11} m^3 in the contemporary system to 1.49×10^{11} m^3 under the largest CSZ earthquake condition.

Changes in shallow water and salmon habitat varied strongly across the lower estuary, and there would be winners and losers in terms of reaches, stocks, and period. At the lower estuary (reach A and B), where subsidence was more than 2 m, the estuary would provide an average of ~26% less shallow water and juvenile Chinook salmon habitat relative to the contemporary system. Reach A would lose habitat during May, when Spring Creek Group fall fingerling was the predominant stock (96%), and during March, when West Cascade fall and Spring Creek Group fall fry were predominant stocks (50%, 40% respectively), while reach B would lose habitat throughout the year. In contrast, reach C, where the subsidence was less than 2 m, provided more habitat relative to the contemporary system because more area was inundated and salt Could not propagate that far.

We did not assess any major change in shallow water habitat and habitat for juvenile Chinook salmon where there is no subsidence at upper reaches.

Determined the influence of SLC on the estuary and its ability to provide estuarine salmon habitat

We described the estuary response to future sea level changes by utilizing habitat-relevant indicators (including, salinity intrusion length, salt volume, shallow water habitat, and juvenile Chinook salmon habitat) for a reference simulation (db33 [year 2010]) of the contemporary system and for six scenarios of sea level changes.

Our result indicated that by passing specific thresholds (approximately ~1 m off the coast), rising sea levels would drastically increase the extent of ocean influence on the

estuary (as measured by salinity intrusion length), and would substantially reduce the seasonal influence of freshwater on the continental shelf (as measured by plume volume during river freshets). Specifically, in response to high-end sea level rise scenario (1.77 m), the Columbia River would be deeply altered by salinity where salinity will propagate upstream to Port of Portland and plume will be disappeared during low river discharge.

On average, almost 12% to 203% of water volume would be permanently changed to saltwater when sea level increases from 0.27 to 1.77 m, respectively, which is seen with the SV indicator.

We identified that salinity propagation inside the estuary is a nonlinear function of river flow, especially in the range of medium to large flow (~ 8000 m3/s). With less than 8000 m3/s river discharge at Bonneville Dam, SIL and SV will extend more than 100% with changing sea levels of more than ~1 m. Rapid changes in the future suggest that there might be an important threshold in river discharge in response of sea level rises more than 1 m.

Consistent with the increase in salinity intrusion, freshwater plume size will decline with sea level rise by 100% passing a 1 m sea level rise relative to the contemporary system.

In a habitat perspective, rising sea levels will alter shallow water—and specifically—salmon estuarine habitat within the estuary in complex spatial and temporal ways. There will be winners and losers in terms of reaches, stocks, and migration periods, which will be critical to consider in designing long-term plans for restoration and hatchery programs.

Reach D, E, F, and G provide more shallow water habitat and habitat for juvenile Chinook salmon under the scenarios of sea level rise relative to the current system. The results showed the middle reaches (D and E), from Longview to the Port of St. Helens, having higher variability than the two ocean-influenced reaches at the lower estuary.

In contrast, with SLR more than 1 m, reach B and H will lose habitat during May, when the Upper Columbia River summer/fall fry and Spring Creek Group fall fingerling are predominant stocks (60%, 90% respectively). When SLR is more than 1.27 m, reach C also loses habitat during May, when West Cascade fall fry, West Cascade fall, and Spring Creek Group fall fingerling are predominant stocks (96%, 40%, 50% respectively).

Though we reported shallow water habitat as an integrated value for each reach, the , spatial pattern of SWH (values for each element) responses were not homogenous within each reach. In fact, SWH may increase in some areas, while decreasing in other areas at the same reach. For instance, in June 14th, part of Cathlamet Bay experiences increased SWH near Marsh Island, while at the same time loses SWH at the mouth of Gray's Bay when sea level rises by 1.77 m relative to the contemporary condition.

Although we determined the impacts of ultimate values of all possible scenarios of sea level changes at year 2100, these changes would happen earlier than 2100 if sea level followed the trend of the high-end scenario.

5.2. Contributions to management

Using a pre-existing regional infrastructure system that consists of a Virtual Columbia River modeling system and SATURN observation network resources, and adding refined indicators of estuarine habitat, our results:

a) Offered a refined method to quantify juvenile Chinook salmon habitat. Although the thresholds were already defined for juvenile Chinook salmon (Bottom et al., 2005; Burla, 2009; McCullough, 1999; Roegner et al., 2011; Roegner and Teel, 2014; Volk et al., 2010), the methodology itself is applicable to other aquatic species when the thresholds are available

b) Suggested that a possible sea level rise threshold of more than ~ 1 m will alter salinity regime and fish habitat; and

c) Provided scientific guidance on the impacts of future changes (sea level change and seismic events) and their effect on long-term design plans for restoration and hatchery programs. Based on the estimated sea level rise threshold, we suggest that restoration project managers and hatchery designers consider the vulnerability of site locations to sea level rise in order to enhance the improvement of freshwater habitat resilience.

There is always a degree of uncertainty about how, when, and where this system will experience the impact of sea level changes. However, an extensive and continuous monitoring system will help track ongoing changes and therefore, prevent permanent system damages.

5.3. Uncertainty

Evaluation of the impact that future changes might have on the Columbia River

estuary comes with some degree of uncertainty, ranging from the definition of the scenarios, to their simulation and the interpretation of the results. In spite of these uncertainties, the potential for massive change in the estuary due to either a CSZ subsidence or sea level rise is too important to be ignored.

Quantifying the degree of uncertainty wasn't an objective of this research; however, we did identify the following sources of uncertainty in our analysis:

- Uncertainty in the 3D hydrodynamic model, which arises as a result of errors in the model configuration, input data (e.g. atmospheric, ocean, and river forcing), and grid resolution.
- Uncertainty in the Cascadia earthquake deformation model for both the structure and input data. For instance, while this grid resolution is adequate for capturing the change in indicators, it may not be sufficient for capturing the detailed changes in bathymetry in the response to the largest CSZ earthquake near small islands in the estuary.
- Uncertainty in global sea level change projections, which originate from three sources of uncertainties: natural variability, future emission of greenhouse gases, and climate modeling.
- Uncertainty in regional sea level change projections resulting from uncertainty in eustatic global sea level rise rate and regional vertical land movement calculation.
- Uncertainties resulting from the use of atmospheric, river, and ocean forces for the year 2010 in future sea level change scenario simulations, as well as for the contemporary condition. We focused only on sea level change

impacts in the Columbia River estuary and the cumulative impacts of climate change, including temperature rise, change in hydrologic stream flow regimes were not considered in this study. Uncertainty in the computation of indicators and the definition of the criteria. For instance, we compute plume volume as a proxy for the freshwater impacts on the continental shelf and its important role in out-migration of some salmon stocks and steelhead. However, the plume volume, which was used by Miller (2013; 2014) and Burla (2010), is defined only based on salinity distribution (salinity less than 28 psu), which is a physical aspect of freshwater plume and we didn't consider the biological and chemical characteristics of the plume, as well as the interactions among chemistry, physics, and biology in the plume.

- Uncertainty in the nature of sedimentary adjustments in sea level change and post-Cascadia Subduction Zone earthquake. There is a range of rebounding rate from decades to nearly a century that coseismically subsided wetland rebounds their pre-earthquake elevation. (Hughes et al., 2002)
- Uncertainty in not considering a sediment model in our analyses. Since there were minor differences between the calculated salmon habitat and salinity intrusion length (calculated from model outputs) by using only a circulation model and by using a sediment model and a circulation model, we only run circulation model.

5.4. Future work

This thesis contributed significantly to characterize contemporary variability and demonstrate the potential for change in magnitude and variability of estuarine habitat in the Columbia River estuary. However, much remains to be learned, and research along the following and other directions deserves consideration:

- There have been several modifications to the juvenile Chinook salmon habitat calculation beginning with Bottom et al. (2005), progressing with Burla (2009), and continuing on with this research. The computation method should continue to advance, by adding penalty for food limitation and predation to the indicator. Also, coupling a hydrodynamic circulation model with a biogeochemical, sediment, and individual-based model, which creates an ecosystem-based model, would more effectively track juvenile salmon movement than just using a hydrodynamic circulation model alone. The products for these models including physical variables, chlorophyll and sediment concentration, net ecosystem metabolism that covers biological production, and a random-displacement particle tracking method would help to accurately track specific juvenile salmon stock movements through the lower estuary.
- Our research used the year 2010 for river, ocean, and atmospheric forces for both the contemporary system and for future change scenarios. For sea level change simulations, we only added sea level rise values to the elevation at the ocean boundary and used the large CSZ earthquake scenario's post-deformation bathymetry map. Atmospheric, River, and ocean Forces were

kept the same for sea level change scenarios and the contemporary condition; however, river and ocean conditions will change by 2100. Recent research regarding future changes in the Columbia Basin reveals decreasing temperatures and precipitation in the summer and earlier and higher river discharge at the Dalles by the year 2100 (Rupp et al., 2016). Future research involving sea level rise simulations should consider the impacts of climate change, including temperature rise, change in hydrologic stream flow regimes individually and cumulatively.

- Because of multiple uncertainties mentioned in the previous section, a formal uncertainty analysis is necessary to best utilize our results for risk-based decisions. An uncertainty analysis can create an entire set of possible results and their likelihood of occurrence. To address the uncertainty associated with the quantification of indicators, the Monte Carlo (MC) method may be used. The variables' (model outputs) uncertainty can be characterized as parametric uncertainty and its propagation to the indicators computation results can be assessed using the MC method. A total of 1,000 realizations of physical variables can be generated and used for the MC simulation. The mean and the 5^{th} and 95^{th} percentiles of each variable can be obtained from 1000 MC simulation and the credible interval between the 5^{th} and 95^{th} percentiles will indicate the predictive variance.

Reference

Atwater, B.F., Hemphill-Haley, E., 1997. Recurrence intervals for great earthquakes of the past 3,500 years at northeastern Willapa Bay, Washington. USGPO; Information Services [distributor].

Baptista, A.M., Seaton, C., Wilkin, M.P., Riseman, S.F., Needoba, J.A., Maier, D., Turner, P.J., Kärnä, T., Lopez, J.E., Herfort, L., 2015. Infrastructure for collaborative science and societal applications in the Columbia River estuary. Frontiers of Earth Science 9, 659-682.

Barnes, C.A., Duxbury, A.C., Morse, B.-A., 1972. Circulation and selected properties of the Columbia River effluent at sea. In: Pruter, A.T., Alverson, D.L. (Eds.), The Columbia River Estuary and Adjacent Ocean Waters. University of
Washington Press, Seattle, WA, pp. 41–80.

Bartz, K.K., Lagueux, K.M., Scheuerell, M.D., Beechie, T., Haas, A.D., Ruckelshaus, M.H., 2006. Translating restoration scenarios into habitat conditions : an initial step in evaluating recovery strategies for Chinook salmon (Oncorhynchus tshawytscha). 1595, 1578-1595.

Battin, J., Wiley, M.W., Ruckelshaus, M.H., Palmer, R.N., Korb, E., Bartz, K.K., Imaki, H., 2007. Projected impacts of climate change on salmon habitat restoration. Proceedings of the national academy of sciences 104, 6720-6725.

Beechie, T., Buhle, E., Ruckelshaus, M., Fullerton, A., Holsinger, L., 2006. Hydrologic regime and the conservation of salmon life history diversity. Biol. Conserv. 130, 560-572.

Borde, a.B., Cullinan, V.I., Diefenderfer, H.L., Thom, R.M., Kaufmann, R.M., Zimmerman, S.a., Sagar, J., Cobertt, C., 2012. Lower Columbia River and Estuary Ecosystem Restoration Program Reference Site Study : 2011 Restoration Analysis. 49.

Bottom, D.L., Baptista, A., Burke, J., Campbell, L., Casillas, E., Hinton, S., Jay, D.A., Lott, M.A., McCabe, G., McNatt, R., 2011. Estuarine habitat and juvenile salmon: current and historical linkages in the lower Columbia River and estuary, Final Report 2002–2008. Seattle: Northwest Fisheries Science Center, Fish Ecology Division. DTIC Document.

Bottom, D.L., Simenstad, C.A.B., Jennifer, Baptista, A.M., Jay, D.A., Jone, K.K., Casillas, E., Schiewe, M.H., 2005. Salmon at river's end: the role of the estuary in the decline and recovery of Columbia River salmon. NOAA Technical Memorandum NMFS-NWFSC-70, U.S. Department of Commerce.

Brett, J., Clarke, W.C., Shelbourn, J., Station, P.B., 1982. Experiments on thermal requirements for growth and food conversion efficiency of juvenile chinook salmon Oncorhynchus tshawytscha. Government of Canada, Department of Fisheries and Oceans, Fisheries Research Branch, Pacific Biological Station.

Burke, J.L., 2004. Life Histories of Juvenile Chinook salmon in the Columbia River Estuary, 1916 to the Present. Master's Thesis, Corvallis, Oregon: Oregon State University.

Burla, M., 2009. The Columbia River Estuary and Plume: Natural Variability, Anthropogenic Change and Physical Habitat for Salmon. Doctoral Thesis, Beaverton, Oregon: Oregon Health & Science University.

Burla, M., Baptista, A.M., Casillas, E., Williams, J.G., Marsh, D.M., 2010. The influence of the Columbia River plume on the survival of steelhead (Oncorhynchus mykiss) and Chinook salmon (Oncorhynchus tshawytscha): a numerical exploration. Can. J. Fish. Aquat. Sci. 67, 1671-1684.

Cederholm, C.J., D. H. Johnson, R. E. Bilby, L.G. Dominguez, A. M. Garrett, W. H. Graeber, E. L. Greda, M. D. Kunze, B.G. Marcot, J. F. Palmisano, R. W. Plotnikoff, W. G. Pearcy, C. A. Simenstad, Trotter., a.P.C., 2000. Pacific Salmon and Wildlife - Ecological Contexts, Relationships, and Implications for Management. Special Edition Technical Report, Prepared for D. H. Johnson and T. A. Oâ€™Neil (Managing directors), Wildlife-Habitat Relationships in Oregon and Washington. WDFW, Olympia, Washington.

Chawla, D.J., AM Baptista, M Wilkin, C Seaton, 2007. Seasonal variability and estuary-shelf interactions in circulation dynamics of a river-dominated estuary. . Estuaries and Coasts, 31, 269-288.

CMOP, 2015. Oxygen Watch, Coastal Margin Observation & Prediction.

Coleman, A.M., Johnson, G.E., Borde, A.B., Diefenderfer, H.L., Sather, N.K., Seiple, T.E., Serkowski, J.A., 2013. The Oncor Geodatabase for the Columbia Estuary Ecosystem Restoration Program : Annual.

Dalton, M.M., Mote, P.W., Snover, A.K., 2013. Climate Change in the Northwest: Implications for Our Landscapes, Waters, and Communities. NCA Regional Input Reports.

Davis, G.E., Foster, J., Warren, C.E., Doudoroff, P., 1963. The influence of oxygen concentration on the swimming performance of juvenile Pacific salmon at various temperatures. Trans. Am. Fish. Soc. 92, 111-124.

Davis, J.C., 1975. Minimal dissolved oxygen requirements of aquatic life with emphasis on Canadian species: a review. Journal of the Fisheries Board of Canada 32, 2295-2332.

De Robertis, A., Morgan, C.A., Schabetsberger, R.A., Zabel, R.W., Brodeur, R.D., Emmett, R.L., Knight, C.M., Krutzikowsky, G.K., Casillas, E., 2005. Columbia River plume fronts. II. Distribution, abundance, and feeding ecology of juvenile salmon.

Elsner, M.M., Cuo, L., Voisin, N., Deems, J.S., Hamlet, A.F., Vano, J.a., Mickelson, K.E.B., Lee, S.-Y., Lettenmaier, D.P., 2010. Implications of 21st century climate change for the hydrology of Washington State. Clim. Change 102, 225-260.

Emmett, R.L., Brodeur, R.D., Orton, P.M., 2004. The vertical distribution of juvenile salmon (Oncorhynchus spp.) and associated fishes in the Columbia River plume. Fish. Oceanogr. 13, 392-402.

Emmett, R.L., Stone, S.L., Hinton, S.a., Monaco, M.E., 1991. Distribution and abundance of fishes and invertebrates in west coast estuaries: specific life history summaries. N.O.A.A. Technical Report Circular 2, 329p.

Everest, F.H., Chapman, D., 1972. Habitat selection and spatial interaction by juvenile chinook salmon and steelhead trout in two Idaho streams. Journal of the Fisheries Board of Canada 29, 91-100.

Ford, M.J., 2011. Status review update for Pacific salmon and steelhead listed under the Endangered Species Act: Pacific Northwest. US Department of Commerce, National Oceanic and Atmospheric Administration, National Marine Fisheries Service, Northwest Fisheries Science Center.

Fresh, K.L., 2006. Juvenile Pacific Salmon in Puget Sound. 28.

Gleason, M.G., Newkirk, S., Merrifield, M.S., Howard, J., Cox, R., Webb, M., Koepcke, J., Stranko, B., Taylor, B., Beck, M.W., 2011. A conservation assessment of West Coast (USA) estuaries. The Nature Conservancy.

Glick, P., Clough, J., Nunley, B., 2007. Sea-level rise and coastal habitats in the Pacific Northwest: An analysis for Puget Sound, southwestern Washington, and northwestern Oregon. National Wildlife Federation.

Goertler, P.A., Simenstad, C.A., Bottom, D.L., Hinton, S., Stamatiou, L., 2015. Estuarine Habitat and Demographic Factors Affect Juvenile Chinook (Oncorhynchus tshawytscha) Growth Variability in a Large Freshwater Tidal Estuary. Estuaries and Coasts, 1-18.

Groffman, P.M., Baron, J.S., Blett, T., Gold, A.J., Goodman, I., Gunderson, L.H., Levinson, B.M., Palmer, M.A., Paerl, H.W., Peterson, G.D., 2006. Ecological thresholds: the key to successful environmental management or an important concept with no practical application? Ecosystems 9, 1-13.

Groot, C., Margolis, L., 1991. Pacific salmon life histories. UBC press.

Hamlet, A.F., Lee, S.-Y., Mickelson, K.E., Elsner, M.M., 2010. Effects of projected climate change on energy supply and demand in the Pacific Northwest and Washington State. Clim. Change 102, 103-128.

Hawkes, A., Horton, B., Nelson, A., Vane, C., Sawai, Y., 2011. Coastal subsidence in Oregon, USA, during the giant Cascadia earthquake of AD 1700. Quaternary Science Reviews 30, 364-376.

Healey, M.C., 1992. Life history of Chinook Salmon (Oncorhynchus tshawytscha). Pacific Salmon Life Histories 1992, 311-394.

Healey, M.C., Jordan, F., Station, P.B., 1982. Observations on juvenile chum and chinook and spawning chinook in the Nanaimo River, British Columbia, during 1975-1981. Department of Fisheries and Oceans, Fisheries Research Branch, Pacific Biological Station.

Hickey, B.M., Kudela, R.M., Nash, J., Bruland, K.W., Peterson, W.T., MacCready, P., Lessard, E.J., Jay, D.A., Banas, N.S., Baptista, A.M., 2010. River influences on shelf ecosystems: introduction and synthesis. Journal of Geophysical Research: Oceans 115.

Hughes, J.F., Mathewes, R.W., Clague, J.J., 2002. Use of pollen and vascular plants to estimate coseismic subsidence at a tidal marsh near Tofino, British Columbia. Palaeogeogr., Palaeoclimatol., Palaeoecol. 185, 145-161.

IPCC, 2001. Climate Change 2001: Synthesis Report. A Contribution of Working Groups I, II, and III to the Third Assessment Report of the Integovernmental Panel on Climate Change [Watson, R.T. and the Core Writing Team (eds.)]. Cambridge University Press, Cambridge, United Kingdom, and New York, NY, USA, 398 pp.

IPCC, 2007. Climate Change 2007: Synthesis Report. Contribution of Working Groups I, II and III to the Fourth Assess- ment Report of the Intergovernmental Panel on Climate Change [Core Writing Team, Pachauri, R.K and Reisinger, A. (eds.)]. IPCC, Geneva, Switzerland, 104 pp.

IPCC, 2013. “Summary for policy makers,”in Climate Change2013;ThePhysical Science Basis. Contribution of Working GroupI to theFifth Assessment Reportof the Intergovernmental Panel on Climate Change, eds T.F.Stocker, D.Qin, G.-K.

Plattner,M.Tignor,S.K.Allen,J.Boschung,etal., Cambridge,UK; NewYork, NY,USA:CambridgeUniversityPress),3–29.

ISAB, 2007. Climate change impacts on Columbia River basin fish and wildlife. Independent Scientific Advisory Board.
Jevrejeva, S., Grinsted, A., Moore, J., 2009. Anthropogenic forcing dominates sea level rise since 1850. Geophys. Res. Lett. 36.
Jorgensen, J.C., Honea, J.M., McCLURE, M.M., Cooney, T.D., Engie, K., Holzer, D.M., 2009. Linking landscape-level change to habitat quality: an evaluation of restoration actions on the freshwater habitat of spring-run Chinook salmon. Freshwat. Biol. 54, 1560-1575.
Kärnä, T., Baptista, A.M., 2016a. Evaluation of a long-term hindcast simulation for the Columbia River estuary. Ocean Model. Online 99, 1-14.
Kärnä, T., Baptista, A.M., 2016b. Water age in the Columbia River estuary. Estuar. Coast. Shelf Sci. 183, 249-259.
Kärnä, T., Baptista, A.M., Lopez, J.E., Turner, P.J., McNeil, C., Sanford, T.B., 2015. Numerical modeling of circulation in high-energy estuaries: A Columbia River estuary benchmark. Ocean Model. Online 88, 54-71.
Levy, D., Northcote, T., 1982. Juvenile salmon residency in a marsh area of the Fraser River estuary. Can. J. Fish. Aquat. Sci. 39, 270-276.
Mains, E.M., Smith, J.M., 1964. The distribution, size, time, and current preferences of seaward migrant chinook salmon in the Columbia and Snake Rivers. Wash. Dep. Fish. Fish. Res. Pap 2, 5-43.
Mantua, N., Tohver, I., Hamlet, A., 2010. Climate change impacts on streamflow extremes and summertime stream temperature and their possible consequences for freshwater salmon habitat in Washington State. Clim. Change 102, 187-223.
Mantua, N.J., Hare, S.R., Zhang, Y., Wallace, J.M., Francis, R.C., 1997. A Pacific interdecadal climate oscillation with impacts on salmon production. Bulletin of the american Meteorological Society 78, 1069-1079.
McCabe Jr, G., Muir, W.D., Emmett, R.L., Durkin, J.T., 1983. Interrelationships between juvenile salmonids and nonsalmonid fish in the Columbia River estuary. Fish. Bull. 81, 815-826.
McCullough, D.A., 1999. A review and synthesis of effects of alterations to the water temperature regime on freshwater life stages of salmonids, with special reference to Chinook salmon.
Miller, J.A., Simenstad, C.A., 1997. A comparative assessment of a natural and created estuarine slough as rearing habitat for juvenile chinook and coho salmon. Estuaries 20, 792-806.
Miller, J.A., Teel, D.J., Baptista, A., Morgan, C.A., 2013. Disentangling bottom-up and top-down effects on survival during early ocean residence in a population of Chinook salmon (Oncorhynchus tshawytscha). Can. J. Fish. Aquat. Sci. 70, 617-629.
Miller, J.a., Teel, D.J., Peterson, W.T., Baptista, A.M., 2014. Assessing the relative importance of local and regional processes on the survival of a threatened salmon population. PloS one 9, e99814.
Morgan, C.A., De Robertis, A., Zabel, R.W., 2005. Columbia River plume fronts. I. Hydrography, zooplankton distribution, and community composition. Marine ecology. Progress series 299, 19-31.
Morgan, J.D., Iwama, G.K., 1991. Effects of salinity on growth, metabolism, and ion regulation in juvenile rainbow and steelhead trout (Oncorhynchus mykiss) and fall chinook salmon (Oncorhynchus tshawytscha). Can. J. Fish. Aquat. Sci. 48, 2083-2094.

Mote, P., Petersen, A., Reeder, S., Shipman, H., 2008. Sea Level Rise in the Coastal Waters of Washington State.

Mote, P.W., Parson, E.A., Hamlet, A.F., Keeton, W.S., Lettenmaier, D., Mantua, N., Miles, E.L., Peterson, D.W., Peterson, D.L., Slaughter, R., 2003. Preparing for climatic change: the water, salmon, and forests of the Pacific Northwest. Clim. Change 61, 45-88.

Mote, P.W., Salathe, E.P., 2010. Future climate in the Pacific Northwest. Clim. Change 102, 29-50.

Nelson, K.D., Zhao, W., Brown, L., Kuo, J., 1996. Partially molten middle crust beneath southern Tibet: synthesis of project INDEPTH results. Science 274, 1684.

NMFS, 1999. Conclusions regarding the updated status of the Columbia River chum salmon ESU and Hood Canal summer-run chum salmon ESU. Memo 12 February 1999 to W. Stelle, NWFSC, and W. Hogarth, Southwest Fisheries Science Center, from M. H. Schiewe, NWFSC, Seattle, WA.

NOAA, 2010a. National Oceanic and Atmospheric Administration. Technical Considerations for Use of Geospatial Data in Sea Level Change Mapping and Assessment. NOAA Technical Report NOS 2010-01. Washington, DC: National Ocean Service, NOAA.

NOAA, 2013b. Estimating vertical land motion from long-term tide gauge records, Technical report NOS CO-OPS 065, U.S. Department of Commerce, National Oceanic and Atmospheric Administration, Center for Operational Oceanographic Products and Services: Silver Spring, MD, [Available at http://tidesandcurrents.noaa.gov/publications/Technical_Report_NOS_CO-OPS_065.pdf].

NPCC, 2014. Northwest Power and Conservation Council, Columbia River Basin Fish and Wildlife Program.

NRC, 1987. National Research Council. Responding to Changes in Sea Level: Engineering Implications. National Academy Press: Washington, D.C.

NRC, 2004b. National Research Council, Managing the Columbia River: instream flows, water withdrawals, and salmon survival. National Academy Press, Washington. National Academy Press, Washington.

NRC, 2012. National Research Council. Sea-Level Rise for the Coasts of California, Oregon, and Washington:: Past, Present, and Future. Washington, DC: The National Academies Press. National Academies Press.

Parris, A., P. Bromirski, V. Burkett, D. Cayan, M. Culver, J. Hall, R. Horton, K. Knuuti, R. Moss, J. Obeysekera, A. Sallenger, Weiss., J., 2012. Global Sea Level Rise Scenarios for the United States National Climate Assessment.

Pearcy, W.G., 1992. Ocean ecology of North Pacific salmonids. Books in recruitment fishery oceanography (USA).

Pfeffer, W.T., Harper, J., O'Neel, S., 2008. Kinematic constraints on glacier contributions to 21st-century sea-level rise. Science 321, 1340-1343.

PFMC, 2011. Pacific Fishery Management Council, Review of 2010 ocean salmon fisheries Pacific Fishery management council, Portland, OR http://www.pcouncil.org.

Richter, A., Kolmes, S.A., 2005. Maximum temperature limits for Chinook, coho, and chum salmon, and steelhead trout in the Pacific Northwest. Rev. Fish. Sci. 13, 23-49.

Roegner, G.C., Dawley, E.W., Russell, M., Whiting, A., Teel, D.J., 2010. Juvenile salmonid use of reconnected tidal freshwater wetlands in Grays River, lower Columbia River basin. Trans. Am. Fish. Soc. 139, 1211-1232.

Roegner, G.C., McNatt, R., Teel, D.J., Bottom, D.L., 2012. Distribution, size, and origin of juvenile Chinook salmon in shallow-water habitats of the lower Columbia River and estuary, 2002–2007. Marine and Coastal Fisheries 4, 450-472.

Roegner, G.C., Needoba, J.A., Baptista, A.M., 2011. Coastal upwelling supplies oxygen-depleted water to the Columbia River estuary. PloS one 6, e18672.

Roegner, G.C., Teel, D.J., 2014. Density and Condition of Subyearling Chinook Salmon in the Lower Columbia River and Estuary in Relation to Water Temperature and Genetic Stock of Origin. Trans. Am. Fish. Soc. 143, 1161-1176.

Rupp, D.E., Abatzoglou, J.T., Mote, P.W., 2016. Projections of 21st century climate of the Columbia River Basin. Climate Dynamics, 1-17.

Sagar, J.P., K. E. Marcoe, A. B. Borde, L. L. Johnson, J. L. Morace, T. Peterson, K. H. Macneale, R.M Kaufmann, V.I. Cullinan, S. A. Zimmerman, R. M. Thom, C.L. Wright, P.M. Chittaro, O. P. Olson, S. Y. Sol, D. J. Teel, G. M. Ylitalo, D. Lomax, W.B. Temple, A. Silva, C. A. Simenstad, M. F. Ramirez, J. E. O'Connor, C. Cannon, and M. Schwartz., 2012. Lower Columbia River Ecosystem Monitoring Program Annual Report for Year 7 (September 1, 2010 to December 31, 2011). Prepared by the Lower Columbia Estuary Partnership for the Bonneville Power Administration.

Satake, K., Shimazaki, K., Tsuji, Y., Ueda, K., 1996. Time and size of a giant earthquake in Cascadia inferred from Japanese tsunami records of January 1700. Nature 379, 246-249.

Savage, J., Prescott, W., Lisowski, M., King, N., 1981. Strain accumulation in southern California, 1973–1980. Journal of Geophysical Research: Solid Earth 86, 6991-7001.

Scavia, D., Field, J.C., Boesch, D.F., Buddemeier, R.W., Burkett, V., Cayan, D.R., Fogarty, M., Harwell, M.A., Howarth, R.W., Mason, C., 2002. Climate change impacts on US coastal and marine ecosystems. Estuaries 25, 149-164.

Scheuerell, M.D., Williams, J.G., 2005. Forecasting climate‐induced changes in the survival of Snake River spring/summer Chinook salmon (Oncorhynchus tshawytscha). Fish. Oceanogr. 14, 448-457.

Scheuerell, M.D., Zabel, R.W., Sandford, B.P., 2009. Relating juvenile migration timing and survival to adulthood in two species of threatened Pacific salmon (Oncorhynchus spp.). J. Appl. Ecol. 46, 983-990.

Sheaves, M., Baker, R., Nagelkerken, I., Connolly, R.M., 2015. True Value of Estuarine and Coastal Nurseries for Fish: Incorporating Complexity and Dynamics. Estuaries and Coasts 38, 401-414.

Simenstad, C.A., Burke, J.L., O'Connor, J.E., Cannon, C., Heatwole, D.W., Ramirez, M.F., Waite, I.R., Counihan, T.D., Jones, K.L., 2011a. Columbia River estuary ecosystem classification—concept and application. US Geological Survey.

Simenstad, C.A., Burke, J.L., O'Connor, J.E., Cannon, C., Heatwole, D.W., Ramirez, M.F., Waite, I.R., Counihan, T.D., Jones, K.L., 2011b. Columbia River Estuary Ecosystem Classification— Concept and Application.

Simenstad, C.A., Fresh, K.L., Salo., E.O., 1982. The role of Puget Sound and Washington USA coastal estuaries in the life history of Pacific salmon Oncorhynchus-spp an unappreciated function. . In Estuarine comparisons, ed. V. Kennedy, 343–364. New York: Academic.

Smith, C.L., 2014. Salmon Abundance and Diversity in Oregon Are We Making Progress ?

Teel, D.J., Bottom, D.L., Hinton, S.a., Kuligowski, D.R., McCabe, G.T., McNatt, R., Roegner, G.C., Stamatiou, L.a., Simenstad, C.a., 2014. Genetic Identification of Chinook Salmon in the Columbia River Estuary: Stock-Specific Distributions of Juveniles in Shallow Tidal Freshwater Habitats. N. Am. J. Fish. Manage. 34, 621-641.

Thom, R., Sather, N., Northwest, P., Roegner, G.C., Bottom, D.L., Marine, N., Service, F., 2013. Columbia Estuary Ecosystem Restoration Program.

Tiffan, K.F., Garland, R.D., Rondorf, D.W., 2002. Quantifying flow-dependent changes in subyearling fall Chinook salmon rearing habitat using two-dimensional spatially explicit modeling. N. Am. J. Fish. Manage. 22, 713-726.

U.S., Environmental Protection Agencey. 1986. Ambient water quality criteria for dissolved oxygen. EPA 440/5-86-003., Washington, DC. Office of Water Regulations and Standards.

U.S., Environmental Protection Agencey. 2003. EPA Region 10 guidance for Pacific Northwest state and tribal temperature water quality standards. EPA 910-B-03-002, Seattle, WA, Region 10 Office of Water

USACE, 2012. A 50% Annual Exceedance Probability Stage Approach for Calculating the Survival Benefit Units Profile for Lower Columbia River Estuary, CENWP EC-HY_536_SBU_Rev2.docx, 6 February 2012.

USACE, 2013a. Engineer Regulation, Incorporating sea-level change in civil works programs, Regulation No. 1100-2-8162, Department of the Army: Washington, DC, [Available at: http://www.publications.usace.army.mil/Portals/76/Publications/EngineerRegulations/ER _1100-2-8162.pdf].

USACE, 2014. Engineer Technical Letter, Procedures to evaluate sea level change: impacts, DRAFT responses, and adaptation, Technical Letter No. 1100-2-1, United States Army Corps of Engineers: Washington, DC, [Available at: http://www.publications.usace.army.mil/Portals/76/Publications/EngineerTechnicalLetter s/ETL_1100-2-1.pdf].

Vermeer, M., Rahmstorf, S., 2009. Global sea level linked to global temperature. Proceedings of the National Academy of Sciences 106, 21527-21532.

Volk, E.C., Bottom, D.L., Jones, K.K., Simenstad, C.A., 2010. Reconstructing juvenile Chinook salmon life history in the Salmon River estuary, Oregon, using otolith microchemistry and microstructure. Trans. Am. Fish. Soc. 139, 535-549.

Weitkamp, L.A., Goulette, G., Hawkes, J., O'Malley, M., Lipsky, C., 2014. Juvenile salmon in estuaries: comparisons between North American Atlantic and Pacific salmon populations. Rev. Fish Biol. Fish. 24, 713-736.

Witter, R.C., Zhang, Y.J., Wang, K., Priest, G.R., Goldfinger, C., Stimely, L., English, J.T., Ferro, P.a., 2013. Simulated tsunami inundation for a range of cascadia megathrust earthquake scenarios at bandon, oregon, USA. Geosphere 9, 1783-1803.

Zervas, C., 2009. Sea Level Variations of the United States 1854-2006.

Zervas, C., 2013. Estimating vertical land motion from long-term tide gauge records, Technical report NOS CO-OPS 065, U.S. Department of Commerce, National Oceanic and Atmospheric Administration, Center for Operational Oceanographic Products and Services: Silver Spring, MD, [Available at http://tidesandcurrents.noaa.gov/publications/Technical_Report_NOS_CO-OPS_065.pdf].

Zhang, Y., Baptista, A.M., 2008. SELFE: a semi-implicit Eulerian–Lagrangian finite-element model for cross-scale ocean circulation. Ocean Model. Online 21, 71-96.